A NEW SPECIES OF *ALLOSAURUS* (DINOSAURIA: THEROPODA) FROM THE MORRISON FORMATION OF BARNUM-KAYCEE, WYOMING

P. GODEFROIT & U. LEFÈVRE

museum

Contents

ABSTRACT

Here we describe 'Arkhane', the skeleton of a 8.7 m long *Allosaurus* (Dinosauria: Theropoda) from the Morrison Formation (Fm) (Kimmeridgian, Upper Jurassic) of the Barnum-Kaycee area of Johnson County, Wyoming, USA. This skeleton was deposited in a floodplain environment, characteristic for the middle part of the Morrison Fm in the Powder River sedimentary basin. The skeleton is complete at about 70% and there is no indication that it is a composite specimen: there are no supernumerary bones and the size of all the collected bones is clearly homogeneous, coherent for a single individual. Detailed osteological description and comparisons with other allosauroid taxa support the hypothesis that Arkhane belongs to a new *Allosaurus* species, characterized by 16 cranial and postcranial synapomorphies. Including Arkhane into the most recent and complete phylogenetic analysis of non-coelurosaurian tetanurans places this specimen within a clade formed by the allosaurid taxa from the Morrison Fm, as the sister-group of *Saurophaganax maximus* and close to *Allosaurus fragilis* and *Allosaurus 'jimmadseni'*. It supports the hypothesis that *Saurophaganax* is in fact a distinct, large, species of *Allosaurus* that should be referred to as *Allosaurus maximus*. *Allosaurus 'jimmadseni'* and likely Arkhane were found in the lower Salt Wash Member of the Morison Fm whereas *Allosaurus fragilis* is likely confined to the higher Brushy Basin Member of the Morrison Fm. *Allosaurus maximus* is younger, only present in the uppermost layers of the Morrison Fm.

INSTITUTIONS

DINO Dinosaur National Monument, Utah, USA
MOR Museum Of The Rockies, Bozeman, Montana, USA
USNM National Museum Of Natural History, Washington DC, USA
YPM Peabody Natural History Museum, Yale University, Connecticut, USA

INTRODUCTION

Objectives of the present study

On June 4, 2018, a spectacular allosaurid specimen was put up for Auction by Aguttes at the Eiffel Tower in Paris. This specimen was excavated in 2014 at the Pinepit digsite in the Barnum-Kaycee area in Wyoming. The 8.7-meter-long skeleton was said to have been legally unearthed on private land in Wyoming (although the palaeontologists who unearthed it want to remain anonymous) and was estimated to be about 70% complete (Figure 1). According to the auction house Aguttes's promotional catalogue, the specimen may belong to a previously unknown species, probably a close relative of the iconic Jurassic predator *Allosaurus fragilis*. The specimen was finally acquired by a French collector (who also wishes to remain anonymous), who immediately contacted Pascal Godefroit, present at the Eiffel Tower during the auction. Godefroit incidentally had the opportunity to examine the skull of this allosaurid specimen in 2016, while visiting the laboratory of a private preparator in Italy and had noticed unusual characters on the skull.

Luckily, the new owner wishes to share this exceptional specimen together with the scientific community and with the general public. He is also aware that professional ethics dictate that a specimen can be the basis for a new name only if it is housed in a recognized museum or other repository. Therefore, he asked Godefroit to appraise this new allosaurid specimen (herein nicknamed 'Arkhane') and to provide an independent report with the following objectives:

- Check that Arkhane is a genuine specimen, not a composite one, about 70% complete as stated in the auction catalogue;
- Check that the original parts of the skeleton can be easily distinguished from the reconstructed parts and that the missing parts are correctly reconstructed, following scientific standards;
- Collect information allowing to replace Arkhane in its precise geological context;
- Describe the original parts of the skeleton and compare them with other allosauroid specimens;
- Assess the systematic status of Arkhane and check that it belongs to a new taxon, as clearly stated in the auction catalogue;
- Assess the phylogenetic relationships of Arkhane.

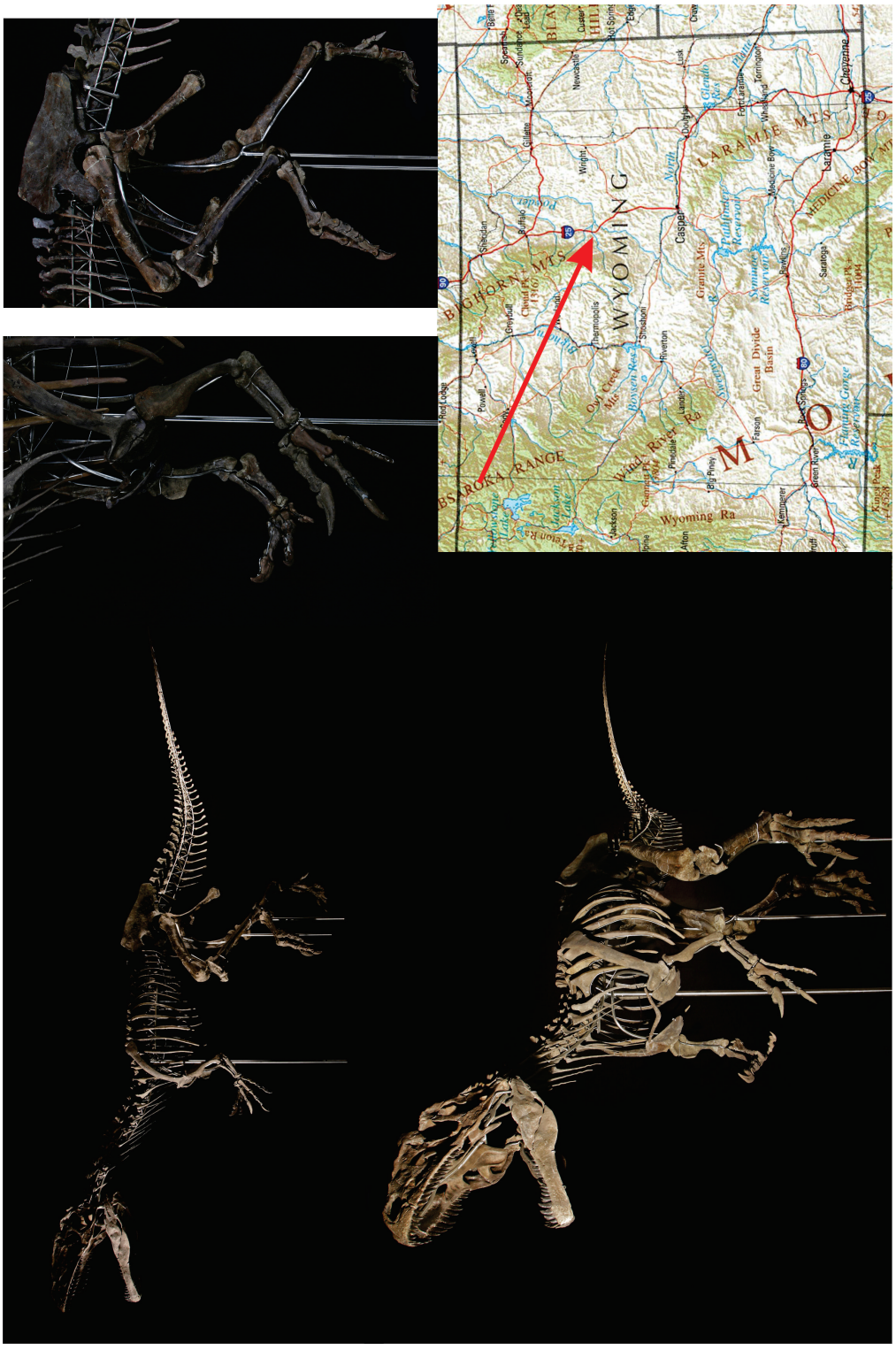

Figure 1
Mounted skeleton of Arkhane, the 8.7 m long skeleton of an 'allosaurid' theropod from the Barnum-Kaycee area of Johnson County, Wyoming.

Allosaurus: a short introduction

Allosaurus is certainly one of the best documented theropod dinosaurs. It was the dominant predator in the Late Jurassic Morrison Formation (Fm), comprising about 60% of the theropod fauna recovered from this formation in Wyoming, Montana, South Dakota, Utah, Colorado, New Mexico, and Oklahoma (Chure 2000) (Figure 2). Moreover, it has also been recognized in the Kimmeridgian of Portugal (Mateus et al. 2006). Chure (2000) demonstrated that other records of *Allosaurus* outside the Morrison Fm are all erroneous.

The first described allosaurid fossil was a fragmentary tail vertebra, probably from Morrison rocks at Middle Park in Colorado. In 1869, F.V. Hayden obtained second-hand this bone and sent it to the famous palaeontologist J.M. Leidy in Philadelphia. Leidy (1873) first assigned this tail vertebra to the European dinosaur genus *Poekilopleuron* as *P. valens*, then he decided it deserved its own genus, *Antrodemus* (Leidy 1873).

Marsh (1877) described *Allosaurus fragilis* based on YPM 1930, a small collection of fragmentary bones including parts of three vertebrae, a rib fragment, a tooth, a toe bone, and a fragmentary humerus, collected from the Morrison Fm of Garden Park, north of Cañon City in Colorado Marsh (1877). The taxonomy of the Morrison Fm allosaurids quickly became a nightmare because of the multiplicity of names coined at the end of the 19th century during the famous 'Bone War' between O.C. Marsh and E.D. Cope, based on sparse material discovered in several localities; these include e.g. *Creosaurus* (Marsh 1878), *Epanterias* (Cope 1878) and *Labrosaurus* (Marsh 1879). On the other hand, several fairly complete skeletons unearthed in Wyoming by Marsh's and Cope's respective excavation teams were not formally described until recently (Chure 2000).

Gilmore (1920) wrote the first monograph on the Morrison Fm allosaurids, concluding that the tail vertebra named *Antrodemus* by Leidy (1873) was indistinguishable from those subsequently described in *Allosaurus*; thus, the older name *Antrodemus* should have priority on *Allosaurus*.

From 1960 onward, the Cleveland-Lloyd Dinosaur Quarry in Emery County, Utah has yielded thousands of bones belonging to at least 44 and possibly as many as 60 disarticulated and mixed *Allosaurus fragilis* individuals of almost all ages and sizes (Madsen 1976b). This abundant material was the base for Madsen's (1976a) famous monograph on the osteology of *Allosaurus fragilis*. Since this detailed study, the name *Allosaurus fragilis* became unanimously adopted by palaeontologists, whereas *Antrodemus*, based on a single tail vertebra, quickly became forgotten. However, the issue of species and potential synonyms is complicated by the fact that the type specimen of *Allosaurus fragilis* is itself extremely fragmentary; because of that, the type specimen is

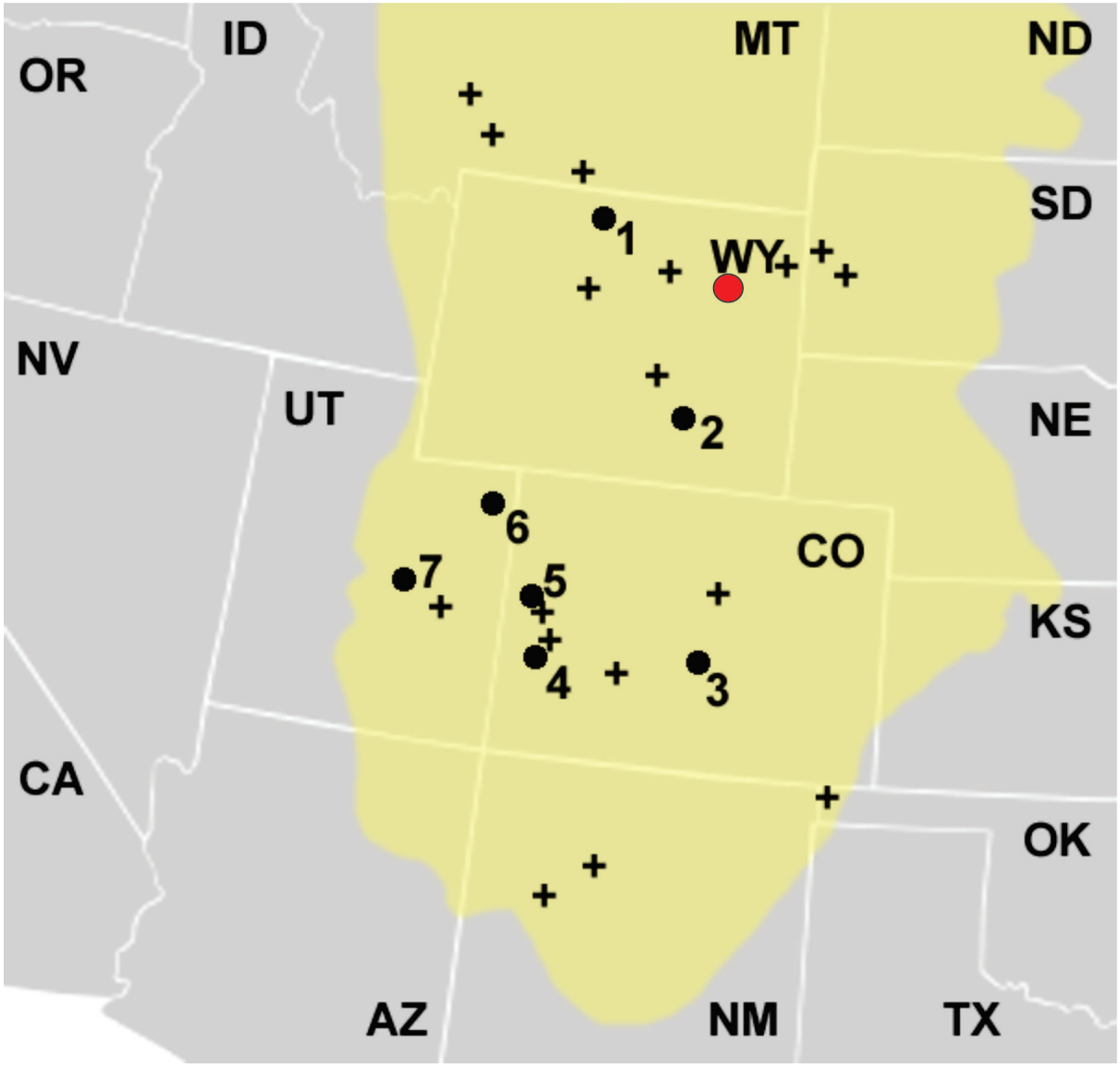

Figure 2

Map of Morrison Fm allosaur quarry locations. The general extent of the Morrison Formation has been overlaid in yellow. Historically or otherwise notable quarries where *Allosaurus* remains have been found include the numbered locations: 1:"Big Al" quarry, Big Horn Co., WY; 2: Como Bluff, Albany Co., WY; 3: Garden Park/Cañon City, Fremont Co., CO; 4: Dry Mesa Quarry, Delta Co., CO; 5: Grand Junction/Fruita, Mesa Co., CO; 6 : Dinosaur National Monument West, Uintah Co., UT; 7: Cleveland-Lloyd Dinosaur Quarry, Emery Co., UT; red point: Barnum Kaysee, Johnson Co, Wy. Other locations where Allosaurus has been found are marked with a "+". Source: https://commons.wikimedia.org/wiki/File:Alloquarrynolang.png.

potentially dubious, and thus the species *Allosaurus fragilis* and even the genus *Allosaurus* itself would be regarded as *nomina dubia* ("dubious name", based on a specimen too incomplete to compare to other specimens or to classify). To address this situation, Paul and Carpenter (2010) submitted a petition to the International Commission of Zoological Nomenclature to have the name *Allosaurus fragilis* officially transferred to the more complete specimen USNM 4734 as a neotype. This request is still currently pending review.

Whathever it might be, *Allosaurus fragilis* is known by more than 60 specimens so far. Particularly complete and spectacular are the skeletons of 'Big Al' (MOR 693) and 'Big Al 2', both discovered in Wyoming by a Swiss team from the Aathal Sauriermuseum (Breithaupt 1996; Hanna 2002; Foth et al. 2015). It is also important to point out that all well identified *Allosaurus fragilis* specimens are apparently confined to the higher Brushy Basin Member of the Morrison Formation (Loewen et al. 2003)(see also Geological Settings).

In his PhD thesis, Daniel Chure (2000) described in detail DINO 11541, one of the best preserved skeletons of *Allosaurus* from the Dinosaur National Monument in Utah, as a new species, *Allosaurus jimmadseni*. Because this new species has not been formally described in a scientific publication yet, we shall refer this specimen as *Allosaurus 'jimmadseni'* (between brackets) in the present report. Unlike *Allosaurus fragilis*, *Allosaurus 'jimmadseni'* was discovered in the lower Salt Wash Member of the Morrison Formation. Besides its older stratigraphic age, numerous osteological characters justify the specific separation of DINO 11541. In his PhD thesis, Chure (2000) also substantially clarified the taxonomy of *Allosaurus* in revising all the numerous species that had been previously classified within or referred to this genus.

Chure (1995) also described the extremely large allosaurid *Saurophaganax maximus*, based on disarticulated material from the top of the Morrison Fm in Oklahoma. Smith (1998) regarded *Saurophaganax maximus* as a species of *Allosaurus*, but this hypothesis has not been followed in the most recent reviews of Tetanurae (e.g. Holtz (2004) and Carrano et al. (2012)).

Galton et al. (2015) reassigned the holotype pes of *Camptonotus amplus* Marsh, 1879 to *Allosaurus*. Whether it belongs to a separate species or can be assigned to one of the existing *Allosaurus* species requires further investigation of the variation of pes osteology in this genus (Galton et al. 2015). Dalman (2014) named *Allosaurus lucasi* from two partial skeletons discovered in the Morrison Fm of southwestern Colorado. However, given the fragmentary preservation of the type material, comparisons with other species is extremely adventurous and we prefer regarding *Allosaurus lucasi* as a *nomen dubium* pending further evidences.

Allosaurus fossils were first reported in Portugal and referred to *Allosaurus fragilis* by Pérez-Moreno et al. (1999). Based on the subsequent discovery of a partial skull and neck in the Lourinhã Fm, Mateus et al. (2006) named a new species, *Allosaurus europaeus*, which differs from other *Allosaurus* species in cranial details. However, Malafaia et al. (2007), based on more abundant material, consider that *Allosaurus europaeus* is a junior synonym of *Allosaurus fragilis*.

The Barnum-Kaycee dinosaur locality: a historical background

At the turn of the 20th Century, the main North American natural history museums organized intensive palaeontological expeditions in the American West, actively looking for colossal and spectacular dinosaur skeletons for their brand-new dinosaur halls. The principal protagonists were the American Museum of Natural History in New York, the Field Museum in Chicago and the Carnegie Museum of Natural History in Pittsburgh (Brinkman 2010). The Late Jurassic Morrison Formation was of course one of their favourite hunting grounds.

On June 25, 1902, William H. Utterback, a field palaeontologist at the Carnegie Museum, was prospecting Jurassic deposits along the Red Fork of the Powder River, about 12 miles from Kaycee in Wyoming, when he found excellent dinosaur material: one completely eroded skeleton besides a second one, which displayed an articulated series of caudal vertebrae, together with limb bones. Utterback started the excavation in this quarry ('Quarry A') and, in July, he already unearthed a significant part of the second skeleton, including 16 caudal vertebrae, the sacrum and limb bones, that he tentatively identified as belonging to the large sauropod *Diplodocus*. Because of the weather conditions, Utterback had to stop fieldwork by mid-September 1902. He covered the bones still showing in the field and returned to Pittsburgh ten boxes containing half a sauropod skeleton (Brinkman 2010).

Utterback returned to Kaycee in May 1903 and started unearthing the rest of the *Diplodocus* skeleton (Brinkman 2010). During a prospection, Utterback located a new dinosaur quarry above Quarry A. In this new quarry ('Quarry B'), he and his team quickly removed more than one hundred dinosaur bones belonging to a least two individuals from a limited area. Strangely, although Quarry B was particularly promising, Utterback felt that the excavation results were unsatisfactory. Utterback closed up the excavations at Quarry B on August 11, shipped 29 boxes of dinosaur fossils to Pittsburgh, including an articulated series of 38 caudal vertebrae of *Diplodocus*, then moved to Montana.

In 1905, the articulated series of caudal vertebrae from Powder River Quarry B were incorporated within the famous Carnegie's mounted *Diplodocus* specimen, together with elements of another skeleton, discovered in the Sheep Creek quarry, also in Wyoming. Andrew Carnegie himself paid to have this skeleton replicated and copies were sent to some of the most prestigious natural history museums, including London, Paris, Vienna, Berlin, Mexico City, Buenos Aires, and Munich.

In 1924, the partial skeleton from Powder River Quarry A was named as a new species of *Diplodocus*, *Diplodocus hayi*, by the director of the Carnegie Museum, William J. Holland. In 2015, Tschopp et al. renamed it as the separate genus, *Galeamopus hayi*.

Institutional palaeontologists completely abandoned excavations and researches in the Barnum-Kaycee area. However, this area still attracted the attention of private fossil collectors. From 2006 onward, an European private company started prospections in this area, looking for potentially productive dig site, in the Morrison Formation. Several quarries were opened in the following years, providing a wealth of particularly well-preserved dinosaur skeletons including:

- several *Allosaurus* skeletons;
- *Torvosaurus*-like isolated teeth;
- several partial skeletons and isolated bones of small theropod dinosaurs;
- one large complete stegosaur skeleton;
- several partial skeletons of small neornithischian dinosaurs ("*Nanosaurus*");
- complete and partial skeletons of diplocid and apatosaurid sauropods.

Besides dinosaurs, crocodiles (teeth), fresh-water turtles (postcranial elements), lungfishes (teeth) and freshwater clams are also abundantly represented in the Barnum-Kaycee fossiliferous quarries.

At the end of the 2013 field season, few theropod bones were discovered cropping out nearby a pine tree at the flank of a small hill, close to the Red Fork of the Powder River in the Barnum-Kaycee area. One day of digging by hand proved that there were more bones coming. So, the decision was made to start new excavations there during the next field season. In 2014, a road to the site was built and the overburden removed using heavy machinery. Pretty soon it was clear that the skeleton of a large allosaurid theropod was present in the "Pinepit" digsite. During the 2014 season, almost all the present skeletal elements of the theropod could be excavated. From the excavation map (Figure 3), it is clear that a single allosaurid specimen is present in Pinepit Quarry. There is no supernumerary bone and the size of all the collected bones is clearly homogeneous,

coherent for a single individual. A few metres from the allosaurid skeleton, the first bones of another skeleton showed up, belonging to a camarasaurid sauropod that was excavated in 2015.

Geological setting

The Kaycee dinosaur locality is located on the western margin of the Powder River Basin (Figure 4). This sedimentary basin, formed mostly during the early Tertiary, covers approximately 22,000 mi^2 in northeastern Wyoming, western South Dakota, and southeastern Montana. It is bordered by the Bighorn Mountains on the west, the Laramie Range and the Hartville Uplift on the south, and the Black Hills on the east. Rocks of Jurassic age are exposed in all of the surrounding uplifts (Johnson 1992).

During the Late Jurassic, marine water withdrew from the Western Interior, probably due to a combination of increased progradation of siliciclastic sediments from the western source area, of reduced subsidence in the seaway, and of eustatic lowering of sea level (Johnson 1992). As the sea withdrew, a vast expanse of sea floor was exposed that was then rapidly covered by alluvial sediments, now represented by the Morrison Formation, that spread from west to east. The Morrison crops out throughout the Western Interior from southern Canada to central New Mexico and from central Utah eastward to the Great Plains. Winslow and Heller (1987) reported the total area of Morrison deposition to exceed 617,600 mi^2. In the area of the Powder River Basin, the Morrison is defined as all of the Jurassic nonmarine rocks above the Sundance Formation (Johnson 1992). In this area, the Morrison is usually a fining-upward sequence composed of dull, variegated, gray, green, and red argillaceous rocks; some sandstone and limestone are in the lower part. The upper part of the formation contains mostly grey and green argillaceous rocks. The Morrison Fm is overlain by the Cretaceous Cloverly Fm; in the area of the powder River Basin, the contact between the two formations can be subtle and appear conformable where fine-grained rocks from the Cloverly overlie the Morrison. In the Powder River Basin, the Morrison Fm likely began in the late Oxfordian; most of the Morrison Fm is probably Kimmeridgian in age and the upper part of the formation maybe extends into the Tithonian (Imlay 1980).

The depositional environments of the Morrison Fm include lacustrine and fluvial, with all the associated subfacies (channel, levee, crevasse splay, floodplain, ...), deposits (Johnson 1992). The lower part of the Morrison Fm was probably deposited under warm, arid to semiarid conditions. The upper part of the formation, which contains mostly floodplain and lacustrine facies, was possibly deposited under cooler, more humid conditions.

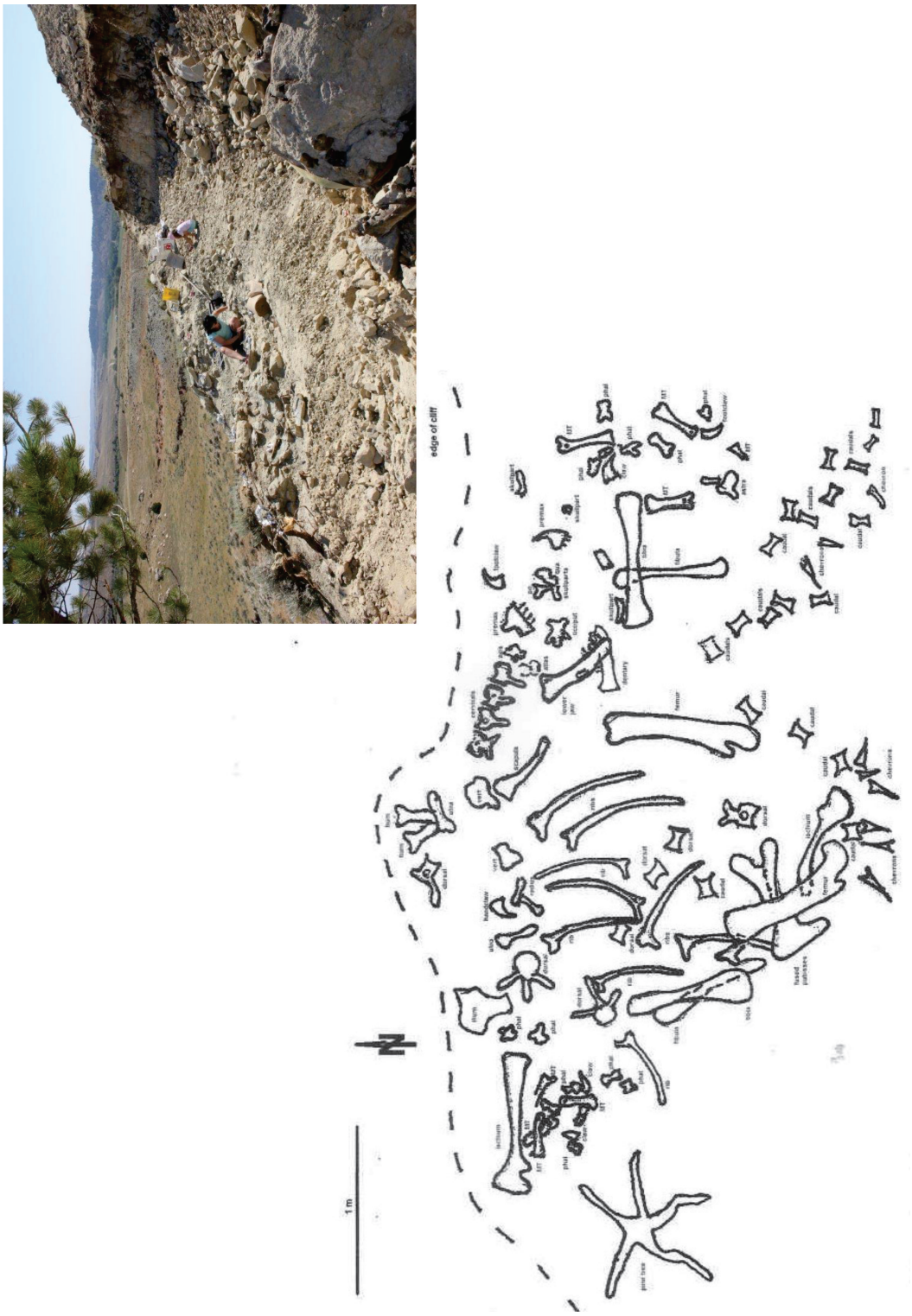

Figure 3

Excavation fieldmap of the *Allosaurus* quarry ("Pinepit" Quarry) at Barnum-Kaycee, Wyoming. The skeleton of a single allosaurid individual is disarticulated, but all the isolated bones remain concentrated in a limited area, without contamination of bones from other individuals. Together with sedimentological data, this 'crime scene' snapshot suggests that the allosaurid died in a floodplain environment and that its skeleton was rather quickly covered with sediments from this floodplain.

A western source for most Morrison sediments is indicated by fluvial palaeocurrent data and is suggested by both regional thickening of the formation and an increase in the amount of sand in the formation toward the west. The mineralogy and clast composition indicate that the source area consisted mostly of sedimentary rocks (Johnson 1992).

The well-known members of the Morrison in the Colorado Plateau (for example, Salt Wash and Brushy Basin Members) have not been formally recognized in the Powder Basin yet. The Pinepit quarry is located in the lower to middle part of the stratigraphic section of the Morrison Fm exposed in the Barnum-Kaycee area. The allosaurid was found in a green siltstone beds that represent relics of an ancient floodplain. The semi-articulated nature of both the allosaurid (Figure 3) and camarasaurid skeletons in the Pinepit quarry is consistent with this interpretation. Based on their position in the Morrison Fm and on their sedimentological composition, it might be hypothesized that the Pinepit Quarry deposits correlate with the Salt Wash Member of the Morrison Fm in the Colorado Plateau. However, this hypothesis needs to be corroborated by a detailed geological survey and sedimentological samplings of the Morrison Fm deposits in the Barnum-Kayce area. As a reminder, the Salt Wash Member has yielded *Allosaurus 'jimmadseni'* in Utah (Chure 2000), although all the well-identified *Allosaurus fragilis* specimens seem confined to the higher Brushy Basin Member (Loewen et al. 2003).

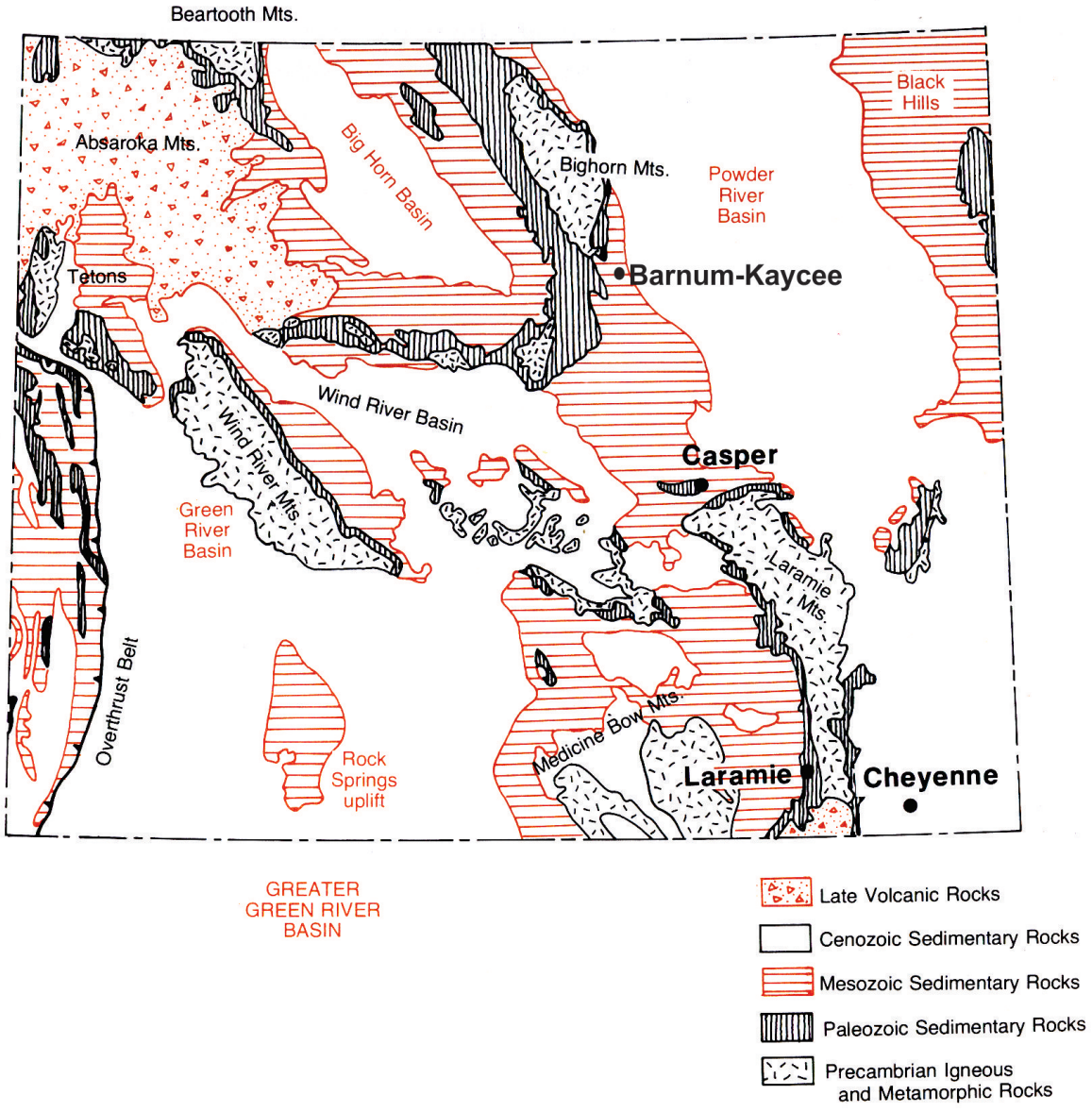

Figure 4
Simplified geological map of Wyoming (after Lageson and Spearing, 1988). Roadside geology of Wyoming. Mountain Press Publishing Company, Missoula

RESULTS

Systematic palaeontology

Neotheropoda Bakker, 1986
Tetanurae Gauthier, 1986
Avetheropoda Paul, 1988
Allosauroidea Marsh, 1878
Allosauria Paul, 1988
***Allosaurus* Marsh, 1877**

1877 *Allosaurus* Marsh,
1878 *Creosaurus* Marsh,
1878 *Epanterias* Cope,
1879 *Labrosaurus* Marsh,

Type-species: *Allosaurus fragilis* Marsh, 1877

Included species: *Allosaurus maximus* Chure et al., 2005; *Allosaurus jimmadseni* Chure et al., 2006 (nomen nudum?); *Allosaurus europaeus* Mateus et al., 2006 ; *Allosaurus* nov. sp. (this report).

Amended diagnosis: Allosauroid theropod with: (1) tall, mediolaterally compressed dorsal projection ('horn') on posterodorsal surface of lacrimal; (2) reduced subnarial process of premaxilla, separate from nasals by maxillary contribution to narial margin; (3) rostral end of jugal excluded from internal antorbital fenestra; (4) jugal not pneumatized; (5) orbital margin of jugal vertical; (6) suborbital flange absent on postorbital; (6) width of basal tubera inferior to occipital condyle width; (7) reduced external mandibular fenestra; (8) neomorphic antarticular bone on lower jaw; (9) low and blunt epipophyses on anterior cervical vertebrae; (10) length/width ratio of scapular blade > 10; (11) humerus distally canted in lateral view, wih distal condyles not parallel to proximal ones; (12) low swollen vertical ridge on lateral surface of iliac blade dorsal to acetabulum.

***Allosaurus* nov. sp.**

Holotype: 'Arkhane', a 70% complete specimen.

***Locus typicus*:** "Pinepit" Quarry, Barnum-Kaycee area, Johnson County, Wyoming, USA.

***Stratum typicum*:** Morrison Formation, Kimmeridgian Upper Jurassic.

Diagnosis: *Allosaurus* species with: (1) single pneumatic recess on lacrimal corneal process ('horn'); (2) nuchal crest of supraoccipital extending up to the foramen magnum; (3) short paroccipital processes extending up to the level of the floor of the foramen magnum; (4) retroarticular process not covered laterally by the surangular; (5) internal mandibular foramen absent on prearticular; (6) narrow lateral exposure of the prearticular at the caudal nd of the mandible; (7) odontoid fused to axis; (8) pleurocoels extending up to dorsal centrum 1; (8) single infradiapophyseal lamina on dorsal 4; (9) massive manual ungual I-2, 2/3 the length of the radius; (10) relatively short pubic foot (craniocaudal length of the pubic foot /proximodistal length of the pubis = 0.49); (11) slender pubic shaft (Proximodistal length of the pubis / craniocaudal width of the pubic shaft = 27); (12) paired pubes widely expanded proximally (greatest width of the paired pubes / proximodistal length of pubis = 0.51); (13) femoral head angled dorsomedially in cranial view; (14) mesial distal condyle of femur extends further distally than lateral condyle; (15) rostrolateral process developed into a ventral spine that overhangs the tibial shaft; (16) no nutrient foramen caudal to distal end of fibular crest.

Osteological description

Head

Skull

***Important preliminary remark*:** Between December 2016 and May 2017, the skull of Arkhane had been partly prepared in Brussels by skilled technicians from Raphus SPRL, who mounted the original bones on a metallic frame and reconstructed the missing parts. The original and reconstructed bones could easily be separated for further subsequent anatomical studies. The skull was returned to Italy in June 2017. Surprisingly, the original mounting has been completely removed in the meantime; the original and reconstructed bones cannot be separated anymore, so that the skull cannot be adequately studied so far. The following description of the skull is therefore based on the observations and iconographic documents while in Brussels. The skull will be completely dismounted, re-prepared and remounted again from April 2018 onwards by Raphus SPRL, to fit the original situation, so a more complete and accurate description of the original elements of the skull will then be possible.

***Premaxilla*:** As in *Allosaurus fragilis* (Madsen 1976b) and *Allosaurus 'jimmadseni'*

(Chure 2000), the body of the premaxilla is quadrangular in lateral view, with subequal sides (Figure 5 A-B). As in those species, there are 5 alveoli for premaxillary teeth. The teeth tend to be uniform in size, with a D-shaped cross section. Randomly-spaced foramina perforate the external aspect of the premaxilla. The ascending nasal process forms the rostral margin of the external naris. The nasal processes of both premaxillae form rostrally a flattened symphysis, but are separated caudally by the thin projections of the nasal, which meet at the midline. The contact area with the maxilla and the subnarial foramen are unfortunately not preserved in Arkhane.

***Maxilla*:** Both maxillae are quite incompletely preserved in Arkhane (Figure 5). It is particularly massive and roughly triangular in lateral view. Its rostrodorsal margin clearly participated in the ventral margin of the external naris. The number of maxillary alveoli cannot be adequately estimated. The broad tapering nasal process rises from the body of the maxilla to meet the nasal dorsally and, more caudally, the rostral process of the lacrimal. A large maxillary fenestra opens laterally at the base of the nasal process. The caudal process of the maxilla is roughly rectangular in lateral view and forms the ventral margin of the large antorbital fenestra. It forms an interdigitating articulation with the rostral process of the jugal.

***Lacrimal*:** The lacrimal participates in the rostral margin of the orbit and in the dorsal margin of the antorbital fenestra (Figure 5 A-B). In lateral view, the dorsal surface of the lacrimal forms a semicircular corneal process, as also observed in *Allosaurus fragilis* (Madsen 1976b), *Allosaurus 'jimmadseni'* (Chure 2000), *Ceratosaurus* (Madsen and Welles 2000), and *Baryonyx* (Charig and Milner 1986). The bone surface of this process is roughened, suggesting the presence of a keratinous covering in life. The lateral aspect of the corneal process is deeply excavated by a large rounded pneumatic recess; in *Allosaurus fragilis*, the lateral aspect of the lacrimal is perforated by two oval openings, the larger one being the caudal one (Gilmore 1920). In *Allosaurus 'jimmadseni'*, two smaller pneumatic recesses are present at the base of the corneal processes (Chure 2000).

***Jugal*:** Both jugals are incompletely preserved. The jugal participates in the rostroventral corner of the infratemporal fenestra and in the ventral border of the orbit (Figure 5 and 6 A-B). The jugal is dorsoventrally expanded underneath the contact with the lacrimal, so that the bone is higher here than in its suborbital part, as observed in many theropods (Rauhut 2003). The jugal participated in the rostral margin of the orbit as in *Allosaurus fragilis* (Madsen 1976b), although it is completely excluded by the lacrimal in *Allosaurus 'jimmadseni'* (Chure 2000). The ascending ramus extends above

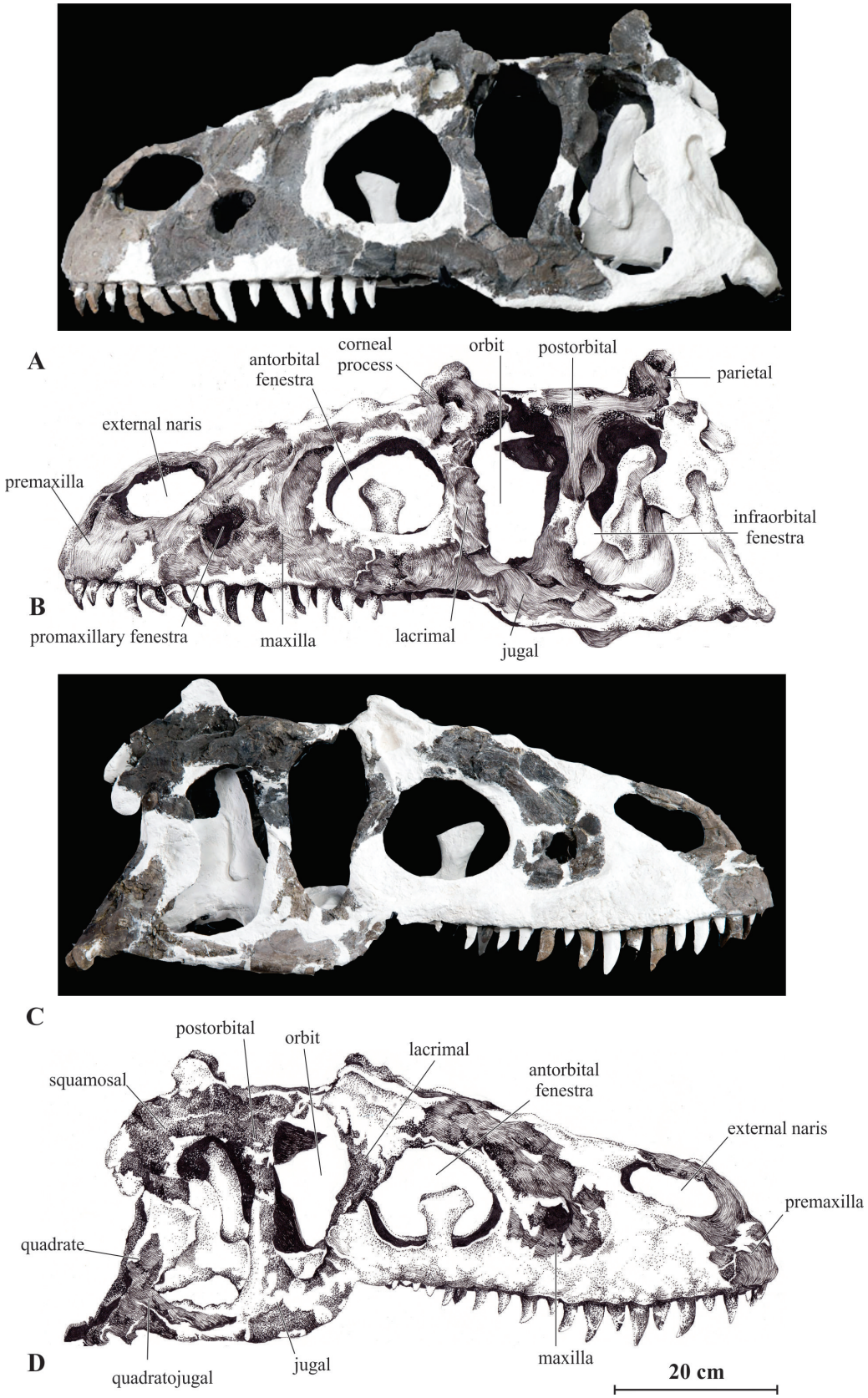

Figure 5
Skull of Arkhane in left lateral (**A**, **B**) and right lateral (**C**, **D**) views.

the mid-height of the postorbital bar. The rostral process of the jugal is triangular in lateral view and tapers rostrally, covering the lateral side of the maxilla. The jugal rostral process of the jugal is excluded from the margin of the internal antorbital fenestra, as also observed in *Allosaurus fragilis* and *Allosaurus 'jimmadseni'*, although it participates in the caudoventral margin of the antorbital fenestra in *Acrocanthosaurus* (Stovall and Langston 1950), *Carcharodontosaurus* (Sereno et al. 1996), *Monolophosaurus* (Zhao and Currie 1993), *Sinraptor dongi* (Currie and Zhao 1993), *Sinraptor hepingensis* (Gao 1992), *Yangchuanosaurus shangyuensis*, and *Yangchuanosaurus magnus* (Dong et al. 1983). Under the orbit, the ventral border of the jugal is regularly convex and deflected ventrally, as also observed in *Allosaurus fragilis*. It is rather straight in *Allosaurus 'jimmadseni'* and most theropods (Chure 2000). There is no pneumatic foramen on the lateral surface of the jugal, as also observed in *Allosaurus 'jimmadseni'*. In *Allosaurus fragilis* the lateral surface is often pierced by several small neurovascular foramina, but those foramina are not pneumatic, according to Chure (2000). Jugal pneumatisation is present e.g. in *Carcharodontosaurus* (Sereno et al. 1996), *Monolophosaurus* (Zhao and Currie 1993), *Sinraptor dongi* (Currie and Zhao 1993).

***Postorbital*:** The postorbital is dorsoventrally high and T-shaped in lateral view (Figure 5 A-B). Its ventral process is triangular in cross-section and curves slightly forward; its caudal margin forms a wide shelf covered by the ascending process of the jugal in a loose contact. The caudal process of the postorbital tapers caudally, lying in a deep groove along the lateral aspect of the squamosal to form a stout dorsal supratemporal arch. The rostral margin of the postorbital is separated from the corneal process of the lacrimal by a deep embayment along the rostrodorsal corner of the orbit. The dorsal aspect of the postorbital above the orbit is ornamented by rugosae as in *Allosaurus fragilis* (Madsen 1976b) and *Allosaurus 'jimmadseni'* (Chure 2000).

***Parietal*:** The parietals meet dorsally but, unlike in *Allosaurus fragilis* (Madsen 1976b), apparently do not form a sagittal crest; laterally, the parietals are deeply excavated to form the concave inner surfaces of the supratemporal fenestra. The parietal expands dorsally into a wide flange and tapers posterolaterally to a thin, pointed projection that fits between the paroccipital process and an anteromedial branch of the squamosal, as also described in *Allosaurus fragilis* (Madsen 1976b). The parietals surround the supraoccipital laterally and dorsally and merge above in the nuchal crest.

***Squamosal*:** The squamosal forms the dorsal and upper caudal half of margin of the infratemporal fenestra (Figure 5 C-D). The descending ramus extends down more than

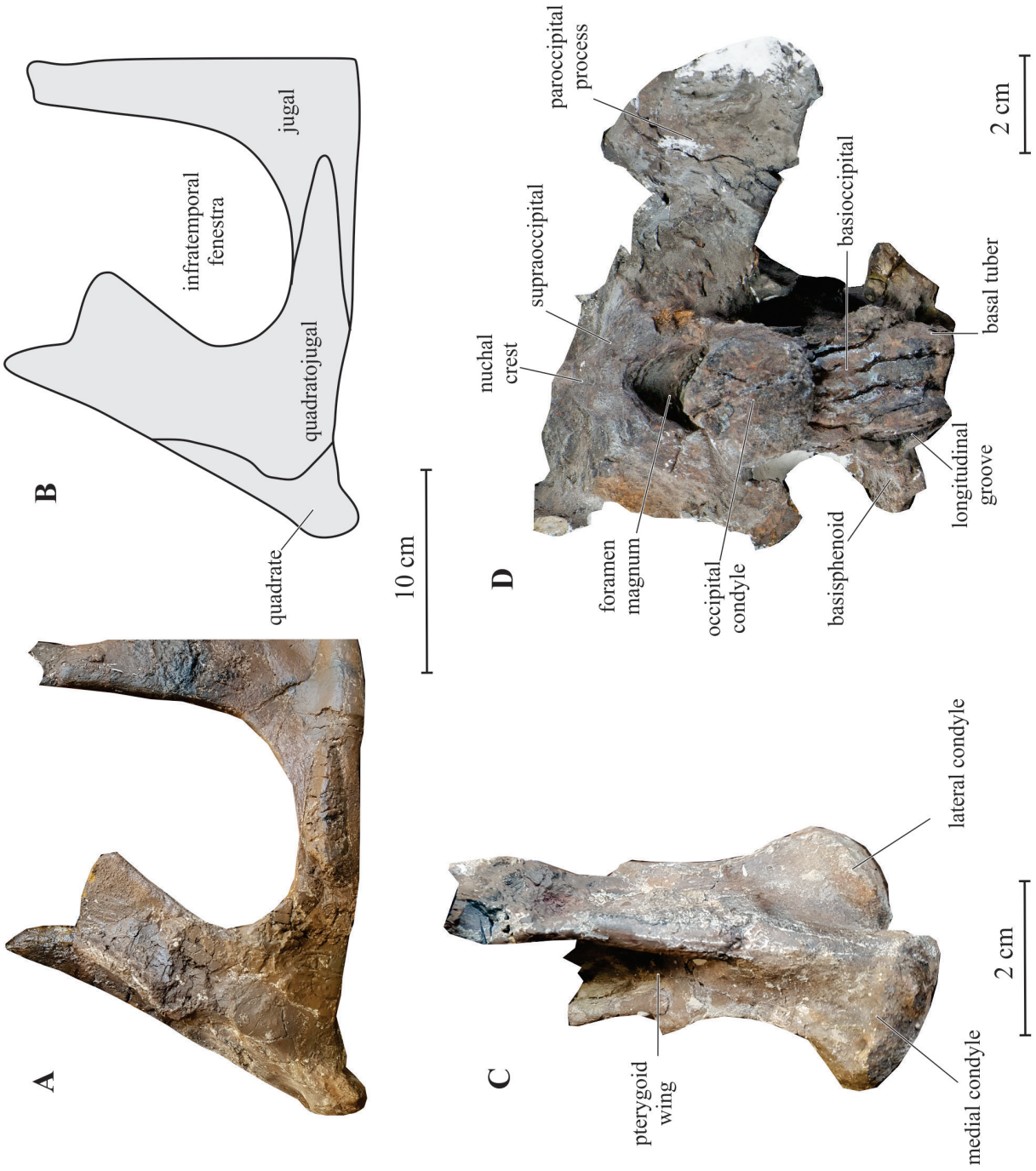

Figure 6
Right infratemporal complex of Arkhane in lateral view (**A**,**B**). Right quadrate of Arkhane in caudal view (**C**). Occiput of Arkhane in caudal view (**D**).

half the height of the infratemporal fenestra and contacts the quadratojugal, excluding the quadrate from the fenestra. The cranial margin of this ramus is strongly convex and partially constricts the infratemporal fenestra. The presence of striations on the lateral surface of the descending process of the squamosal, regarded as a synapomorphy for the genus *Allosaurus*, cannot be ascertained in Arkhane. The cotylus for the head of the quadrate is well developed ventrally.

***Quadrate*:** The quadrate and quadratojugal are intimately fused together, their respective limits cannot be easily discerned (Figure 6 A-C). In lateral view, the body of the quadrate is slightly bowed rostrally, as also observed in *Allosaurus fragilis* (Madsen 1976b), and the bone is noticeably inclined rostrodorsally. The quadrate head is rounded and not significantly expanded. The distal articular surface is mediolaterally expanded: its width is about one-half of the quadrate height, as also observed in *Allosaurus fragilis* (Madsen 1976b). The lateral condyle is wider than the medial one, but the latter extends further ventrally. Both condyles are separated by a narrow, deep, and oblique groove along the caudal surface of the quadrate. From the lateral edge of the medial condyle, a strong rounded ridge extends dorsally along the caudal surface of the quadrate; this ridge forms the lateral border of the medially-directed pterygoid wing, characterized by a particularly depressed caudal surface. A slit-like quadrate foramen is present at mid-height on the caudolateral aspect of the quadrate, close to the quadratojugal contact.

***Quadratojugal*:** The quadratojugal is L-shaped, composed of of a subvertical dorsal process and a horizontal rostral process (Figure 6 A-B). It forms the caudoventral margin of the infratemporal fenestra. The ascending process is inclined craniodorsally and is particularly wide craniocaudally, covering most of the lateral surface of the quadrate shaft, as also observed in *Allosaurus fragilis* (Madsen 1976b), *Allosaurus 'jimmadseni'* (Chure 2000), *Cryolophosaurus* (Hammer and Hickerson 1994), and *Monolophosaurus* (Zhao and Currie 1993). The caudal base of the rostral process is dorsoventrally high, as also observed in *Allosaurus fragilis* (Madsen 1976b), *Allosaurus 'jimmadseni'* (Chure 2000), and *Yangchuanosaurus shangyuensis* (Dong et al. 1983); it tapers to a point rostrally as in most allosauroids except *Sinraptor dongi*, in which it is forked (Currie and Zhao 1993).

***Basioccipital/basisphenoid*:** The basioccipital forms the largest part of the occipital condyle and contributes to the floor of the foramen magnum, although it is completely excluded by the exoccipital-opisthotics in *Allosaurus 'jimmadseni'* (Chure 2000). In caudal view, it also forms the entire median part of the ventrally-extending basal tubera

(Figure 6 D). The basal tubera are framed laterally by caudally-extending walls of the basisphenoid, which are separated from the basioccipital by shallow longitudinal grooves. These grooves are sharper and the lateral contribution of the basisphenoid to the basal tubera is more important in *Allosaurus fragilis* and *Sinraptor dongi* (Currie and Zhao 1993; Rauhut 2003). The rostral part of the basisphenoid is too eroded to be adequately described.

***Supraoccipital*:** The supraoccipital is intimately fused with the medial part of the exoccipital-opisthotic, so the limits of the bones cannot be discerned (Figure 6 D). It likely forms the main part of the dorsal margin of the foramen magnum, although its participation is more limited in *Allosaurus fragilis* (Madsen 1976b) and *Allosaurus 'jimmadseni'* (Chure 2000). The nuchal crest is particularly prominent and extends along the whole height of the supraoccipital. Unlike in *Allosaurus 'jimmadseni'*, the nuchal crest is much wider ventrally and it extends up to the foramen magnum. There is no trace of openings on each side of the supraoccipital dorsolaterally to the foramen magnum.

***Exoccipital-opisthotic*:** The exocipital-opisthotics form the lateral margin of the foramen magnum (Figure 6 D). Unlike in *Allosaurus 'jimmadseni'*, they do not completely exclude the basioccipital from the floor of the foramen magnum (Chure 2000). The right paroccipital process is well preserved; it is rather massive and extends laterally and slightly ventrally, extending more or less to the level of the base of the foramen magnum as also observed in *Monolophosaurus* (Zhao and Currie 1993). It has not the characteristic pending aspect, extending well below the level of the foramen magnum, as observed in *Allosaurus fragilis* (Madsen 1976b), *Allosaurus 'jimmadseni'* (Chure 2000), *Sinraptor dongi* (Currie and Zhao 1993), and *Ceratosaurus* (Madsen and Welles 2000). In dorsal view, the paroccipital process is only slightly directed caudally, although it forms a 135° angle with the sagittal axis of the skull as in *Allosaurus fragilis* (Madsen 1976b), *Allosaurus 'jimmadseni'* (Chure 2000), *Sinraptor dongi* (Currie and Zhao 1993), and *Acrocanthosaurus* (Currie and Carpenter 2000). A deep notch separates the caudoventral pedicel of the exoccipital-opisthotic from the basal tubera in occipital view, as also observed in other allosauroids (Currie and Zhao 1993). The pedicel extends dorsal to the level of the basal tubera, as observed in most theropods including *Allosaurus fragilis*, although it extends further ventrally in *Sinraptor dongi* (Currie and Zhao 1993).

Mandible

***Dentary*:** The dentary is elongated and appears more slender than in *Allosaurus fragilis*, more closely resembling the condition in *Marshosaurus* (Figure 7). The caudal part of the dentary is thin and dorsoventrally expanded. Its height progressively diminishes rostrally along its caudal third, then its depth remains uniform up to the symphysis. The caudal third of its ventral margin is therefore concave, then it remains straight rostrally as in *Allosaurus fragilis*, contrasting with the condition in *Marshosaurus* and *Ceratosaurus*, in which the rostral half of the dentary curves upwards (Madsen 1976a; Madsen and Welles 2000). The mandibular symphysis is short and forms a flattened surface, inclined rostrolaterally. Two centimeters below its dorsal margin, the lateral surface of the dentary is pierced by a series of aligned neurovascular foramina, each more or less corresponding to an alveolus. As in *Allosaurus 'jimmadseni'* (Chure 2000), there are 18-19 alveoli in the complete tooth row (16 +/- 1 in *Allosaurus fragilis*; 21 in *Marshosaurus*; Madsen (1976a) and Madsen (1976b)). In dorsal view, the dentary is nearly straight, in any case, not as laterally bowed as in *Allosaurus fragilis* (Holtz 2004). The medial side of the dentary is slightly convex dorsoventrally. The Meckelian canal extends along its whole length, up to the symphysis.

***Supradentary*:** The supradentary is a long and particularly thin bone that lies along the mediodorsal margin of the dentary, medial to the base of the teeth (Figure 7 B).

***Surangular*:** The surangular is dorsoventrally elevated, reflecting the weak development of the external mandibular fenestra (Figure 8). In lateral view, caudal to the external mandibular fenestra, the ventral aspect of the surangular is covered by the angular. Caudally, the surangular covers the lateral aspect of the articular, but does not extend onto the retroarticular process; in *Allosaurus 'jimmadseni'* and, particularly, *Allosaurus fragilis*, the surangular extends further caudally, covering laterally most of the articular at the level of the retroarticular process (Madsen 1976b; Chure 2000). A horizontal ridge is particularly well developed along the lateral aspect of the surangular. As in *Allosaurus fragilis* and *Allosaurus 'jimmadseni'*, a smaller foramen is present at midlength beneath this ridge (Madsen 1976b; Chure 2000). A wide groove extends along the rostrolateral side of the surangular, just beneath its dorsal margin. This groove is also developed in *Allosaurus 'jimmadseni'* (Chure 2000), but is apparently absent in *Allosaurus fragilis*, in which a foramen opens rostrally on the lateral surface of the surangular (Madsen 1976b). The surangular as a quite limited medial exposure, dorsal to the coronoid, as also decribed in *Allosaurus 'jimmadseni'* (Chure 2000).

Figure 7
Left dentary of Arkhane in lateral (**A**) and medial (**B**) views.

***Angular*:** The angular is an elongated and ventrally curved bone that forms, in lateral view, the caudal part of the ventral margin of the mandible (Figure 8). Rostally, its dorsal border participates in the ventral margin of the external mandibular fenestra, then it overlaps the ventral border of the surangular. It extends caudally under the articular, ending short of the caudal end of the mandible, as also observed in *Allosaurus fragilis*, *Allosaurus 'jimmadseni'* (Chure 2000), *Cryolophosaurus* (Hammer and Hickerson 1994), and *Monolophosaurus* (Zhao and Currie 1993). At all, the angular appears more slender than in *Allosaurus fragilis*, forming less than one quarter of the total height of the caudal aspect on the mandible.

***Splenial*:** The splenial is too incompletely preserved to be adequately described.

***Prearticular*:** The prearticular is a large bowlike element that forms most of the median part of the caudal half of the mandible (Figure 8). It is ventrodorsally elevated along its caudal portion, where it covers the articular and the antarticular. Its dorsal border is thickened and regularly concave, forming the ventral margin of the adductor fossa. Rostrally, it forms a large triangular spur between the splenial, ventrally, and the coronoid, dorsally. Unlike in *Allosaurus fragilis* and *Allosaurus 'jimmadseni'*, there is no trace of an internal mandibular foramen along the rostroventral margin of the prearticular; this foramen is absent in other allosauroids described so far and was therefore regarded as a synapomorphy for *Allosaurus* by Chure (2000). The prearticular has a narrow lateral exposure along the caudal end of the mandible, as also observed in *Acrocanthosaurus* (Chure 2000), *Sinraptor dongi* (Currie and Zhao 1993), and *Yangchuanosaurus magnus* (Dong et al. 1983). It does not have a lateral exposure at all in *Allosaurus fragilis*, *Allosaurus 'jimmadseni'*, *Cryolophosaurus*, *Sinraptor hepingensis*, and *Yanchuanosaurus shangyuensis* (Chure 2000).

***Coronoid*:** The coronoid is an elongated bone that forms the rostrodorsal margin of the adductor fossa (Figure 8). It is deflected ventrally and overlapped by a ventral flange from the medial side of the surangular at the level of the rostral end of the adductor fossa. Rostrally, it is inserted between the surangular and the prearticular. The coronoid of *Allosaurus fragilis* and *Allosaurus 'jimmadseni'* appear much higher rostrally and triangular in medial view (Madsen 1976b; Chure 2000).

***Articular*:** The articular is squeezed between the surangular and the prearticular rostrally (Figure 8). Dorsolaterally, the articular and surangular contribute equally to form the lateral glenoid fossa, as also observed in *Allosaurus fragils* (Madsen 1976b).

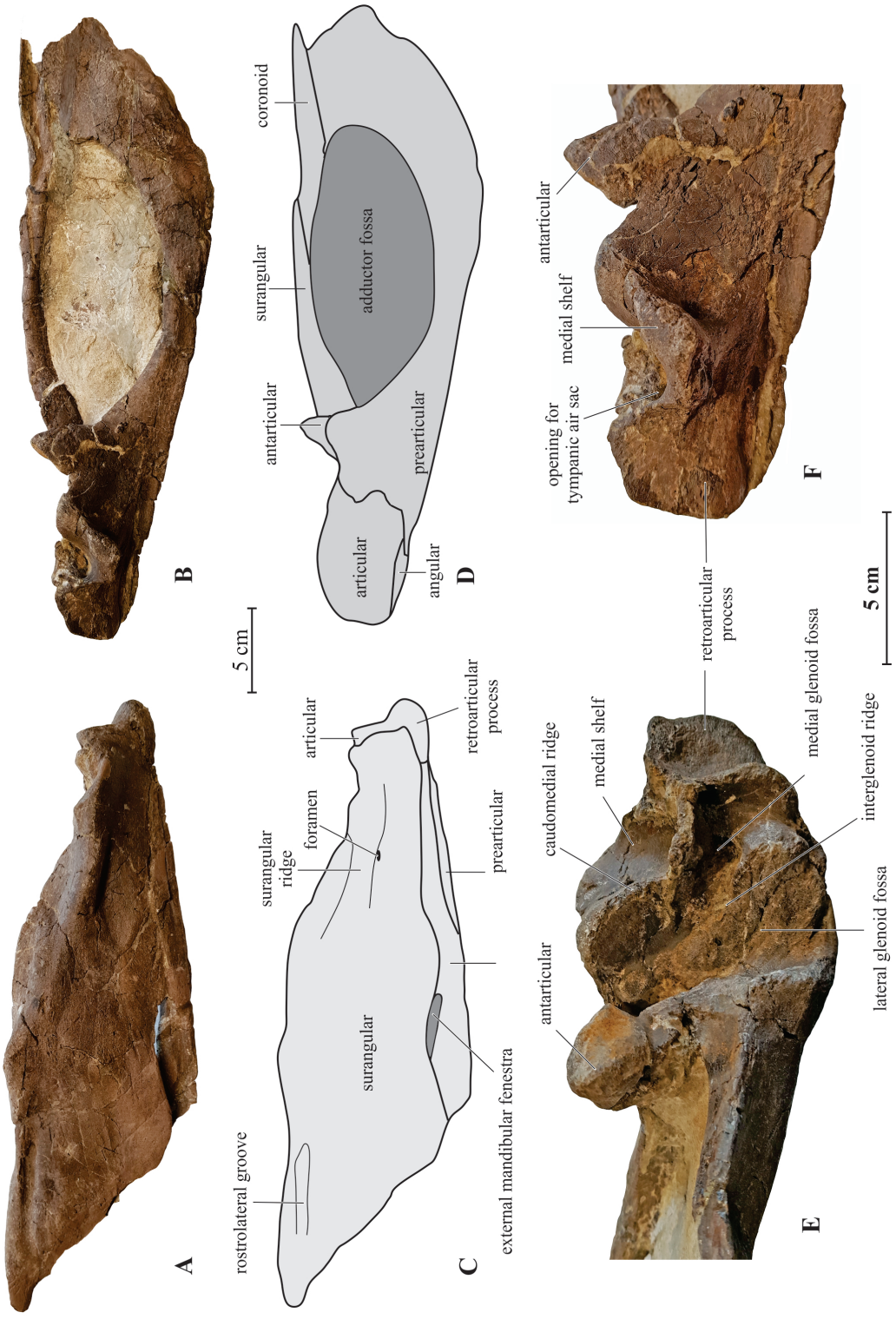

Figure 8

Photographs (**A**-**B**) and interpretative drawings (**C**-**D**) of left postdentary bones of Arkhane in lateral (**A**, **C**) and medial (**B**, **D**) views. Details of the left mandibular glenoid region in dorsal (**E**) and medial (**F**) views.

The interglenoid ridge is oblique (rostromedial-caudolateral). The medial glenoid fossa is narrower, but deeper than the lateral one and separated from the retroarticular process by a high and sharp ridge. The retroarticular process is mediolaterally broadened; it appears more robust than in *Allosaurus fragilis* and is directed caudally, although it is rather oriented caudomedially from the medial glenoid in *Allosaurus fragilis* (Currie and Zhao 1993). The caudal end of the retroarticular process is flexed ventrally, so that the attachment area for *M. depressor mandibulae* faces caudodorsally. Between the antarticular and the retroarticular process, the articular forms a high, sharp and sinuous caudomedian ridge, absent in *Allosaurus*. Medially to this ridge the median part of the articular is expanded into a wide medial shelf that slopes medioventrally; its dorsal surface is deeply excavated, marking the insertion area for *M. depressor madibulae*, whereas its thickened medial edge likely marks the insertion of the retroarticular aponeurosis of *M. pterygoideus posterior* (Chure 2000). A foramen enters rostrolaterally in the wall of this medial shelf. This opening presumably carried a diverticulum of the tympanic air sac into the hollow core of the articular (Molnar 1991; Currie 2003). This pendant medial shelf of the articular is also particularly prominent in *Allosaurus 'jimmandseni'*, although it is distinctly more incipiently developed in *Allosaurus fragilis* (Madsen 1976b).

***Antarticular*:** A prominent antarticular, also identified in *Allosaurus fragilis* and *Bagaraatan* (Madsen 1976b; Osmólska 1996), is present between the articular, prearticular, and surangular; it may have acted as a strop to prevent caudal disarticulation of the jaw joint (Madsen 1976b; Holtz 2004). It is apparently even more prominent than in *Allosaurus fragilis*.

Axial skeleton

Atlas

The atlas is complete with the exception of the tip of its posterior process, which has been reconstructed (Figure 9). Laterally, the concave cranial surface of the intercentrum for the articulation of the occipital condyle is craniodorsally directed at an angle of 45° to the craniocaudal of the axis as in *Allosaurus fragilis* (Gilmore 1920). This facet is not as concave as in *Sinraptor dongi*, *Ceratosaurus*, and *Torvosaurus* (Currie and Zhao 1993). As in *Allosaurus fragilis*, the intercentrum of Arkhane can be distinguished from that of *Ceratosaurus* in being craniocaudally, shorter with its cranial and caudal sides nearly parallel when viewed laterally (Gilmore 1920). Unlike *Allosaurus fragilis* but like *Sinraptor dongi*, *Carnotaurus*, and *Torvosaurus*, a slight distinct ventrolateral

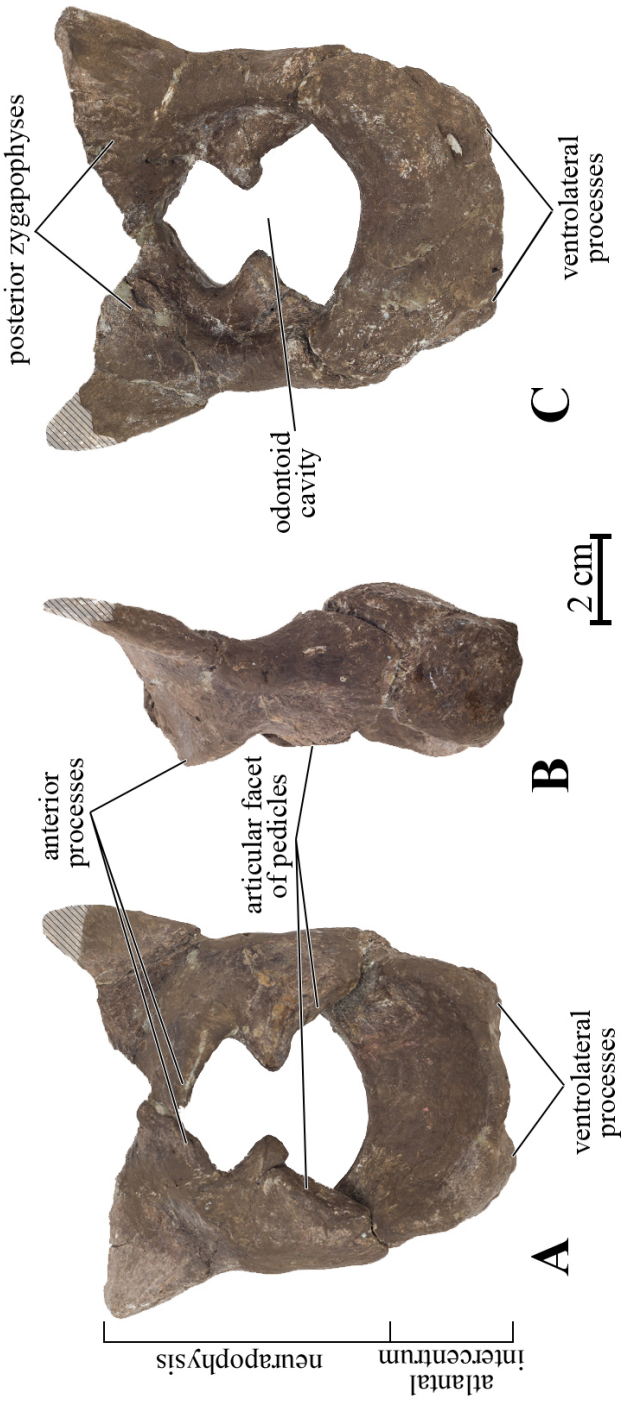

Figure 9
Atlas of Arkhane in cranial (**A**), left lateral (**B**), and posterior (**C**) views. Hatched region corresponds to a reconstructed area.

process is present on each side of the atlantal intercentrum (Bonaparte et al. 1990; Britt 1991; Currie and Zhao 1993). The neurapophysis is completely fused to the atlantal intercentrum although a suture line is still visible by X-Ray (Figure 10). The neurapophysis of Arkhane differs from that of *Ceratosaurus* and *Sinraptor dongi* in being more expanded transversally at the level of the articular facet of the pedicle and craniodorsally shorter (Gilmore 1920; Currie and Zhao 1993). In being more triangular, the neurapophysis of Arkhane resembles that of *Allosaurus fragilis* and more advanced Tetanurae (Currie and Zhao 1993). As in *Sinraptor dongi*, there is no prezygapophysis on the anterior side of the neurapophysis, indicating that there was no proatlas (Currie and Zhao 1993). Unlike *Ceratosaurus*, the posterior zygapophyses are more dorsally located on the caudal side of the caudal process of the neurapophysis. As in *Allosaurus fragilis* and *Ceratosaurus*, the vertical concave surfaces at the cranial side of the pedicle contribute to the formation of the cup for the occipital condyle (Gilmore 1920). Above these articular surfaces, and as in *Allosaurus fragilis*, the neurapophysis widens into a thin, mesially-directed plate (i.e. the cranial process) that joins the opposite side in order to form the covering for the neural arch throught which the spinal cord passes from the foramen magnum (Gilmore 1920; Madsen 1976b).

Axis

Only the cranial half of the axis is preserved, together with the distal portion of the right postzygapophysis (Figure 11). Only the central portion of the axial intercentrum is preserved. The remnant intercentrum is circular in cranial view and firmly attached to the centrum as in *Allosaurus 'jimmadseni'* (Chure 2000). As the intercentrum is not complete, it is impossible to know whether the axial intercentrum is rotated dorsally to bring the vertebral column up under the occipital condyle as in *Allosaurus 'jimmadseni'*, *Sinraptor dongi*, *Monolophosaurus*, and *Yangchuanosaurus* (Currie and Zhao 1993; Chure 2000). The odontoid is fused to the axis as in *Ceratosaurus* (Chure 2000), whereas it is unfused to the centrum and the intercentrum in *Allosaurus fragilis* and *Allosaurus 'jimmadseni'* (Chure 2000). Although the odontoid is deformed, it is largely reniform in outline when viewed cranially, as in *Allosaurus fragilis*, *Yangchuanosaurus*, *Piatnizkysaurus*, *Acrocanthosaurus* and *Ceratosaurus* (Gilmore 1920; Madsen 1976b; Chure 2000; Madsen and Welles 2000), whereas it is tall and narrow in *Allosaurus 'jimmadseni'* (Chure 2000). In contrast to *Acrocanthosaurus* but similar to *Allosaurus 'jimmadseni'*, the odontoid process is apneumatic (Chure 2000). As in *Allosaurus fragilis* and *Ceratosaurus*, the upper surface of the odontoid is concave from side to side in Arkhane (Gilmore 1920). As in *Allosaurus fragilis*, the cranial surface of the

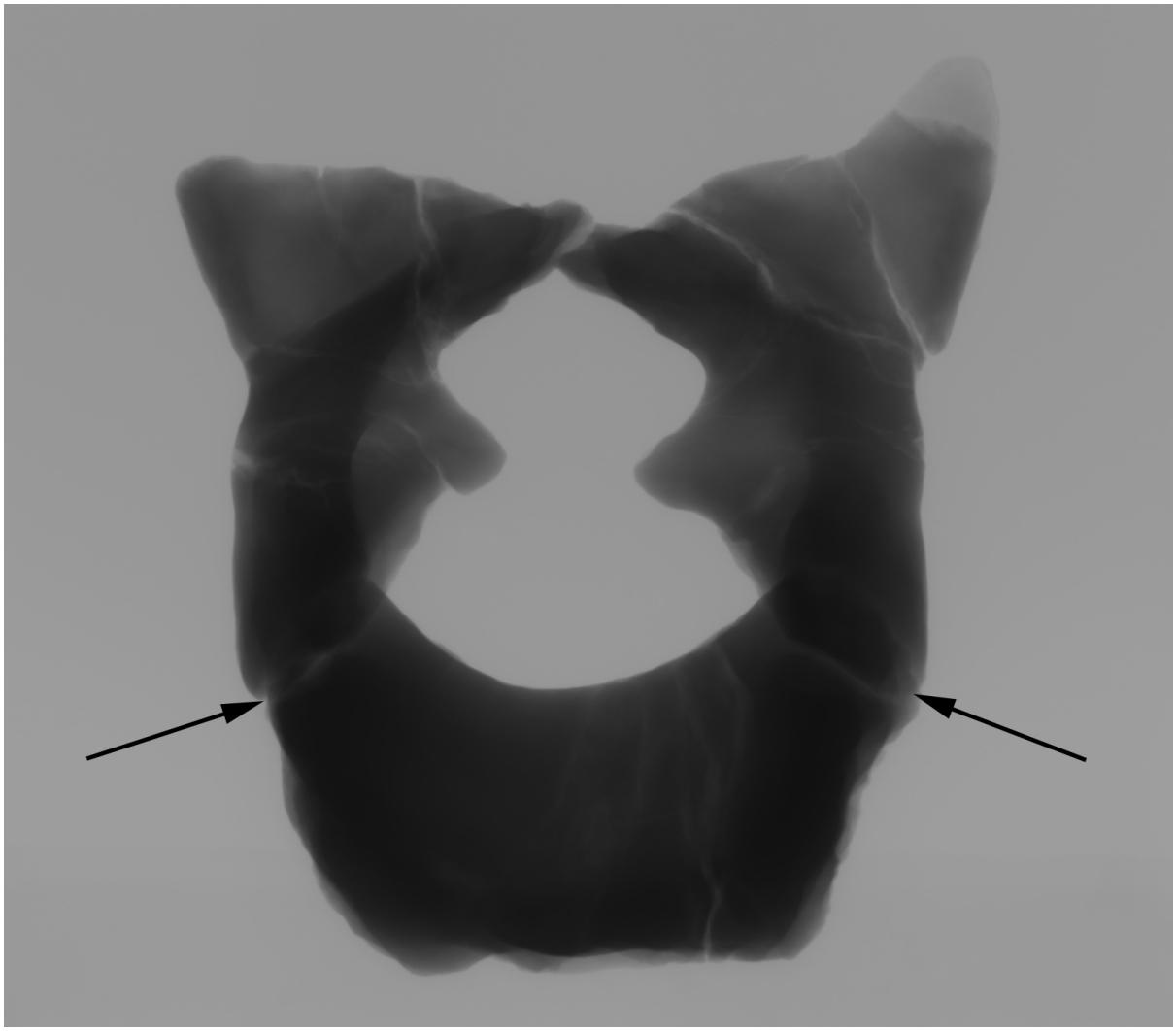

Figure 10
Atlas of Arkhane in RX view. Arrows point to the suture between atlantal intercentrum and neurapophyses.

odontoid shows a subcircular depression (Gilmore 1920). The axial intercentrum is firmly attached to the axial centrum as in *Sinraptor dongi* (Currie and Zhao 1993). As in *Allosaurus fragilis*, the ventral surface of the axis is smooth without keel and a small elongated opening toward the back is preserved on the right side of the vertebra (Gilmore 1920). As in *Sinraptor dongi*, there is a pleurocoel near the craniodorsal contact between the intercentrum and the centrum (Currie and Zhao 1993). The preserved portion of the right postzygapophysis forms a large subcircular articular facet directed downward and slightly outward, as in *Allosaurus fragilis* (Gilmore 1920). However because of the preservation, it is impossible to know whether there is an epipophysis close to the postzygapophyses as in *Allosaurus fragilis* (Madsen 1976b). The ventral border of the hypocentrum is rounded from side to side beneath the insertion of the odontoid. The articular facet that underlaps the articular end of the atlas intercentrum is concave as in *Allosaurus fragilis* (Gilmore 1920). The parapophysis of Arkhane more closely resembles that of *Ceratosaurus* than that of *Allosaurus fragilis* in being very low on the lateral side of the vertebra (Gilmore 1920; Madsen and Welles 2000).

3rd to 9th cervical vertebrae

The rest of the cervical column is partially preserved. Only a right part of the centrum is preserved for the fourth, the fifth, the sixth, and the eighth cervicals. The seventh one is only known by the distal tip of the right diapophysis while the ninth cervical completely preserves this anatomical region. The only neural spine preserved among the cervical column belongs to the eighth cervical (Figure 12).

The ventral surface of the centrum of the fourth, the fifth, and the sixth cervicals is smoothly rounded as reported also in *Allosaurus fragilis* and *Allosaurus 'jimmadseni'* (Gilmore 1920; Currie and Zhao 1993). In contrast to *Allosaurus 'jimmadseni'*, no hypapophysis is present on the fourth cervical of Arkhane (Currie and Zhao 1993). However, the presumed eighth cervical shows a smooth ventral keel along the ventral surface of the centrum, unlike in *Allosaurus fragilis*, in which only the third cervical is keeled (Gilmore 1920). All preserved centra show a wide-cupped caudal articular surface as in *Allosaurus fragilis*, *Allosaurus 'jimmadseni'*, and *Sinraptor dongi* (Gilmore 1920; Currie and Zhao 1993; Chure 2000) and only the fourth, the fifth, and the eighth centra can be clearly defined as opisthocoelus as in *Allosaurus fragilis*, *Allosaurus 'jimmadseni'*, *Saurophaganax*, and *Sinraptor dongi* (Gilmore 1920; Madsen 1976b; Currie and Zhao 1993; Chure 1995). As in the latter species, the cranial articular facets are cranioventrally oriented, whereas the caudal ones are craniodorsally inclined to the longer axis of the

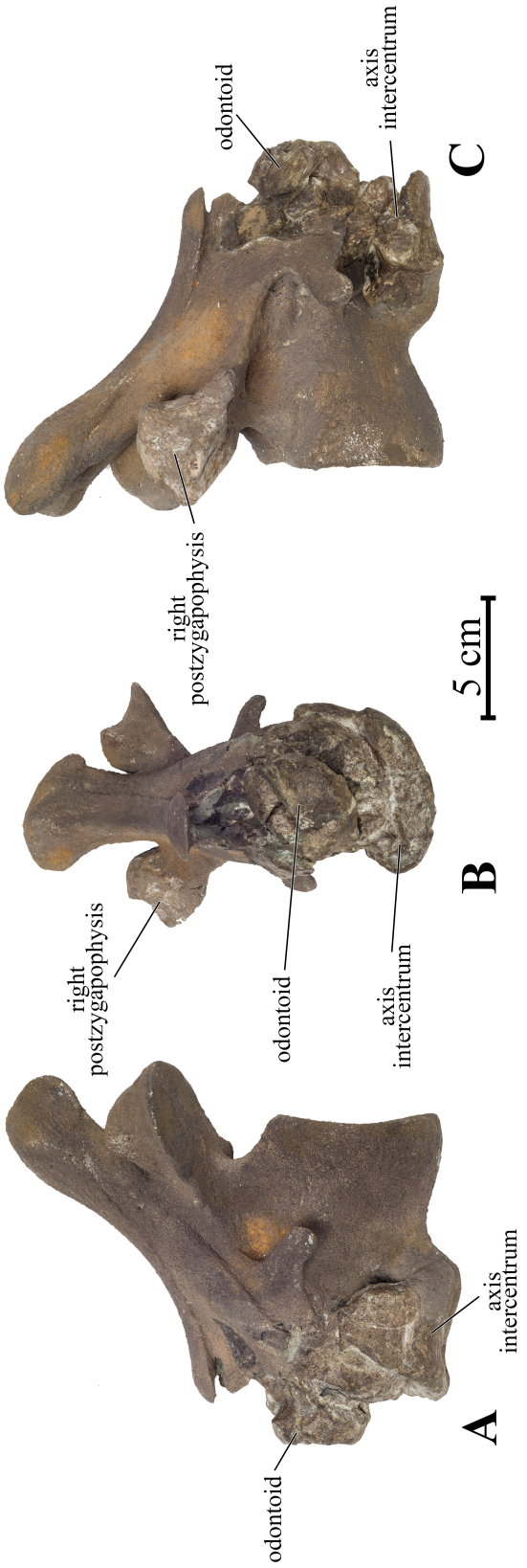

Figure 11
Axis of Arkhane in left lateral (**A**), cranial (**B**), and right lateral (**C**) views.

Dorsal vertebrae

Fourteen dorsal vertebrae are reported in *Allosaurus fragilis* (Madsen 1976b). Considering the state of preservation of Arkhane, the total number of dorsal vertebrae cannot be determined. Only the cranial four vertebrae and the eighth one are almost completely preserved, whereas only fragments of the neural spine are present in the eleventh, the twelfth, and the thirteenth dorsal vertebrae (Figure 13).

***First dorsal*:** As in *Allosaurus fragilis*, *Allosaurus 'jimmadseni'*, and *Saurophaganax*, the first dorsal is marked by a transfer of the parapophysis from a low to an higher position on the lateral side of the centrum and the transition of an opisthocoelus centrum to a more amphiplatyan type, whereas the first dorsal of *Sinraptor dongi* clearly remains opisthocoelus (Gilmore 1920; Madsen 1976b; Currie and Zhao 1993; Chure 1995; Chure 2000). Contrary to Saurophaganax, no deep elliptical depressions are present just below the contact between the centrum and the neural arch in none of the dorsals (Chure 1995). The caudal part of the ventral surface is more ventrally located when compared to the ventral region of the eighth cervical vertebra. There is weak keel along the ventral surface of the centrum and a spur-like anterior projection as in *Allosaurus fragilis* and *Allosaurus 'jimmadseni'* (Madsen 1976b; Chure 2000). As in *Allosaurus fragilis*, the median portion of the centrum is more pinched than on the cervical vertebrae (Gilmore 1920). Caudal to the parapophysis, there is an oval pit on each side of the vertebra that likely leads into chambers inside the centrum, as also observed in *Allosaurus fragilis* and *Allosaurus 'jimmadseni'* (Chure 2000).

***Second dorsal*:** The centrum is much more amphiplatyan than the first dorsal, with completely flattened cranial articular surface, unlike in *Allosaurus fragilis* (Currie and Zhao 1993). The ventral border of the caudal articular surface is less lowered compared to the first dorsal. Although the right parapophysis is not completely preserved, the diameter of the parapophyses is larger than that of the first dorsal, as also described in *Allosaurus 'jimmadseni'* (Chure 2000). The upper edge of each parapophysis reaches the neurocentral suture as in *Allosaurus fragilis* (Gilmore 1920). Pleurocoels are absent on both side of the second dorsal, unlike in *Allosaurus fragilis*, in which pneumatization reaches the third dorsal vertebra (Gilmore 1920). The ventral surface of the centrum bears a much more pinched ventral keel, which widens out toward the front as in *Allosaurus fragilis* (Gilmore 1920). As in *Allosaurus 'jimmadseni'*, a hypapophysis is present along the ventral margin of the vertebra (Chure 2000).

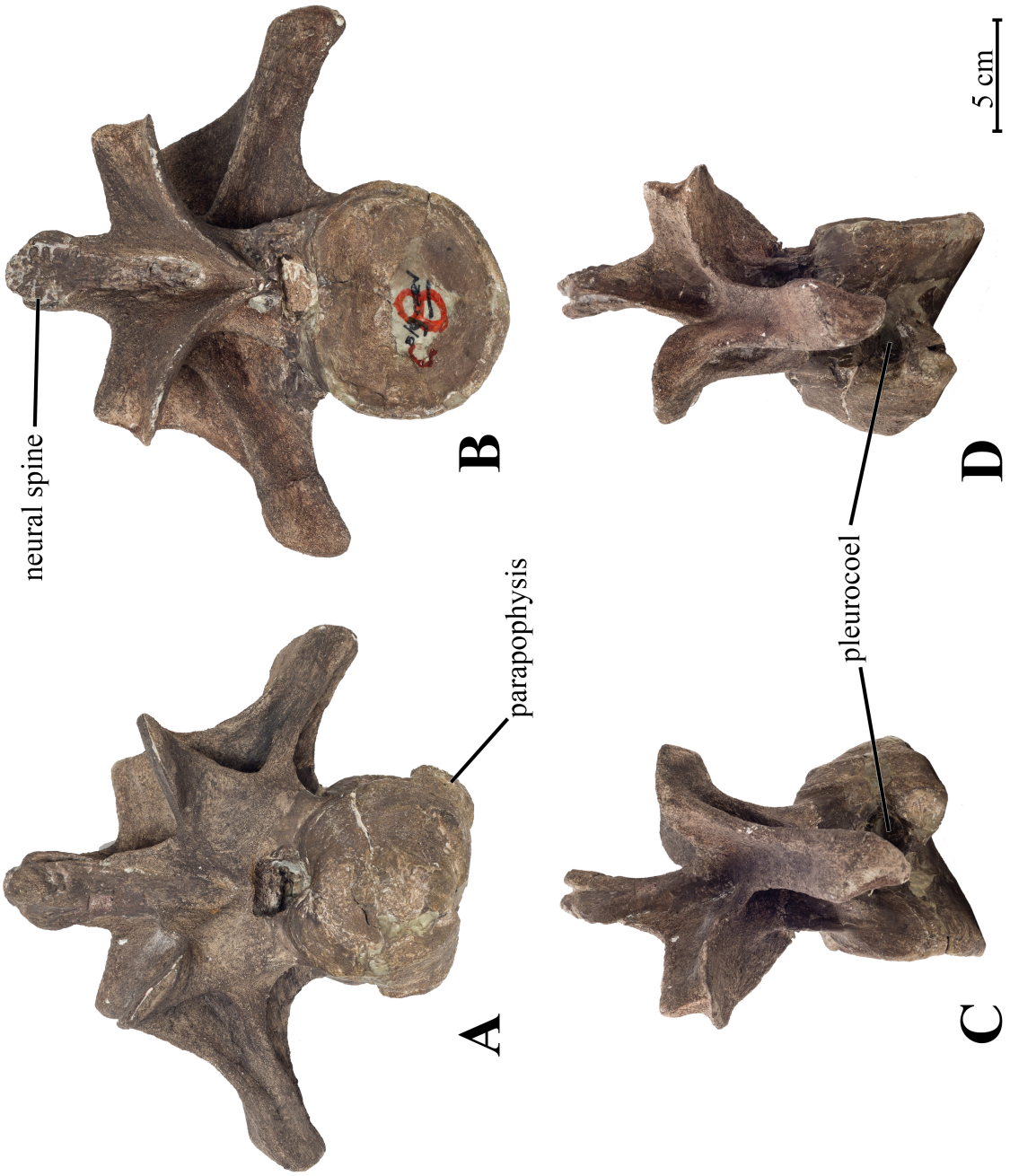

Figure 12
Eighth cervical vertebrae of Arkhane in cranial (**A**), caudal (**B**), right lateral (**C**), and left lateral (**D**) views.

Although the diapophyses are not completely preserved, they are dorsally elevated with an angle exceeding 90° with the ventrodorsal axis of the vertebra as in *Allosaurus fragilis* (Gilmore 1920). As in *Allosaurus 'jimmadseni'*, the neural arch in lateral view extends over three-quarters on the centrum (Chure 2000). The infraprediapophysial, infradiapophysial, and infrapostdiapophysial fossa are present as in *Allosaurus fragilis* and *Allosaurus 'jimmadseni'* (Gilmore 1920; Chure 2000).

***Third dorsal*:** The caudal surface of the centrum is only slightly cupped and the cranial one is flat as in *Allosaurus fragilis* (Madsen 1976b). The ventral borders of both articular surfaces reach the same level when viewed laterally. The ventral keel is sharp and, as in the two preceding vertebrae, is separated from the cranial articular surface by a shallow transverse groove that is also reported in *Allosaurus fragilis* (Gilmore 1920). Contrary to *Allosaurus fragilis*, there is no pleurocoel on the lateral sides of the centrum (Gilmore 1920; Madsen 1976b). As in *Allosaurus fragilis*, the neural arch of the third dorsal is relatively low and craniocaudally shorter than the centrum (Gilmore 1920). A deep cavity located back to the prezygapophyses lightens the vertebra as in *Allosaurus fragilis* (Gilmore 1920). The prezygapophyses project slighlty beyond the cranial articular surface as in *Allosaurus fragilis* (Gilmore 1920). Because of their respective deformation, it is impossible to know whether the prezygapophyses are medialo-dorsaly oriented as in *Allosaurus fragilis* (Gilmore 1920). As in *Allosaurus 'jimmadseni'*, the transverse process extends more dorsally than in the previous dorsal vertebrae (Chure 2000).

***Fourth dorsal*:** When compared to the second and the third dorsal vertebrae, the fourth dorsal differs by stouter spinous and transverse processes, with a more elevated position as in *Allosaurus fragilis* (Gilmore 1920). The dorsal margin of the middle part of the parapophysis is located on pedicles as in *Allosaurus 'jimmadseni'* (Chure 2000). Unlike in *Saurophaganax*, there is no horizontal lamina along the base of each side of the neural spine (Chure 1995). As also observed on the third dorsal, the prezygapophyses are projected cranially beyond the cranial articular surface of the centrum and they are mediodorsally oriented as in *Allosaurus fragilis* (Gilmore 1920). Starting from the fourth dorsal, the ventral keel begins to be poorly defined as in *Allosaurus fragilis* (Madsen 1976b). In contrast to *Allosaurus 'jimmadseni'*, the ventral surface of this dorsal centrum is still slighlty pinched (Chure 2000). The transverse processes are supported by a single infradiapophysial laminae instead of two converging laminae in *Allosaurus fragilis* and *Allosaurus 'jimmadseni'* (Gilmore 1920; Madsen 1976b; Chure 2000). No lateral pit are present on both side of the centrum, unlike in *Allosaurus fragilis* (Gilmore 1920; Madsen 1976b). As in *Allosaurus 'jimmadseni'*, the neural spine is inclined caudally and extends

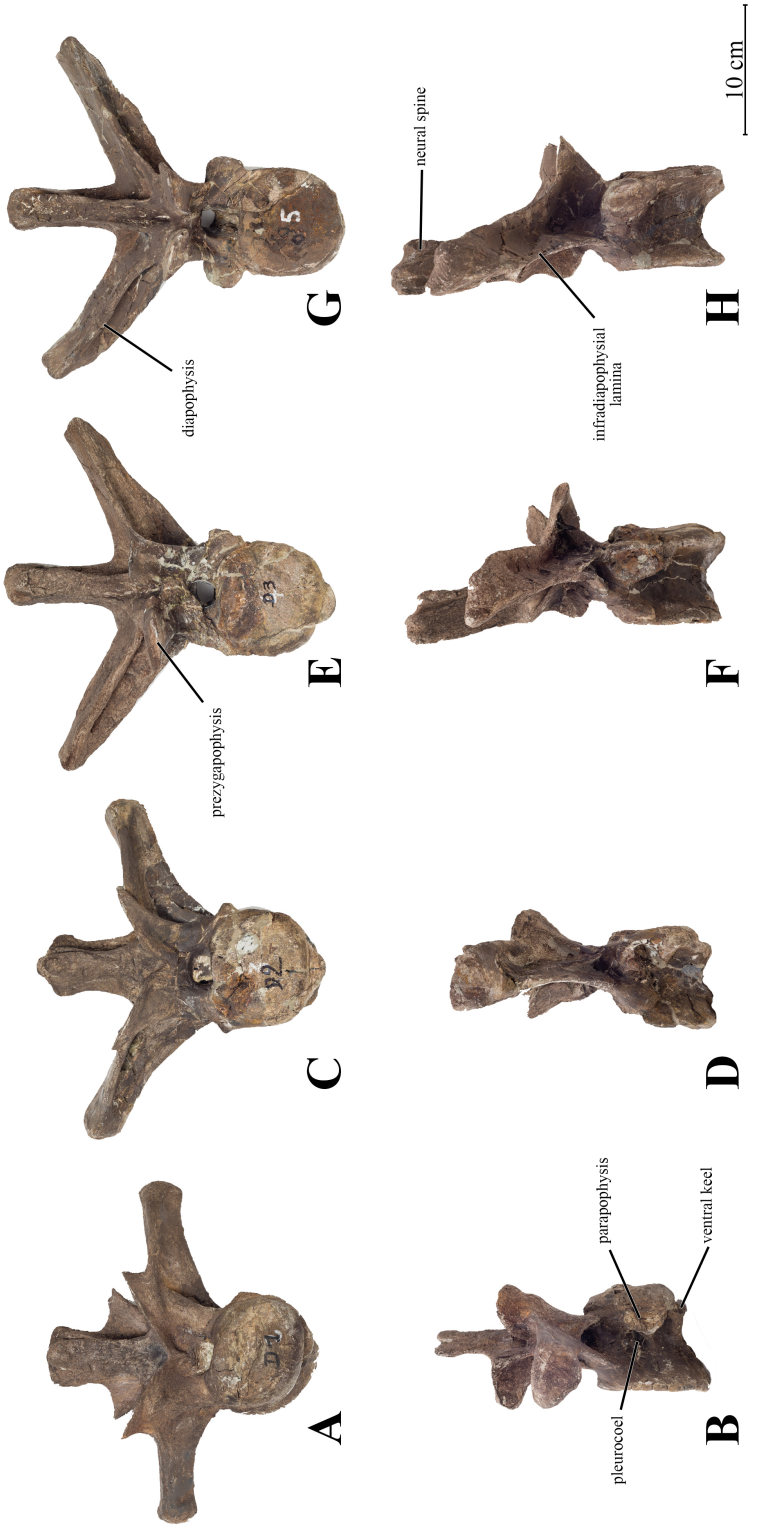

Figure 13

First four dorsal vertebrae of Arkhane. First dorsal (**A,B**) in cranial (**A**) and right lateral (**B**) views. Second dorsal (**C,D**) in cranial (**C**) and right lateral (**D**) views. Third dorsal (**E,F**) in cranial (**E**) and right lateral (**F**) views. Fourth dorsal (**G,H**) in cranial (**G**) and right lateral (**H**) views.

beyond the caudal articular surface of the centrum (Chure 2000). The neural spines of the first four dorsal vertebrae are not as wide craniocaudally than those of *Sinraptor dongi* (Currie and Zhao 1993).

***Eighth dorsal*:** The eighth dorsal is larger than the preceding ones. The ventral side of the centrum is pinched, whereas this area is rounded in *Allosaurus 'jimmadseni'* (Chure 2000). The ventrolateral sides of the centrum are deeply excavated as in *Allosaurus fragilis* (Gilmore 1920). No pleurocoel are present in Arkhane as in *Allosaurus fragilis* and *Allosaurus 'jimmadseni'* (Gilmore 1920; Chure 2000). As in *Allosaurus fragilis*, the cranial articular surface is slightly concave (Gilmore 1920) and the cupped parapophyses occupy the median side of the cranial pedicle of the neural arch (Gilmore 1920; Madsen 1976b). The prezygapophyses are oriented dorsally and slightly medially. The postzygapophyses are separated by a thin zygosphene as in *Allosaurus fragilis* (Gilmore 1920; Madsen 1976b). As in *Sinraptor dongi*, a hypoposphene-hypantrum articulation is present throughout the dorsal series (it is at least present on the eighth dorsal in Arkhane), whereas this articulation is restricted to the first five dorsals in *Allosaurus fragilis* (Chure 2000). The neural spine is large and robust with a significant increase in height as in *Allosaurus fragilis* (Gilmore 1920), unlike in *Sinraptor dongi*, in which the neural spine is comparatively wider in lateral view (Currie and Zhao 1993).

***Tenth, eleventh, and twelfth dorsals*:** Only the distal end of the neural spine is preserved in these vertebrae. They are large and robust and gradually increase in height as in *Allosaurus fragilis* (Gilmore 1920; Madsen 1976b), whereas they are shorter and more quadrangular in lateral view in *Sinraptor dongi* (Currie and Zhao 1993). The cranial and caudal surfaces are roughened for ligamentous attachment. As in *Allosaurus fragilis*, *Gorgosaurus*, and *Tyrannosaurus*, the upper median portion of the spines extends cranially and slightly caudally (Gilmore 1920).

Caudal vertebrae

Only the region between the sixteenth and the twenty-ninth caudal vertebrae is almost completely preserved and articulated. On the proximal portion of the tail, only the second, fifth, seventh, tenth, twelfth and fourteenth caudals are preserved, although they are partly reconstructed. The distal portion of the tail is not preserved in Arkhane.

The centra of the proximal caudals are heavy, stout, and higher than long as in *Allosaurus fragilis* and *Allosaurus 'jimmadseni'* (Gilmore 1920; Chure 2000) (Figure 14).

They are amphiplatyan as in *Allosaurus fragilis* whereas they are reported as moderately procoelus in *Saurophaganax* (Madsen 1976b; Chure 1995). The caudal articular facet is not higher than the cranial one unlike in *Sinraptor dongi* (Currie and Zhao 1993). Unlike in *Allosaurus fragilis* but as in *Allosaurus 'jimmadseni'*, *Sinraptor dongi*, and *Ceratosaurus*, the ventral surface of the caudal centra is longitudinally grooved along the caudal serie (Gilmore 1920; Currie and Zhao 1993; Chure 2000; Madsen and Welles 2000). The articular facets are slightly biconcave but the concavity is much more pronounced on the cranial facet than on the caudal one, as in *Allosaurus fragilis* (Gilmore 1920). The ventral side of both articular facets is beveled for the articulation with the chevron as in *Allosaurus 'jimmadseni'* and *Sinraptor dongi* (Currie and Zhao 1993; Chure 2000). As in *Allosaurus fragilis*, the transverse processes of the anterior caudals are attached on the side of the neural arch and are caudodorsally oriented (Gilmore 1920). They are thick at their point of attachement and become plate-like at their distal end. In dorsal view, the distal end of the transverse process is squared as in *Allosaurus fragilis* (Gilmore 1920). The neural spines of the anterior vertebrae are wide at their base and become narrower at their very distal end, where the spine widens transversely. The neural spine of Arkhane differs from that of *Allosaurus 'jimmadseni'* in being bifid cranially, as also observed in *Allosaurus fragilis* (Chure 2000). The neural spines are strongly inclined caudally, with their distal end overhanging the caudal articular surface of the centra as in *Allosaurus fragilis* (Gilmore 1920). As in *Allosaurus 'jimmadseni'*, the transverse processes of the proximal caudals are long, rise slightly dorsolaterally, and their wide distal ends have striated dorsal and ventral surfaces (Chure 2000).

In the mid-portion of the tail, the centra become cylindrical and longer than high (Figure 15). As in *Allosaurus fragilis*, the mid-caudal centra are concave laterally and ventrally (Gilmore 1920). The neural spines become smaller compared to the height of their corresponding centrum and they become quickly reduced to a short thin plate of bone without a distal expansion. There is a drastic reduction in the size of the neural spine between the eighteenth and the nineteenth caudal vertebrae, where the neural spine is reduced to a small plate of bone inserted between the postzygapophyses. The complete disappearance of the neural spine occurs between the twenty-fourth and the twenty-fifth caudal vertebrae, unlike in *Ceratosaurus*, in which the neural spine disappears on the thirty-first caudal vertebra (Gilmore 1920). The transverse processes in the mid-portion of the tail are reduced in size and are set at mid-height of the centrum as in *Allosaurus fragilis* (Gilmore 1920). This process completely disappears at the level of the tweenty-third caudal vertebra. From the twentieth vertebra, the prezygapophyses extend far beyond the cranial articular surface. Their articular faces are directly medially oriented with widely expanded ends as in *Allosaurus fragilis* (Gilmore 1920).

Figure 14
Seventh caudal vertebra of Arkhane in cranial (**A**) and left lateral (**B**) views.

Chevrons

Twenty-three chevrons (= haemal arches) are partially preserved in Arkhane (Figure 16). Cranially, the chevrons are long and blade-like with a slight caudoventral curve as in *Allosaurus fragilis* and *Allosaurus 'jimmadseni'* (Chure 2000). The proximal chevrons of Arkhane can be distinguished from those of *Ceratosaurus* by their greatly expanded articular proximal ends and their craniocaudally wider shaft, with a more curved lateral profile (Gilmore 1920). They become shorter and more curved towards the distal end of the tail, with the distal elements being more laterally compressed and hook-like as in *Allosaurus fragilis* and *Allosaurus 'jimmadseni'* (Chure 2000). Unlike in *Saurophaganax*, the distal end of the mid and distal chevrons are not craniocaudally enlarged (Chure 1995). As in *Allosaurus fragilis* and *Allosaurus 'jimmadseni'*, the cranial processes at the proximal end of each chevron are well developed (Madsen 1976b). As in *Allosaurus fragilis*, the cranial processes joined together by bone above the haemal arch (Gilmore 1920).

Ribs

No cervical and sacral ribs are preserved in Arkhane.

Almost all dorsal ribs are preserved in Arkhane although the distal ends are frequently missing as reported by Madsen (1976b) in *Allosaurus fragilis* and *Allosaurus 'jimmadseni'* (Figure 17). As in latter two species, the shaft of the dorsal ribs is curved ventromedially with the last dorsal ribs more rounded than the first ones (Madsen 1976b). The tuberculum and capitulum facets of the first dorsal ribs are wide apart and lie in the same plane with equal articular surfaces as in *Allosaurus fragilis* (Gilmore 1920). Caudally the ribs become shorter in length and more slender as in *Allosaurus fragilis* (Gilmore 1920). The tuberculum facet is pointing upward whereas the capitulum facet is raised up to an angle of 90°.

Appendicular skeleton

Scapula

The scapula and coracoid are not fused together. The scapula is particularly elongated (Figure 18), being 86% the length of the femur (77% in *Allosaurus fragilis* USNM 4734;

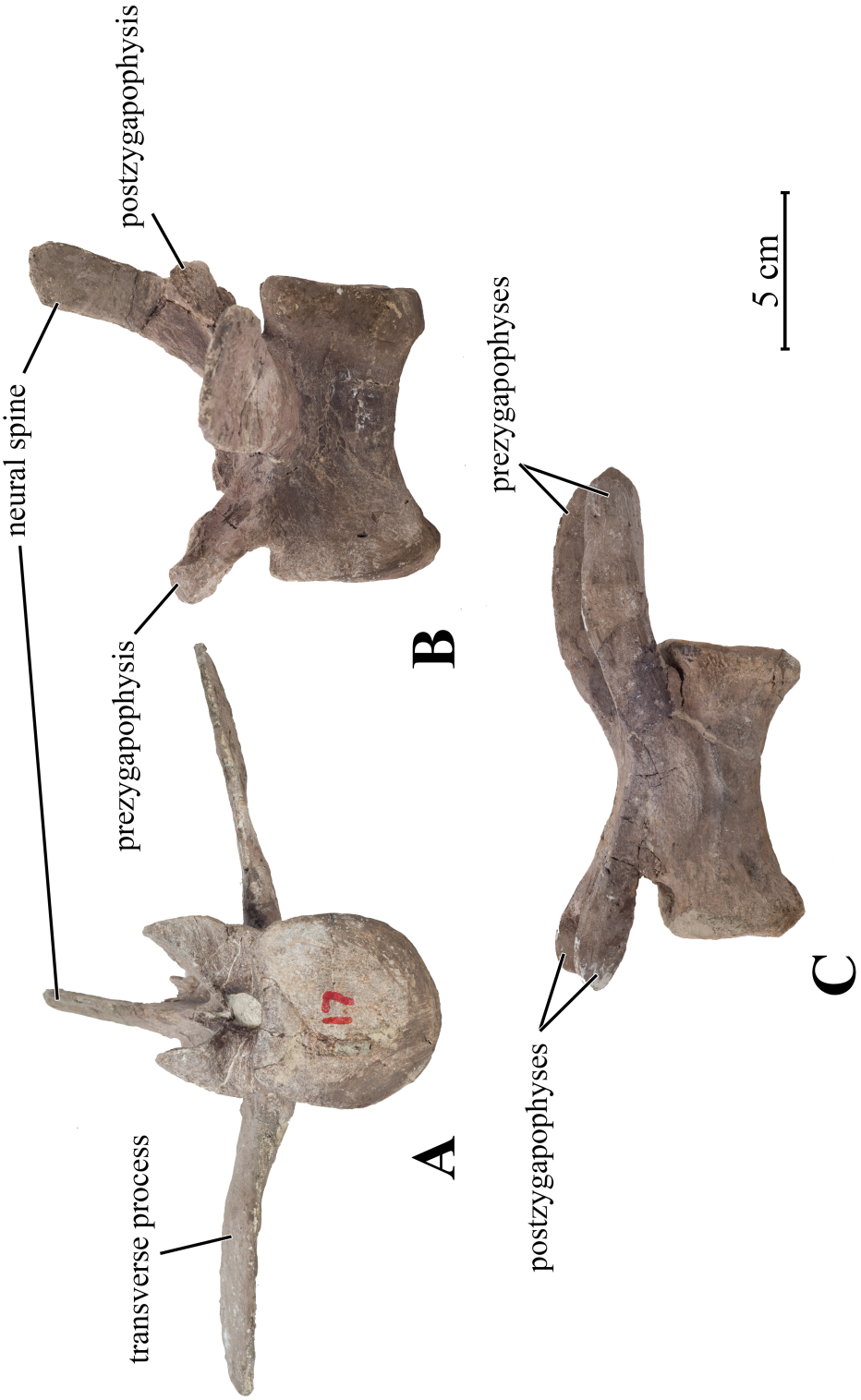

Figure 15
Seventeenth (**A**,**B**) and twenty-fifth (**C**) caudal vertebrae of Arkhane in cranial (**A**), left lateral (**B**), and right lateral (**C**) views.

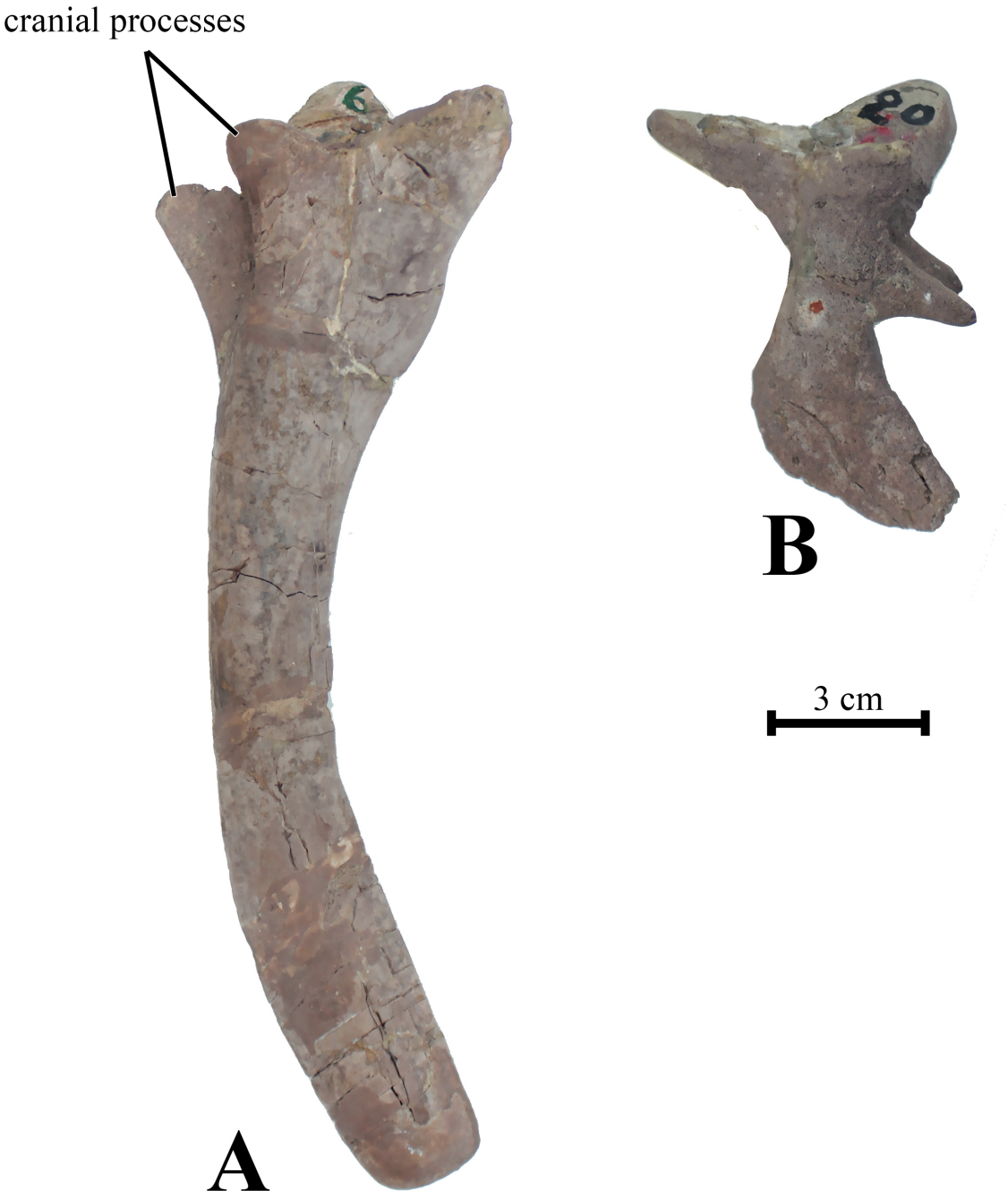

Figure 16
Cranial (**A**) and caudal (**B**) chevrons of Arkhane left lateral view.

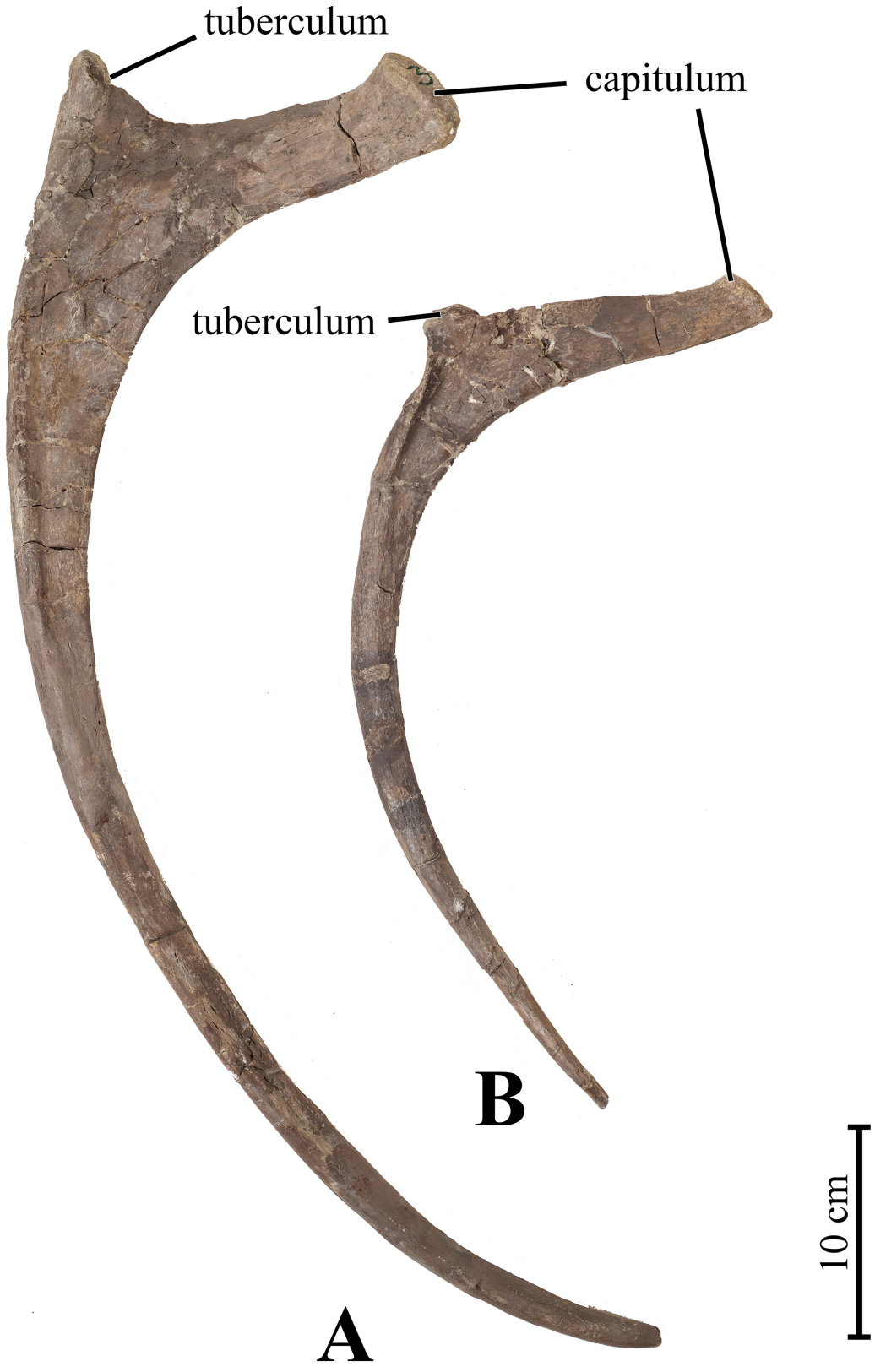

Figure 17
Cranial (**A**) and caudal (**B**) dorsal ribs of Arkhane in cranial view.

Gilmore (1920)). In ventral and dorsal view, it is regularly curved so that it perfectly followed the profile of the ribcage. The acromion is more sharply expanded, forming a 90° angle with the craniodorsal margin of the scapular blade, than in *Allosaurus fragilis* (Madsen 1976b), *Allosaurus 'jimmadseni'* (Chure 2000), *Acrocanthosaurus* (Currie and Carpenter 2000), and *Sinraptor dongi* (Currie and Zhao 1993). The glenoid is also sharply demarked from the rostroventral margin of the scapular blade. The coracoid facet and the glenoid form an angle of approximately 115°. A horizontal sulcus extends from the coracoid suture along the medial side of the proximal plate, as also observed in *Allosaurus fragilis* (Madsen 1976b) and *Neovenator* (Brusatte et al. 2008). Caudal to the proximal plate, the dorsal border of the scapula remains nearly straight, whereas the distal third of the scapula regularly expands ventrally; the distal portion of the scapular blade appears consequently more expanded in this specimen than in *Allosaurus fragilis* and *Allosaurus 'jimmadseni'*, although this character is too dependent from the preservation state of this fragile region of the skeleton to be really diagnostic.

Coracoid

Only the articular portion of the right coracoid is partly preserved (Figure **??**). As in *Allosaurus fragilis*, the coracoid is pierced by a foramen running diagonally trough the bone (Gilmore 1920). When articulated with the scapula it forms a wider glenoid facet than in *Allosaurus fragilis* (Gilmore 1920). As in *Allosaurus 'jimmadseni'* a biceps tubercule (= coracoid tuber) is well-developped on the lateral side of the coracoid (Madsen 1976b).

Furcula

The furcula of Arkhane has been mostly reconstructed but the RX photograph shows that the symphyseal region is mostly intact although only a small portion of each ramus is preserved (Figure 19). They are not anteroposteriorly compressed as in most tyrannosaurids and oviraptorosaurids (DePalma et al. 2015). The rami of the furcula meet at an angle of 138° (130° in *Allosaurus 'jimmadseni'*; Chure (2000)). There is no sign of a caudoventrally triangular projection, unlike in *Allosaurus 'jimmadseni'* where this projection is located at the symphyseal junction (=hypocleideum) (Chure 2000). As in *Allosaurus 'jimmadseni'*, the caudal surface of the rami bear a series of ridges (Chure 2000).

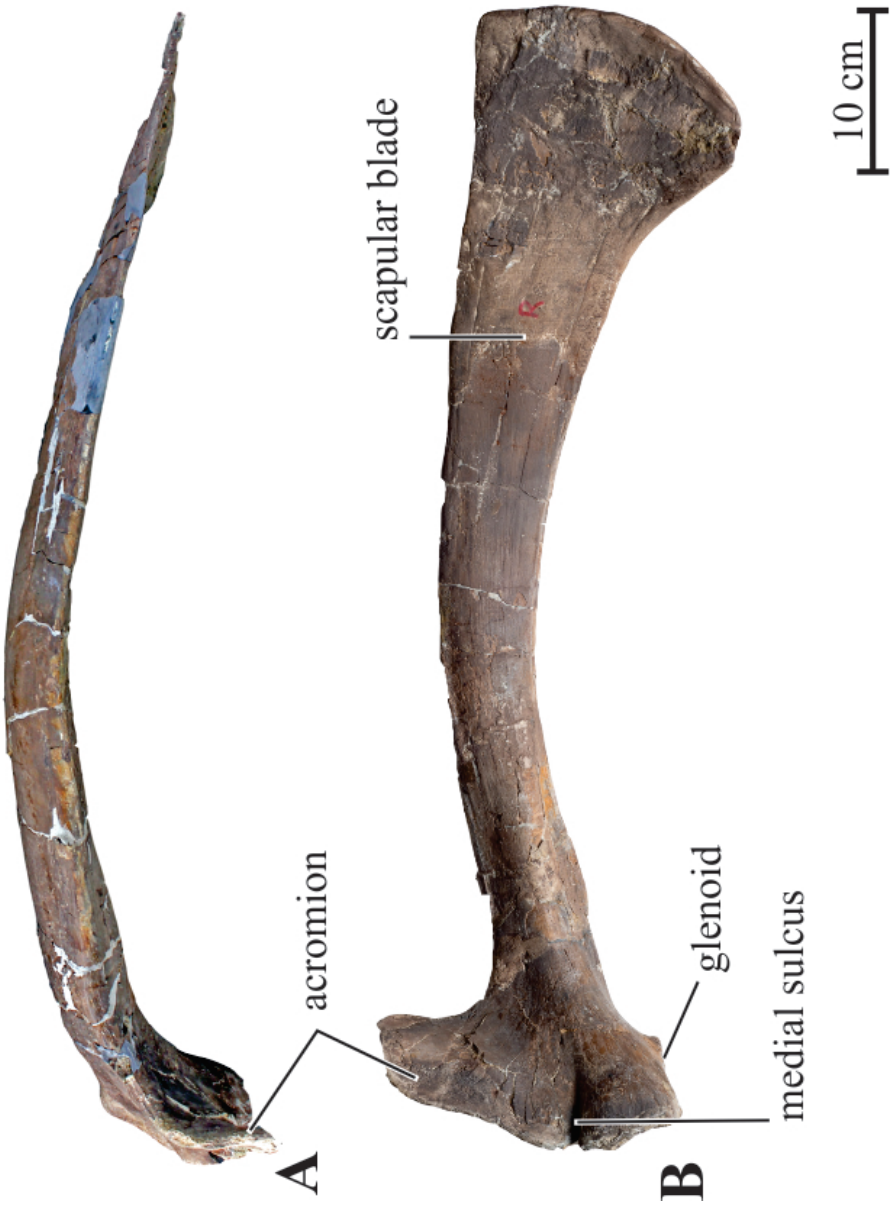

Figure 18
Left scapula of Arkhane in dorsal (**A**) and medial (**B**) views.

Figure 19
Furcula of Arkhane (**A**) and RX (**B**).

Humerus

Only the distal parts of both humeri are preserved, together with the proximalmost portion of the right one (Figure 20). This latter part is however poorly preserved, and the humeral head is flattened and deformed. In cranial view, the proximal surface is regularly convex. The distal end of the humerus is mediolaterally enlarged and craniocaudally compressed. The entocondyle is more salient distally than the ectocondyle. The ectepicondyle is particularly salient, whereas the entepicondyle is a thin crest. The cubital fossa is better developed than the olecranon fossa.

Ulna

The ulna closely resembles that of *Allosaurus fragilis* in being proportionally short and stocky (Figure 21). It is distinctly more gracile in *Allosaurus 'jimmadseni'* (Chure 2000). As in *Allosaurus fragilis*, it is slightly bowed laterally (Madsen 1976b). The olecranon process is robust and quadrangular in cross-section; it is proximodistally longer and mediolaterally narrower in *Allosaurus 'jimmadseni'* (Chure 2000). Its whole surface is particularly roughened. The medial surface of the olecranon process is concave for insertion of *M. brachialis* (Baumel 1993). The proximal radial incisure froms a triangular surface on the proximolateral aspect of the ulna. The ectocotylar process forms a blunt knob; its proximal end participates in the cotyle for the ectocondyle of the humerus. The entocotylar process is particularly well developed and triangular, giving the proximal end of the humerus a high aspect in lateral view. Its proximal end forms the cotyle for the entocondyle of the humerus. The entocotylar process appears proportionally lower in *Allosaurus 'jimmadseni'* (Chure 2000). The distal articular surface is quadrangular in cross-section, although it is triangular, with a salient ventral expansion, in *Allosaurus 'jimmadseni'* (Chure 2000). Its lateral side forms a large contact pedestal-like radial surface. The proximal and distal ends of the ulna are offset at about 45°, as also described in *Allosaurus 'jimmadseni'*, although this offset is close to 90° in *Allosaurus fragilis* (Chure 2000). There is no nutrient foramen on the ulnar shaft near midlength, as described in *Allosaurus fragilis* (Madsen 1976b).

Radius

At all, the radius closely resembles that of *Allosaurus fragilis* (Madsen 1976b) and *Allosaurus 'jimmadseni'* (Chure 2000) (Figure 21). Both the proximal and distal ends are more expanded in *Acrocanthosaurus* (Currie and Carpenter 2000). The proximal

Figure 20
Right humerus of Arkhane before (**A**, **C**) and after (**B**, **D**) preparation, in cranial (**A**, **B**) and caudal (**C**, **D**) views.

end of the radius is transversely flattened and craniocaudally expanded. Its proximal articular surface is flat and roughened. Its slightly concave medial side fits onto the proximal radial incisure of the ulna. The ulnar shaft is perfectly straight and elliptical in cross-section. The distal end of the radius is expanded both mediolaterally and craniocaudally and triangular in cross-section; its distal articular surface is globular and roughened.

Carpals

Distal carpal 1 (intermedium of Gilmore (1920) and semilunate carpal of Sereno et al. (1994)) is a complex bone that covers the proximal end of MC I and also contacts the proximal and mediolateral surfaces of MT II (Figure 22). Its proximal saddle-shaped surface is for contact with the radiale. As in *Allosaurus fragilis* (Gilmore 1920) and *Allosaurus 'jimmadseni'* (Chure 2000), this bone has the same relations as the semilunate carpal of coelurosaurs, but is somewhat rectangular and flattened rather than truly semilunate in ventral views, as is typical for coelurosaurs (Rauhut 2003).

Metacarpals

Metacarpal I is parallelogram-shaped in dorsal view and approximately as broad as long, as also observed in *Allosaurus fragilis* (Madsen 1976b), *Allosaurus 'jimmadseni'* (Chure 2000), *Torvosaurus* (Galton and Jensen 1979), and *Afrovenator* (Rauhut 2003) (Figure 22). The proximal articular surface, which articulates with carpal I, is triangular and cup-shaped. In dorsal view, the proximal portion of metacarpal I is formed by a medial and a larger lateral condyles. The medial and lateral sides of metacarpal I are parallel and inclined laterally, forming an angle of about 45° with the proximal articular surface. The distal end of metacarpal I is formed by two dorsoventrally-enlarged condyles, offset laterally relative to the medial and lateral sides of the bone, so that the distal articular surface is roughly parallel with the proximal one, and ventrolaterally inclined; both condyles are subequal in size, although the lateral distal condyle is clearly larger in *Allosaurus 'jimmadseni'* (Chure 2000). The intercondylar sulcus is particularly deep and extends along both the ventral and dorsal surfaces of metacarpal I, allowing extensive dorsopalmar movements for digit I. The medial collateral pit forms a smooth depression, although the lateral pit is better defined, as also observed in *Allosaurus 'jimmadseni'* (Chure 2000).

Metacarpal II is not preserved on both hands. Metacarpal III is particularly slender

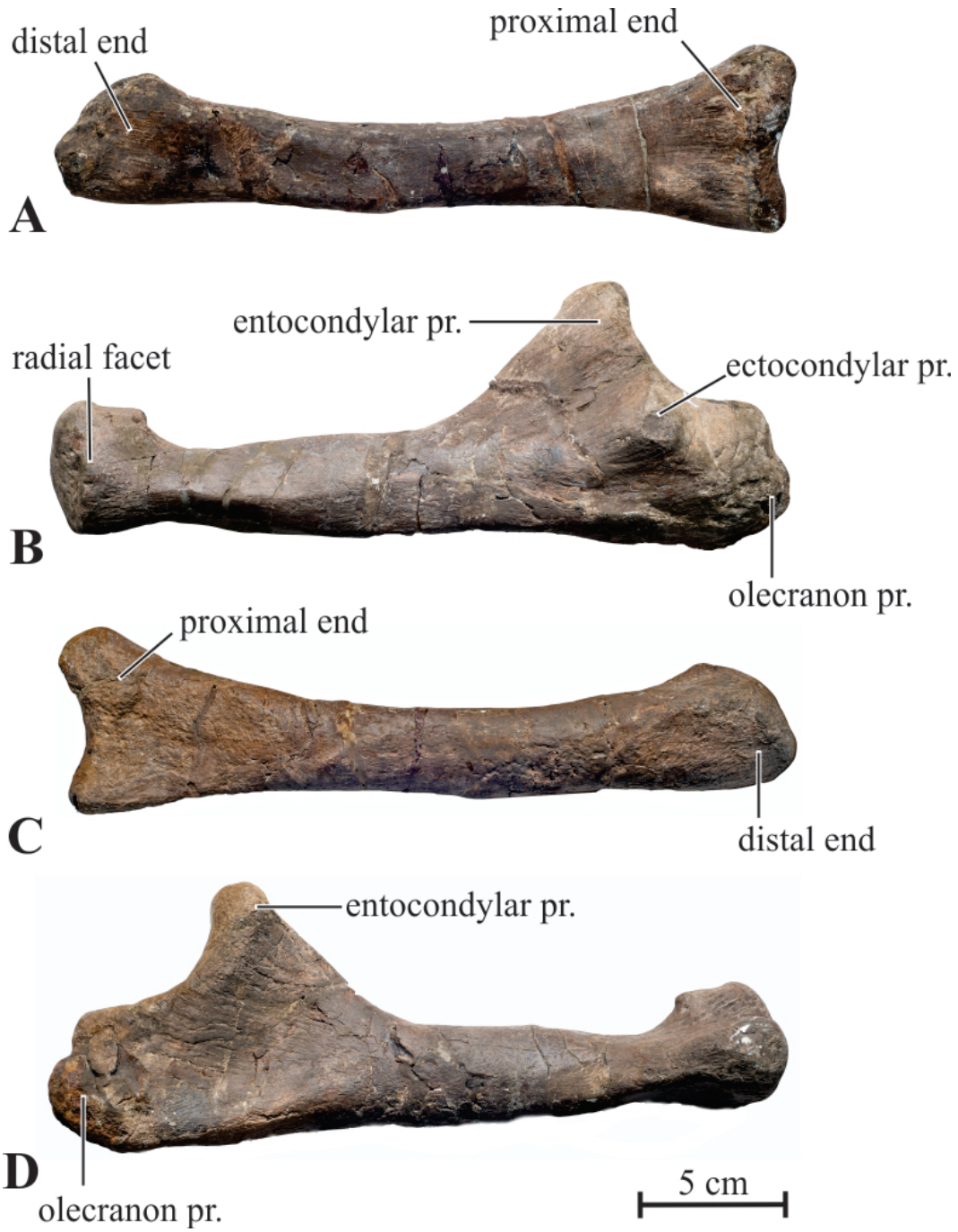

Figure 21
Left radius (**A**, **C**) and ulna (**B**, **D**) of Arkhane in lateral (**A**, **B**) and medial (**C**, **D**) views.

(Figure 22). Its proximal articular surface is smoothly convex and triangular in cross-section, with well-defined apices, and concave medial, lateral and ventral margins. The proximal half of the shaft remains triangular, although its mediolateral and dorsoventral diameters quickly lessen distally. The distal half of the shaft is elliptical in cross-section and mediolaterally compressed. The distal end of metacarpal III is roughly triangular in cross-section; it forms a single condyle, divided into two by a ventral sulcus along its flexor side. In dorsal view, the distal articular surface is offset medially, so that digit III rotates medially when flexed, as also observed in *Allosaurus 'jimmadseni'* (Chure 2000). The medial collateral pit is better defined than the lateral one.

Manual phalanges

Phalanx I-1 is particularly robust (Figure 22). Its proximal end is expanded both mediolaterally and dorsopalmarly. A vertical ridge subdivides its proximal articular surface into two unequal vertically concave facets, the lateral one being the larger. This ridge is particularly robust along its palmar part and slightly overhangs the proximal margin on the palmar side of phalanx I-1, forming a small flexor tubercle. In dorsal view, the proximal margin is regularly but markedly convex. The shaft is straight and subcircular in cross-section. The distal end is slightly expanded palmodorsally. The two distal condyles are subequal in size. The intercondylar groove is particularly deep and extends far along the palmar side of the phalanx, allowing important flexor movements of the claw. Both collateral pits are similarly developed.

Although it is much smaller, phalanx II-1 closely resembles phalanx I-1. Phalanx II-2 is too fragmentary to be adequately described.

Phalanx III-1 differs from the other proximal phalanges in being bowed medially and in having a single cup-shaped proximal articular surface; this surface is perfectly vertical, although it is rather sloped distodorsally in *Allosaurus 'jimmadseni'* (Chure 2000). The distal articular surface forms a single condyle. The lateral collateral pit is much better defined than the medial one. Although it is fragmentary, phalanx III-2 likely resembles phalanx III-1. Phalanx III-3 is longer than the proximal ones. It is transversely compressed along its whole length. Its proximal end is dorsopalmarly elevated. Unlike the proximal phalanges, the proximal end is subdivided into vertically concave articular facets, the medial one being the larger. The distal articular surface is also bicondylar, although the intercondylar sulcus remains rather shallow. The medial condyle extends further distally than the lateral one, whereas the lateral collateral pit is deeper than the medial one.

Unguals I-2 and III-4 are finely preserved. Ungual I-2 is particularly robust and is

the longest manual phalanx, being about two-third the length of the radius, although it is about the half of the radius in *Allosaurus fragilis* (Gilmore 1920) and *Allosaurus 'jimmadseni'* (Chure 2000). It is regularly curved and sharply pointed. Well-defined grooves extend from the tip of the claw along its medial and lateral sides; proximally, the claw grooves are deflected ventrally, progressively forming a broad concave surface at the base of the robust flexor tubercle. The proximal articular surface is subdivided by a low ridge into a larger medial and a lateral vertical concavities. The dorsal lip is well-developed and separated from the rest of the ungual by a transverse dorsal groove. Manual ungual III-4 is about half the size of ungual I-2, as also observed in *Allosaurus fragilis* (Gilmore 1920), although it appears proportionally shorter in *Allosaurus 'jimmadseni'*, being about one third the size of ungual I-2 (Chure 2000).

Pubis

The paired pubes are fused together along most of their length (Figure 23). With a 'craniocaudal length of the foot / proximodistal length of the pubis' = 0.49, the distal foot is not as elongated in lateral view as in *Allosaurus fragilis* (0.63 in USNM 83687) and *Allosaurus 'jimmadseni'* (0.61). A hypertrophied pubic boot, measuring greater than 60% of the length of the pubis, is also present in *Neovenator*, *Giganotosaurus* (Brusatte et al. 2008), and *Acrocanthosaurus* (Stovall and Langston 1950). The pubic boot is only 30% the pubic length in *Sinraptor dongi*(Currie and Zhao 1993) and is incipiently developed in *Torvosaurus* (Britt 1991). The angle between the proximodistal axis of the pubic shaft and the craniocaudal axis of the foot is about 75°, although it is distinctly more inclined caudodorsally in *Allosaurus fragilis* (55°, Madsen (1976b)). The distal surface of the distal foot is triangular in ventral view and straight in lateral view, although it is distinctly convex in lateral view in *Allosaurus fragilis* (Gilmore 1920; Madsen 1976b). Its surface is particularly rugose, indicating the presence of an important cartilaginous cap in life, and a narrow but deep median furrow arising from the cranial margin marks the separation of the paired pubes. The cranial expansion of the distal foot appears less salient than in *Allosaurus fragilis* and *Allosaurus 'jimmadseni'*, although this character cannot be adequately quantified. With a ratio ' proximodistal length of the pubis / minimal craniocaudal width' = 27, the pubic shaft is straight and much more gracile in lateral view than in *Allosaurus fragilis* (about 14 in USNM 8367) and *Allosaurus 'jimmadseni'*. In cranial view, the articulated pubes form a broad apron, an elongate oval opening is present between the joined pubes above the distal foot, contrasting with the continuous suture between the pubes in *Torvosaurus* (Britt 1991). In cranial view, the lateral sides of the pubic shafts are distinctly bowed externally, so

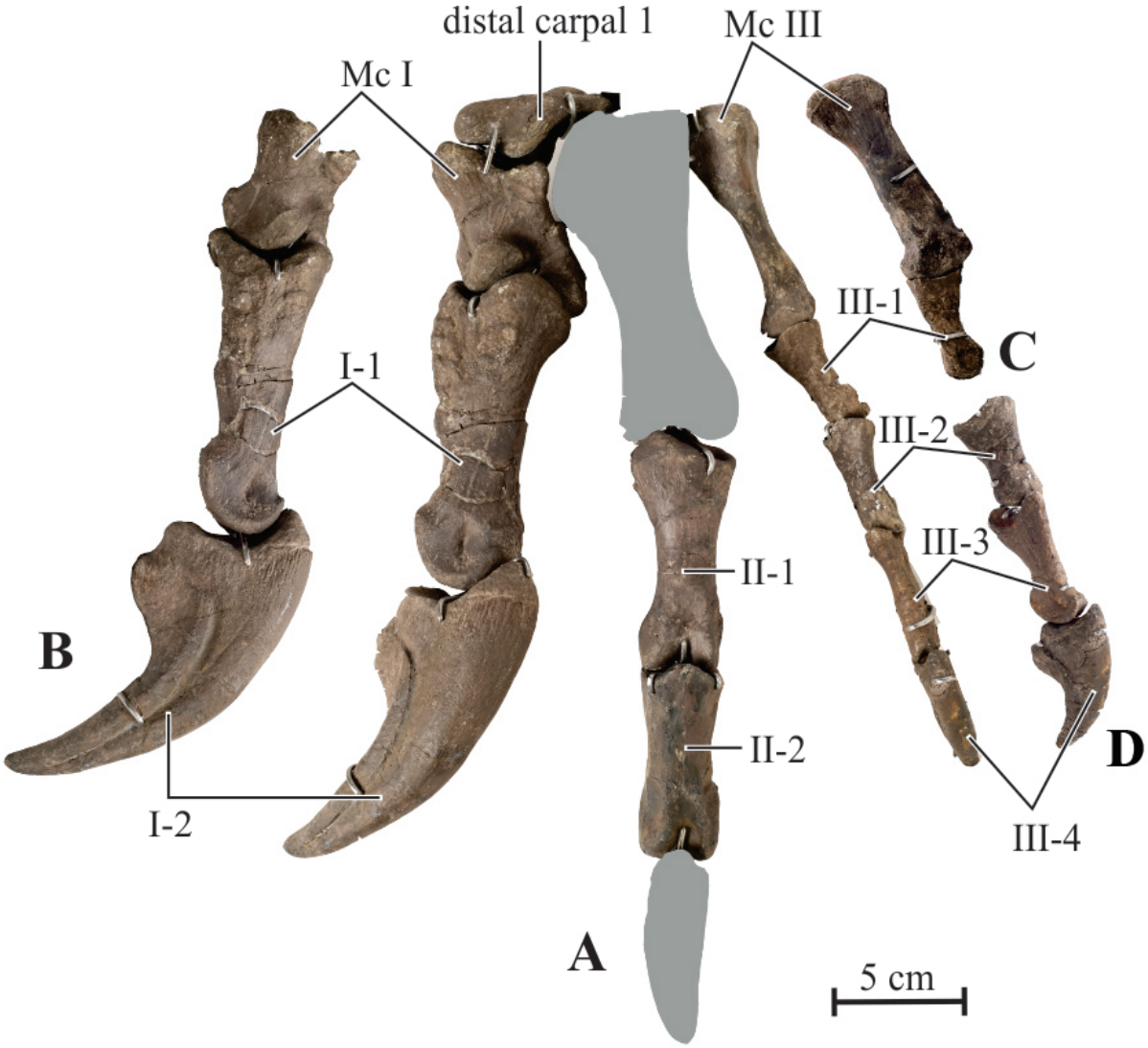

Figure 22
Left manus of Arkhane. Articulated manus in dorsal view (**A**). Digit I in medial view (**B**). Metarcapal III and phalanx III-1 in lateral view (**C**). Phalanges III-2 to III-4 in medial view (**D**). **Mc**: metacarpal

that the proximal part of the fused pubes appear particularly wide: the ratio 'greatest width of the paired pubes / proximodistal length of the pubis' is 0.51, although it is respectively 0.3 and 0.38 in USNM 4734 and USNM 8367 *Allosaurus fragilis* specimens (Gilmore 1920). The lateral sides of the proximal heads are nearly parallel in cranial view. The articular facets for the ilia are elliptical in outline and cup-shaped. Because the proximal heads of both pubes are incompletely preserved, the acetabular part of the proximal heads are not completely preserved and the development and morphology of the pubic notch cannot be observed.

Ischium

The ischium is subequal in size to the pubis, as also observed in *Allosaurus fragilis* (Madsen 1976b), *Allosaurus 'jimmadseni'* (Chure 2000), *Torvosaurus* (Galton and Jensen 1979), it is distinctly shorter, with a more massive aspect, in *Sinraptor dongi* (Currie and Zhao 1993), *Monolophosaurus* (Zhao and Currie 1993), and *Acrocanthosaurus* (Stovall and Langston 1950) (Figure 24). The pubic peduncle is larger than the iliac peduncle and the articulation with the pubis is vertical. A caudally directed flange is present on the iliac peduncle, as observed in *Allosaurus fragilis* (Madsen 1976b), *Allosaurus 'jimmadseni'* (Chure 2000), *Acrocanthosaurus*, *Carcharodontosaurus*, *Giganotosaurus*, and *Mapusaurus* (Brusatte and Sereno 2008), it is absent in *Torvosaurus*, *Sinraptor dongi*, and *Neovenator* (Brusatte and Sereno 2008). The obturator process is located on the proximal third of the shaft and separated from the pubic peduncle by a deep notch. There is no trace of an elongated cranial lamina extending up to the level of the end of the pubic peduncle, as described in *Allosaurus 'jimmadseni'* (Chure 2000) and in a partial specimen from the Upper Jurassic of Portugal (Pérez-Moreno et al. 1999). Chure (2000) suggests that this lamina should be a synapomorphy for the genus *Allosaurus*, although this feature is often not preserved due to preservation or damage during preparation. The ischial shaft is straight in lateral view, but bowed medially in dorsal view. There is no evidence of a longitudinal crest arising from the proximocaudal region of the ischium, as observed in *Sinraptor dongi* (Currie and Zhao 1993) and *Yangchuanosaurus shangyuanensis* (Dong et al. 1983). The distal end of the ischium is distinctly better developed than in *Allosaurus fragilis*, being more than twice the minimum craniocaudal diameter of the ischial shaft and forming a small distinct boot. In this aspect, it more closely resembles the condition in *Allosaurus 'jimmadseni'*, *Sinraptor dongi* (Currie and Zhao 1993), and *Neovenator* (Brusatte et al. 2008). The distal expansion is primarily in the caudal direction, as also observed in *Allosaurus fragilis* (Madsen 1976b), *Allosaurus 'jimmadseni'* (Chure 2000), *Acrocanthosaurus* (Harris 1998), *Torvosaurus* (Galton and

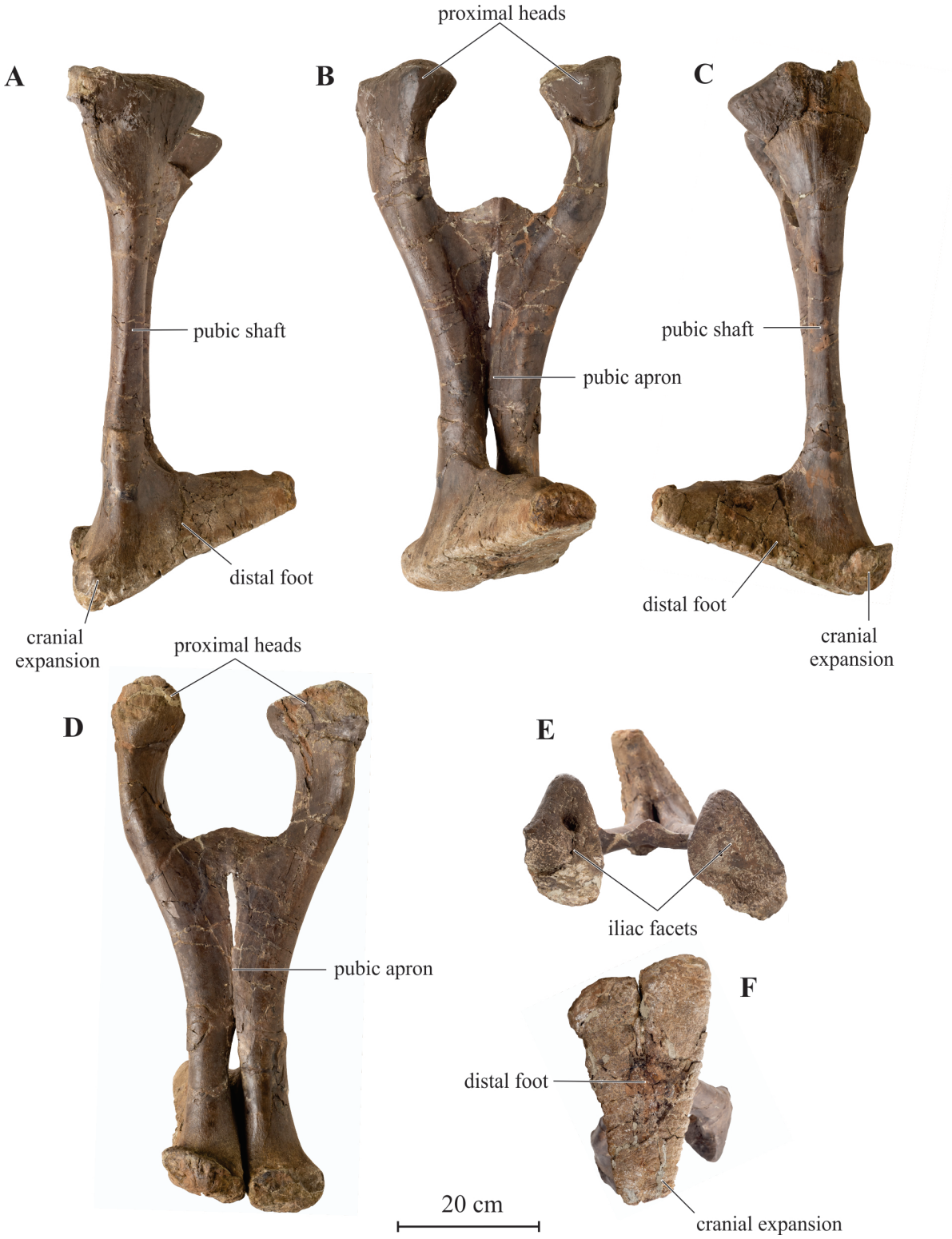

Figure 23
Fused pubes of Arkhane in left lateral (**A**), caudal (**B**), right lateral (**C**), cranial (**D**), proximal (**E**), and distal (**F**) views.

Jensen 1979), and *Giganotosaurus* (Coria and Salgado 1995), *Neovenator* (Brusatte et al. 2008), *Sinraptor dongi* (Currie and Zhao 1993), *Yangshuanosaurus shangyuensis*, *Yangshuanosaurus magnus* (Dong et al. 1983), and likely *Monolophosaurus* (Zhao and Currie 1993), the cranial distal expansion of the ischium is important, although there is virtually no caudal expansion.

Femur

The femur is straight in cranial view, but bowed cranially in lateral view (Figure 25). With a 'circumference at midshaft / total length' ratio = 0.36, its proportions resemble the femora of *Allosaurus fragilis* specimens of similar size (0.33-0.39,Madsen (1976b), tab. 5). In cranial view, the femoral head is angled dorsomedially, so that its apex lies dorsal to the greater trochanter, as also observed in carcharodontosaurids, including *Neovenator*, *Acrocanthosaurus*, *Giganotosaurus* (Brusatte et al. 2008), *Carcharodontosaurus* (Stromer 1931), and *Mapusaurus* (Coria and Currie 2006). In contrast, the femoral head is oriented medially in *Allosaurus fragilis* (Madsen 1976b), *Allosaurus 'jimmadseni'* (Chure 2000) and *Sinraptor dongi* (Currie and Zhao 1993), so that the apex of the femoral head lies about the level of the greater trochanter. In *Ceratosaurus*, the apex of the greater trochanter lies above the femoral head (Madsen and Welles 2000). In medial view, the femoral head is circular in outline and faces slightly ventrally, as also observed in *Allosaurus 'jimmadseni'* (Chure 2000), it faces directly medially in *Allosaurus fragilis*. In proximal view, the femoral head is strictly oriented medially, as in *Allosaurus fragilis* (Madsen 1976b), *Allosaurus 'jimmadseni'* (Chure 2000), *Sinraptor dongi* (Currie and Zhao 1993), *Mapusaurus* (Coria and Currie 2006), and *Giganotosaurus* (Brusatte et al. 2008), although it is oriented craniomedially in *Neovenator* (Brusatte et al. 2008) and basal theropods (Rauhut 2003). The proximal surface of the femoral head remains subequal in width craniocaudally along its entire mediolateral length. In some *Allosaurus fragilis* specimens, the head narrows progressively as it approaches the greater trochanter, whereas in other specimens, only the lateral third of the lateral head becomes narrower (Brusatte et al. 2008). A deep oblique ligament groove for *M. iliofemoralis* extends along the caudal surface of the femoral head. A shallower depression is present lateral to this groove and just below the proximal margin of the femur, as also observed in *Allosaurus 'jimmadseni'* (Chure 2000). In cranial view, the greater trochanter is confluent with the femoral head and the proximal margin is slightly concave. In proximal view, the greater trochanter is progressively narrowing towards the lateral side of the femur. The lesser trochanter is craniocaudally broadened and wing-like. It is separated from the greater trochanter by a deep cleft and its lateral side is striated, marking the insertion of *M.*

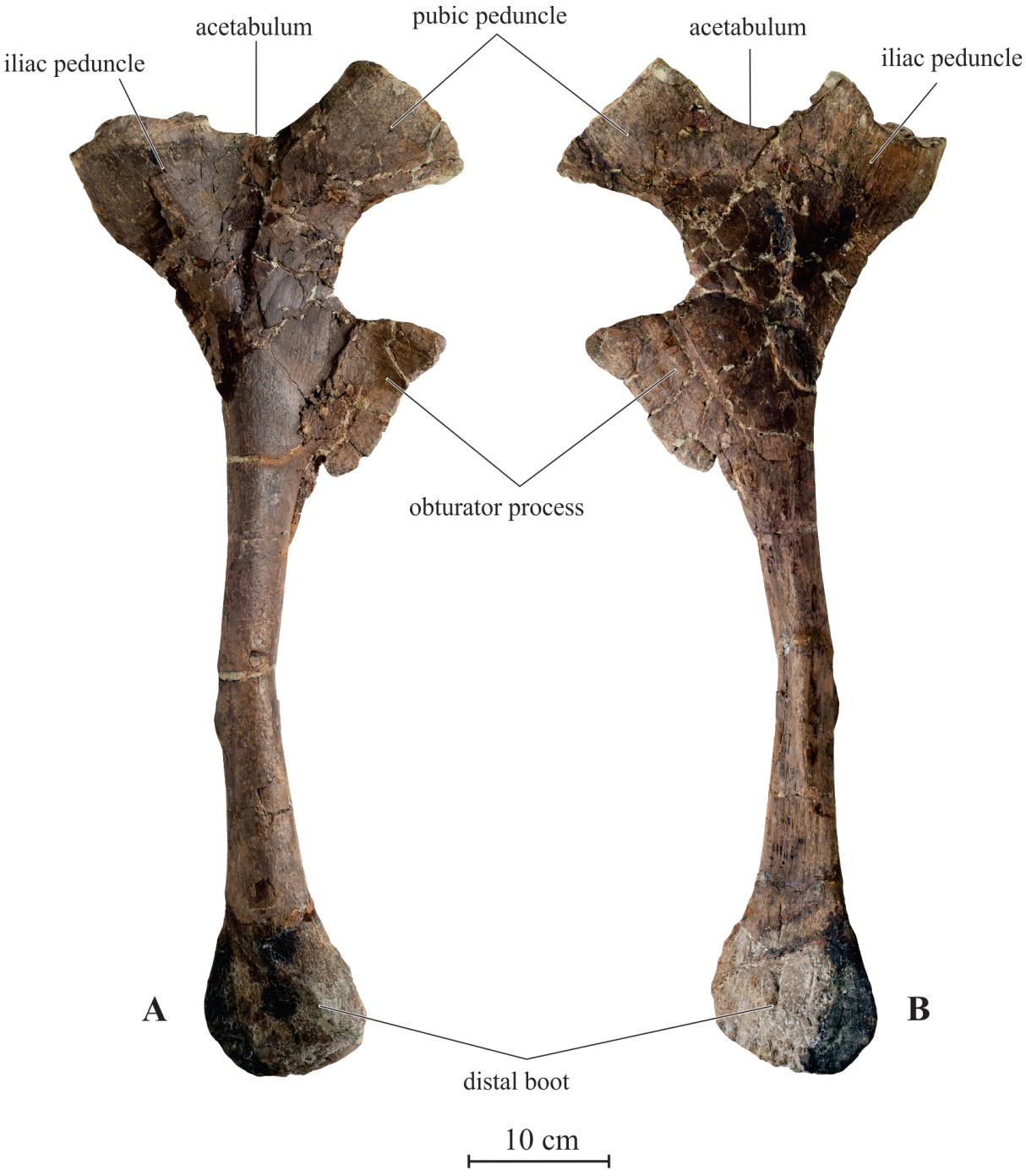

Figure 24
Right ilium of Arkhane in lateral (**A**) and medial (**B**) views.

vertical ridges extend along the central region of the flexor groove.

Tibia

The tibia is proportionally elongated, being 94% the length of the femur; it is 81% and 83% the length of the femur, respectively in *Allosaurus fragilis* specimens USNM 4734 (Gilmore 1920) and DNM 2560 (formerly UUVP 6000, Madsen (1976b)) (Figure 26). On the proximal end of the tibia, the medial condyle is stout, slightly curved laterally, and extends caudally beyond the lateral condyle. In *Allosaurus 'jimmadseni'*, the medial condyle does not project caudal to the shaft (Chure 2000). Both condyles are separated by a deep proximocaudal notch. The lateral condyle is craniocaudally elongated and considerably overhangs the tibial shaft. Its lateral side is smoothly concave in proximal view. In proximal view, the lateral condyle extends rostrally as triangular rostrolateral process that projects into the *incisura tibialis*. This process is present in *Allosaurus fragilis* and *Neovenator* (Brusatte et al. 2008), but is absent in *Sinraptor dongi* (Currie and Zhao 1993). As in *Neovenator*, but unlike in *Allosaurus fragilis*, this rostrolateral process develops into a ventral spine that overhangs the tibial shaft. In lateral view, the cnemial crest extends dorsally above the level of the proximal articular surface. It is distinctly less curved laterally than in *Allosaurus fragilis*, more closely resembling the condition in *Allosaurus 'jimmadseni'*. A strong caudoventrally-oriented crest extends along its lateral side, as also observed in *Neovenator* (Brusatte et al. 2008). This crest is also present, although much less pronounced, in *Allosaurus fragilis* (Madsen 1976b), *Sinraptor dongi* (Currie and Zhao 1993), and *Torvosaurus* (Brusatte and Sereno 2008). The medial side of the proximal tibia is regularly convex craniocaudally. The tibial shaft is rather slender (ratio 'minimal circumference of the shaft / total length of the tibia' = 0.33), straight in both cranial and lateral views, and elliptical in cross-section. The fibular crest is particularly salient on the proximal third of the lateral side of the tibial shaft and is clearly separated from the proximal articular surface, its caudal side forms an elongated articular surface for the fibula. There is no trace of a nutrient foramen caudal to the distal end of the fibular crest, as e.g. observed in *Allosaurus fragilis* (Madsen 1976b), *Allosaurus 'jimmadseni'* (Chure 2000), *Sinraptor dongi* (Currie and Zhao 1993), and *Neovenator* (Brusatte et al. 2008). Ventral to the fibular crest, the lateral side of the shaft forms an elongated facet that marks the close contact with the fibula. The distal end of the tibia is craniocaudally expanded and mesiolaterally compressed, with a triangular outline in distal view. The lateral malleolus is larger than the medial one and extends further distally. The cranial side of the distal end of the tibia forms a triangular facet for articulation with the ascending process of the astragalus. This surface is bounded mediodorsally by a strong oblique

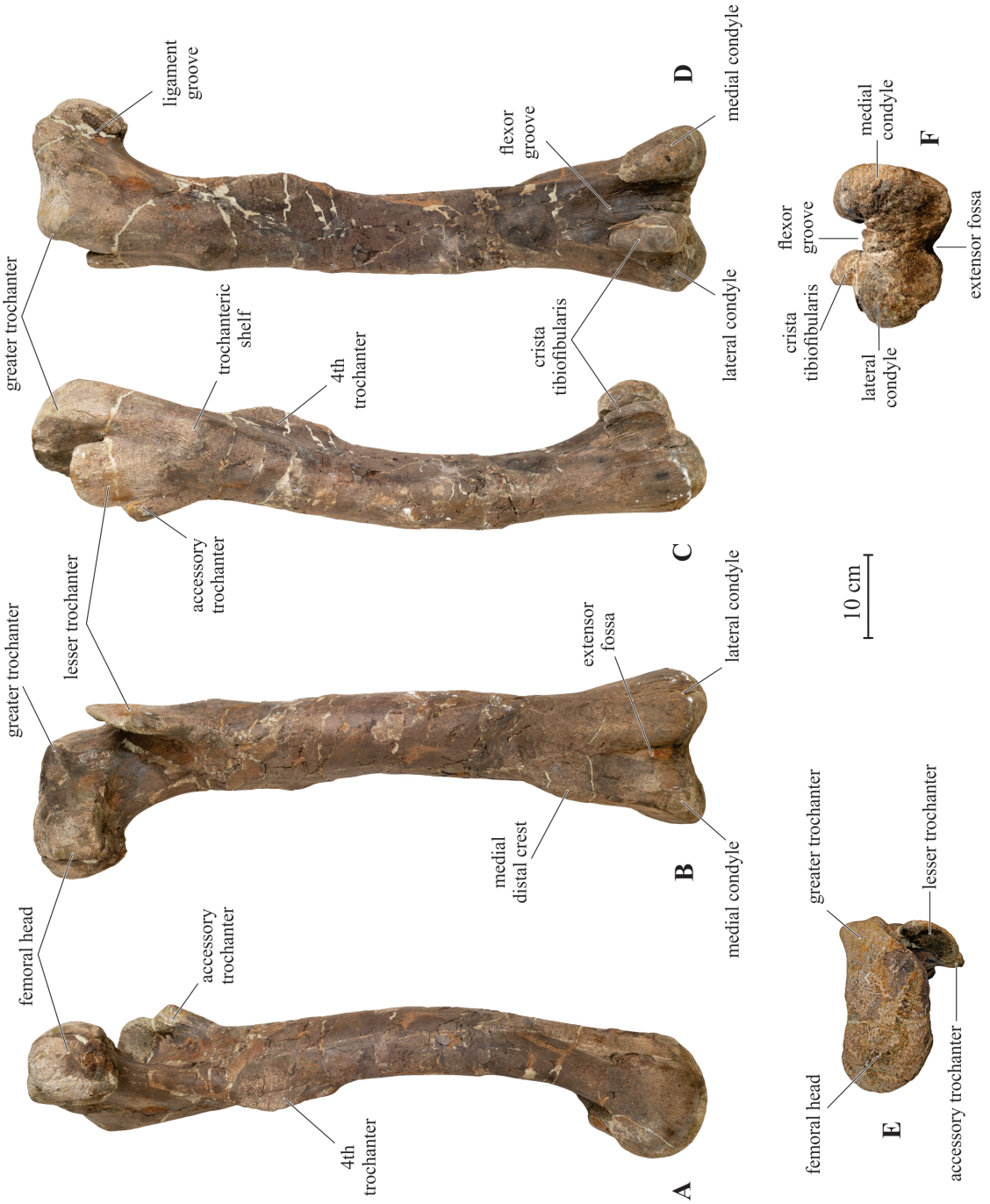

Figure 25
Left femur of Arkhane in medial (**A**), cranial (**B**), lateral (**C**), caudal (**D**), proximal (**E**), and distal (**F**) views

suprastragalar buttress that extends from the medial malleolus, as observed in most basal Tetanurae (Rauhut 2003). A low vertical ridge divides the caudal distal side of the tibia into a smaller mean and a larger lateral parts. In distal view, there is a long contact area for the astragalus and, at the lateral end of this contact area, a deep pit.

Fibula

With a ratio 'total length / distal width' = 10.5, the fibula looks more gracile than in *Allosaurus fragilis*, more closely resembling the condition in *Sinraptor dongi* (Currie and Zhao 1993) (Figure 27 A-B). The proximal head is craniocaudally expanded and crescentic in outline, with a convex lateral margin and a concave medial margin toward the tibia. As in many theropods, a deep groove is present on the medial side of the proximal end of the tibia. This groove starts 45 mm from the proximal margin of the tibia and extends distally along 130 mm; it is rather wide craniocaudally, covering about the cranial two-thirds of the width of the fibula. This groove is limited cranially by a high crest, better developed than in *Allosaurus fragilis* (Madsen 1976b). The fibular shaft gradually narrows to the level of the mid-shaft. About one-third down the cranial margin of the fibular shaft, a swelling marks the insertion of *L. interosseum tibiofubulare*. The distal end of the fibula is slightly bowed laterally and moderately expanded into a distal knob, with a spherical distal surface. Its medial side is flattened, with fine vertical striations marking the distal articulation with the tibia. A vertical crest extends along the cranial side of the distal end of the fibula.

Astragalus

The astragalus is roughly rectangular in plantar view and mediolaterally expanded (Figure 27 C-E). The ascending process is restricted to the lateral two-thirds of the cranial side; it is triangular in cranial view, with a vertical lateral edge, and inclined cranially. The basal part of the cranial side of the ascending process is depressed and a upper horizontal groove marks its base. A lower horizontal groove extends along the whole width of the cranial side of the astragalus; this groove opens laterally as a well-developed notch for reception of the calcaneum. Dorsal and ventral to this notch, the astragalus forms well developed buttresses. There is a deep circular depression at the base of the caudal side of the ascending process. The astragalus is saddle-shaped in plantar view, forming a larger medial and a smaller lateral malleoli. The proximal articular surface of the astragalus forms two distinct articular surfaces. The surface

Figure 26
Left tibia of Arkhane in cranial (**A**), lateral (**B**), medial (**C**), proximal (**D**), and distal (**E**) views.

for the medial malleolus of the tibia faces medially; it is limited cranially by a ridge extending from the base of the ascending process, whereas it is limited caudally by a stout buttress along the mediocaudal rim of the astragalus. The articular surface for the lateral malleolus of the tibia, limited cranially by the ascending process, is mediolaterally elongated and craniocaudally narrow.

Metatarsals

Metatarsal I is short, with a truncated proximal portion (Figure 28 B); its proximolateral and proximomedial sides form an angle of about 30° in dorsal view. Its proximolateral side is dorsoplantarly concave, where it articulates with the medial aspect of metatarsal II. The distal articular surface is roughly rectangular in outline and is offset medially from the body of the metatarsal; a well-developed intercondylar groove is developed along its flexor surface. The lateral collateral ligament pit is better developed than the medial one.

Metatarsal II is shorter, but as robust as metatarsal III (Figure 28 C,D). Its proximal articular surface is slightly depressed and roughly semi-circular in cross-section, with a flattened lateral margin and a convex lateral margin; there is a salient lateroventral keel, as also observed in *Allosaurus fragilis* (Madsen 1976b). Metatarsal II is closely appressed to metatarsal III along its whole length, except its distal end, which is slightly divergent medially. The metatarsal shaft is quadrangular in cross-section. The distal articular surface is quadrangular in outline. The lateral condyle is much larger than the medial one; along their plantar surface, both condyles are separated by a deep and wide sulcus that does not extend towards the dorsal aspect of the bone. Dorsally, the distal condyle is marked by a shallow transverse depression. The lateral collateral ligament pit is much deeper, with better-defined margins, than the medial one.

Metatarsal III is the longest metatarsal and is about one half the length of the tibia, as also observed in *Allosaurus fragilis* (Gilmore 1920). Its proximal end is hour-glass shaped in proximal view and mediolaterally compressed, with a long axis that forms a 45° angle with the metatarsal shaft (Figure 28 E,F). Its dorsomedial side forms a depressed triangular surface for articulation with metatarsal II, whereas its ventrolateral side forms a particularly enlarged flattened surface for articulation wit metatarsal IV. The metatarsal shaft is rather straight and mediolaterally wider distally than proximally, as also observed in *Allosaurus 'jimmadseni'* (Chure 2000). The plantar side of the metatarsal shaft is mediolaterally flat, whereas its dorsal surface is convex, as also observed in *Ceratosaurus* (Gilmore 1920); in *Allosaurus fragilis* (Gilmore 1920), *Allosaurus 'jimmadseni'* (Chure 2000), and *Sinraptor dongi* (Currie and Zhao 1993), the dorsal side of the shaft is wider than the plantar side, giving a V-shaped cross-section. This latter character is

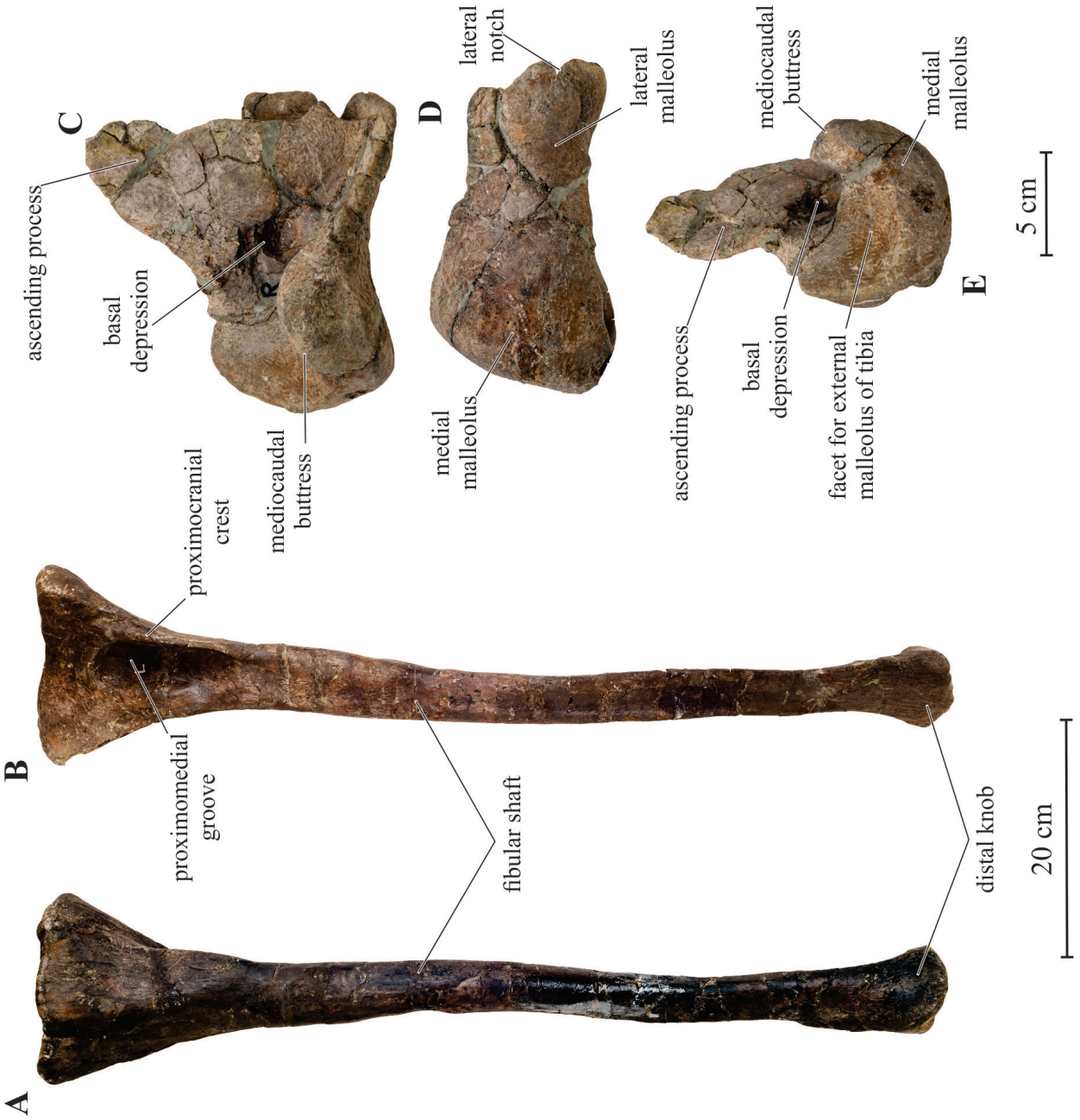

Figure 27
Left fibula of Arkhane in lateral (**A**) and medial (**B**) views. Right astragalus of Arkhane in caudal (**C**), plantar (**D**), and medial (**E**) views.

regarded as a synapomorphy for Tetanurae by Gauthier (1986) and as a synapomorphy for Avetheropoda by Holtz (2004). Distally, the shaft of metatarsal III does not form a distinct medial shoulder as observed in *Allosaurus fragilis* (Gilmore 1920; Holtz 2004). The distal end of metatarsal III forms a ginglymoid surface with deep collateral fossae. Unlike in *Allosaurus 'jimmadseni'* (Chure 2000), the medial half of the distal articular surface is larger than the lateral one and the distal condyles are separated by a deep sulcus.

Metatarsal IV is about the same size as metatarsal II, but more gracile (Figure 28 G,H). Its proximal articular surface is triangular in outline and mediolaterally expanded, contrasting with the broader, subquadragular proximal surface in *Ceratosaurus* (Gilmore 1920). The caudolateral margin is markedly concave as in *Allosaurus fragilis* (Gilmore 1920) and *Sinraptor dongi* (Currie and Zhao 1993), although it is rather convex in *Torvosaurus* (Britt 1991). The shaft is distinctly and regularly bowed laterally; its plantar side is mediolaterally flat, whereas its dorsal side is regularly convex. The distal articular surface is triangular in outline and mediolaterally compressed. The distal condyles are developed only along the plantar side of metatarsal IV. The medial condyle is distinctly stouter than the lateral one. The medial collateral ligament pit is shallowly developed, whether the lateral one is not developed at all.

Metatarsal V is reduced, but distinctly longer than metatarsal I (Figure 28 I). It is completely devoid of articular surfaces, transversely flattened along its whole length; its distal end tapers through a gentle curve. Its medioplantar edge forms a rugose ridge, presumably for ligamentous articulation with metatarsal IV.

Pes phalanges

The phalangeal formula of the pes is 2-3-4-5-0. As is usual in basal Tetanurae (Holtz 2004), digit III is the longest and digit I is reduced, not long enough to touch the ground, and directed slightly towards the plantar side of the pes (Figure 29). The pes phalanges are proportionally shorter and stouter than those of the manus. The proximal articular surfaces of the proximal phalanges are concave, whereas those of more distal phalanges are saddle-shaped, subdivided by a vertical ridge. Those surfaces are roughly trapezoidal outline, with a convex dorsal margin, a concave ventral margin, and straight to slightly convex lateral and medial margins, as also observed in *Allosaurus fragilis* (Madsen 1976b); the latter margins are rather concave in *Sinraptor dongi* (Currie and Zhao 1993) and *Neovenator* (Brusatte et al. 2008). Rugosities for the collateral ligaments and digit flexors are present along the periphery of the proximal surface. The distal articular surfaces of non-ungual phalanges are saddle-shaped, formed by two bulbous condyles separated by a

Figure 28

Left metatarsus of Arkhane. Articulated metatarsals II-IV in proximal view (**A**); Metatarsal I in dorsal view **B**; Metatarsal II **C,D** in dorsal (**C**) and lateral (**D**) views; Metatarsal III (**E,F**) in dorsal (**E**) and lateral (**F**) views; Metatarsal IV (**G,H**) in medial (**G**) and dorsal (**H**) views; Metatarsal V in lateral view (**I**).

sulcus extending onto the flexor and extensor surfaces. On digit II-1, the lateral condyle is distinctly larger than the medial, unlike the condition in *Neovenator* (Brusatte et al. 2008). On digit II, the collateral ligament pits are broader and deeper laterally than medially, whereas on digit IV, the medial pits are better developed than the lateral ones. As is usual in theropods, the dorsal surface of each phalanx is excavated on its extensor surface proximal to the distal articulation.

The pedal unguals are broad and well-rounded in cross-section. A deep groove extends along both their medial and lateral sides. This groove is located closer to the plantar margin of the ungual than in *Allosaurus fragilis* (Madsen 1976b) and *Sinraptor dongi* (Currie and Zhao 1993), more closely resembling the condition in *Neovenator* (Brusatte et al. 2008). Unlike in *Neovenator*, there is no median shallow groove on the dorsal surface of the unguals (Brusatte et al. 2008).

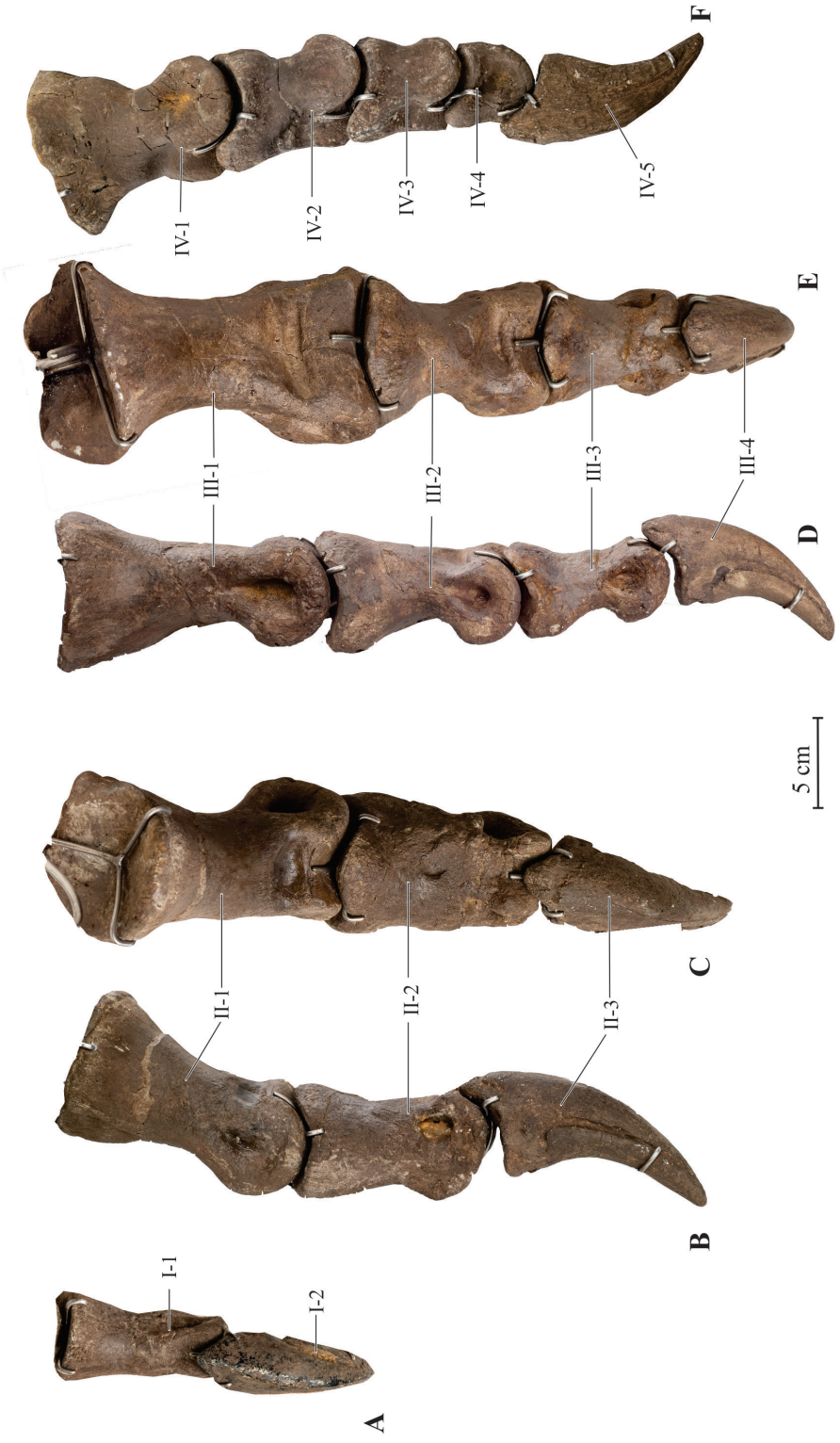

Figure 29
Phalanges of the left pes of Arkhane. Digit I in dorsal view (**A**); Digit II (**B,C**) in medial (**B**) and dorsal (**C**) views; Digit III (**D,E**) in medial (**D**) and dorsal (**C**) views; Digit IV in lateral view (**F**).

PHYLOGENETIC ANALYSIS

In order to recover the phylogenetic position of Arkhane, we included this specimen into the data matrix of Carrano et al. 2012, which is the most recent and comprehensive phylogenetic study focussing on the relationships of non-coelurosaurian tetanurans. This data matrix consists of 351 informative characters originally scored for 61 operational taxonomic units (OTUs). In the present report, we score *Allosaurus fragilis* and *Allosaurus 'jimmadseni'* separately as two distinct OTUs rather than considering them as part of the same hypodigm. Because of the discussions still pending on its validity, we have not included *Allosaurus europaeus* in the present analysis. The character list is detailed in Appendix 2 and the nexus file, in Appendix 3.

During the scoring process, we changed several character states coded by Carrano et al. 2012 in *Allosaurus fragilis*, as following:

- char. 28 $1 \rightarrow 0$
- char. 46 $0\&1 \rightarrow 1$
- char. 55 $0 \rightarrow 1$
- char. 118 $2 \rightarrow 0$
- char. 122 $1 \rightarrow 0$
- char. 161 $1 \rightarrow 0$
- char. 187 $0 \rightarrow 1$
- char. 192 $1 \rightarrow 0$
- char. 248 $1 \rightarrow 0$
- char. 285 $0 \rightarrow 1$
- char. 289 $1 \rightarrow 2$

We also add a third character state to describe the relative position of the lateral and the medial distal condyles of the femur, in adding the possibility that the medial condyle can be projected further distally than the lateral one, as observed in Arkhane (character 315:2).

The matrix was analyzed using the TNT software package (Goloboff et al. 2008). As in (Carrano et al. 2012), *Eoraptor* and *Herrerasaurus* serve as outgoup taxa, with the former rooting the analyses. One thousand 'New Technology search' runs with default settings were computed. Then the shortest tree islands were explored by the tree-bisection-reconnection algorithm to only hold the shortest trees. Our analysis

recovered 1296 shortest trees with each a length of 1025 steps. Bremer supports were recovered using the bremer.run script in TNT software.

The 50% consensus tree is presented in Figure 30. The general topology of the consensus tree is quite consistent with that of Carrano et al. 2012, so that we refer to this paper for detailed descriptions and discussions of the results. Our phylogenetic analysis places Arkhane as the sister-taxon of *Saurophaganax maximus* in a clade supported by one ambiguous synapomorphies: **342.0**: metatarsal III, midshaft of metarsal III rectangular in cross-section. Two ambiguous synapomorphies and one autapomorphy (*) support Arkhane as a separate taxon: **161.0**: atlas, moderately elongated epipophyses; **302.2**: femur, head of femur is dorsomedialy directed; **315.2***: femur, distal medial condyle is more distaly located than lateral condyle.

Our analysis also shows that Arkhane and *Saurophaganax* are closely related to *Allosaurus fragilis* and *Allosaurus 'jimmadseni'* (Figure 30). The four 'allosaurid' taxa from the Morrison Fm form a clade supported by one unambiguous synapomophy (*) and ten ambiguous synapomorphies: **3.1**: premaxilla, subnarial process is reduced and separate from nasals by maxillary contribution to narial margin; **47.2**: lacrimal, presence of a triangular horn; **51.1**: jugal, the anterior end of the bone is excluded from internal antorbital fenestra; **52.0**: jugal, absence of pneumatisation; **55.1**: jugal, orbital margin vertical; **58.0**: postorbital, suborbital flange absent: **94.1***: basioccipital, width of basal tubera is inferior to occipital condyle width; **177.0**: epipophyses of anterior cervical vertebrae are low and blunt; **223.2**: scapula, length:width ratio of blade is superior to 10; **236.1**: humerus, distaly canted in lateral view with distal condyles not parallel to proximal ones; **263.1**: ilium, low swollen vertical ridge on lateral surface of blade dorsal to acetabulum.

This phylogenetic analysis supports the hypothesis that Arkhane does belong to a new, separate species. It also suggests that it should be referred to *Saurophaganax* rather than to *Allosaurus* itself. However, the general morphology of Arkhane is quite consistent with *Allosaurus*: if differences are numerous and clearly documented, they remain minor and do not really affect the general morphology of the skeleton. Moreover, *Saurophaganax maximus* is known from fragmentary material and is characterized by only two autapomorphies (= expanded chevrons as those of primitive theropods and lamina along the base of the neural spine; Chure, 1995). Smith 1998 already noticed that, despite of its very large size, the material identified as *Saurophaganax* lies on the same growth trajectory as *Allosaurus fragilis* in almost every case, suggesting that *Saurophaganax* is a distinct, large, species of *Allosaurus* that should be referred to as *Allosaurus maximus*. The results of the present phylogenetic analysis entirely support Smith's (1998) hypothesis. We consider that the clade including the four 'allosaurids' from

the Morrison Fm represents in fact the genus *Allosaurus* itself, then well-supported by one unambiguous and ten ambiguous synapormorphies. In a strict taxonomical perspective, the family Allosauridae is therefore limited to its type-genus *Allosaurus*.

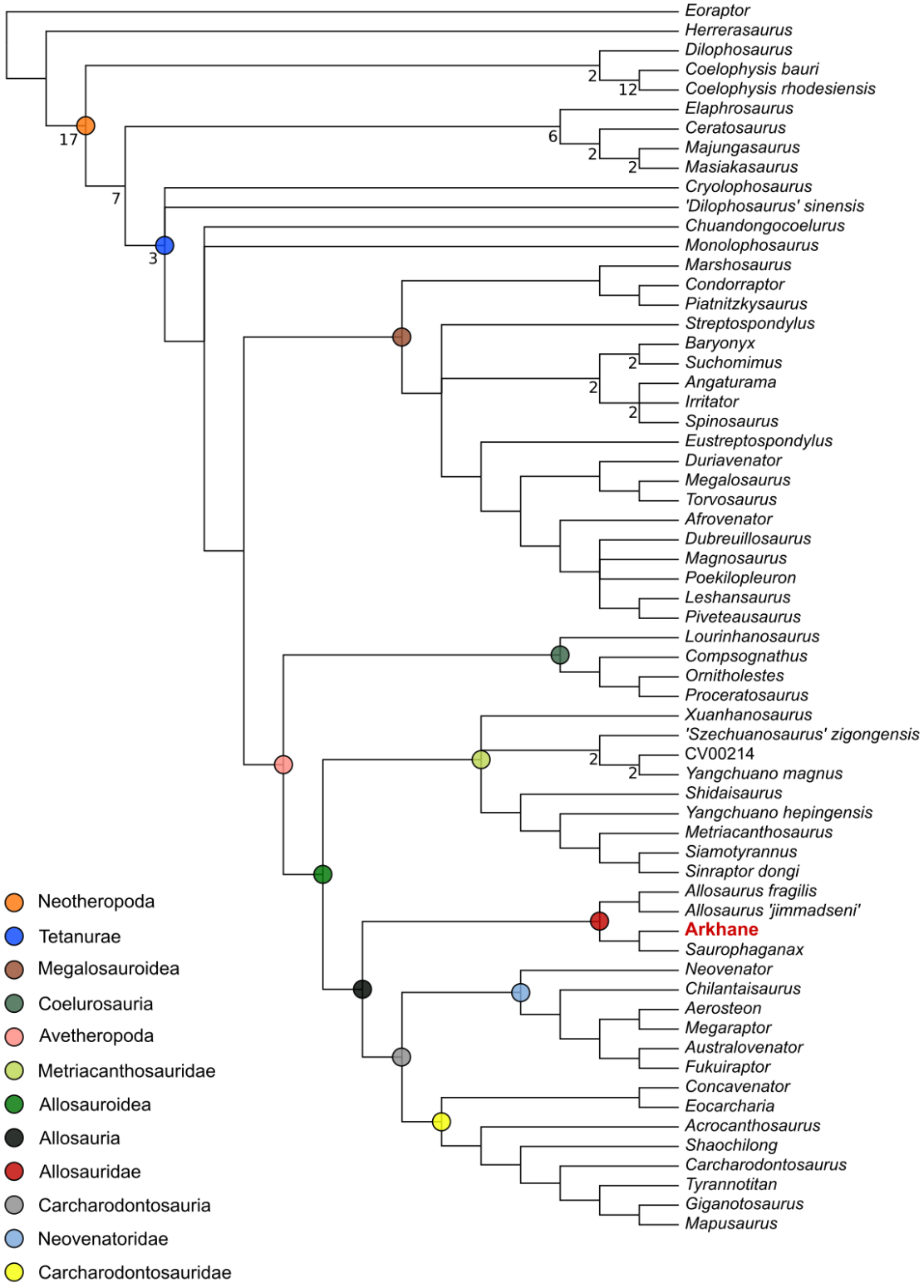

Figure 30
Consensus tree (50% majority rule) resulting of 1296 shortest trees of 1025 steps. CI = 0.40 and RI = 0.69.

CONCLUSIONS

Arkhane is the skeleton of an allosaurid theropod discovered in the Morrison Fm of the 'Pinepit Quarry' in Barnum-Kaycee, Wyoming. This site is close to the type locality of the *Galeomopus hayi* (Holland 1906) specimen (Sauropoda, Diplodocidae) discovered by W.H. Utterback in 1902-1903. Sedimentological and taphonomic data suggest that the skeleton of Arkhane was deposited in a floodplain environment, characteristic for the middle part of the Morrison Fm in the Powder River sedimentary basin. The skeleton is complete at about 70% and there is no indication that it is a composite specimen: there is no supernumerary bones and the size of all the collected bones is clearly homogeneous, coherent for a single individual.

Detailed osteological description and comparisons with other 'allosaurid' taxa already described from the Morrison Fm support the hypothesis that Arkhane belongs to a new species, as already stated in the auction house Aguttes's promotional catalogue. The main differences between the different *Allosaurus* species from the Morrison Fm are summarized in Table 1.

Including Arkhane into the most recent and complete phylogenetic analysis of non-coelurosaurian tetanurans places this specimen within a clade formed by the allosaurid taxa from the Morrison Fm, as the sister-group of *Saurophaganax maximus* and close to *Allosaurus fragilis* and *Allosaurus 'jimmadseni'*. It supports the hypothesis that *Saurophaganax* is a distinct, large, species of *Allosaurus* that should be referred to as *Allosaurus maximus*, as already suggested by Smith (1998).

Interestingly, the four *Allosaurus* species from the Morrison Fm were not strictly contemporaneous, as already noticed by Loewen et al. (2003). *Allosaurus fragilis* is likely confined to the higher Brushy Basin Member of the Morrison Fm, whereas *Allosaurus 'jimmadseni'* and likely Arkhane were found in the slightly older Salt Wash Member. *Allosaurus maximus* is younger, as it was found in the uppermost layers of the Morrison Fm.

A more detailed study of the skull of Arkhane requires further preparation of this specimen: the skull has not been prepared according to scientific standards and the original and reconstructed bones cannot be separated anymore. Therefore, the skull has to be dismounted, re-prepared and remounted again from April 2018 onwards by skilled technicians. Only after this operation, a more complete and accurate description of the original elements of the skull will be possible.

It will be extremely important to study in detail the other *Allosaurus* skeletons already discovered in the Morrison Fm of Barnum-Kaycee area. Indeed, several specimens have already been excavated and sold abroad to official museums, but also to private collectors. It will be important to retrace them and to collect all available information about them. Hopefully those specimens were not too heavily affected during their preparation

process. This global study will allow to better understand the variability of the *Allosaurus* hypodigm in this limited area and to compare it with the abundant information already collected about the *Allosaurus fragilis* population from the Cleveland-Lloyd Dinosaur Quarry in Emery County, Utah.

A detailed geological survey of the Barnum-Kaycee area will also be important for better constraining the stratigraphic age of Arkhane and its fellows and to follow the micro-evolutionary patterns of the *Allosaurus* populations in western North America at the end of the Jurassic.

Table 1: Main osteological differences between the different species of *Allosaurus* from the Morrison Fm.

Character	**Arkhane**	***A. fragilis***	***A. 'jimmadseni'***	***A. maximus***
Stratigraphic age	? Salt Wash Member	Brushy Basin Member	Salt Wash Member	Top of Morrison Fm
Lacrimal corneal process	Single pneumatic recess	Two oval openings	Two small pneumatic recesses	
Jugal participates in orbital margin	Yes	Yes	No	
Ventral margin of jugal	Deflected ventrally	Deflected ventrally	Straight	
Parietal sagittal crest	Absent	Deflected Smooth	?	
Basioccipital contributes to floor of foramen magnum	Yes	Yes	No	
Nuchal crest extends up to the foramen magnum	Yes	?No	No	
Ventral extension of paroccipital processes	Up to the level of FM	Well below the level of FM	Well below the level of FM	
Caudal orientation of paroccipital processes	Slight	Pronounced	Pronounced	
Number of dentary teeth	18-19	16+/-1	19	
Surangular covers laterally the retroarticular process	No	Yes	Yes	
Rostrolateral groove on surangular	Present	Absent, one foramen present	Present	
Internal mandibular foramen on prearticular	Absent	Present	Present	
Lateral exposure of prearticular	Narrow caudal end	Absent	Absent	
Articular medial shelf	Pendant	More incipiently developed	Pendant	
Atlas ventrolateral process	Small	Absent	?	
Odontoid	Fused to axis	Unfused	Unfused	
Hypapophysis on 4th cervical vertebra	Absent	?	Present	

Continuation of Table 1

Pleurocoels on 4th vertebra	Two distinct pits	Single pit	Single pit	Two distinct pits
Elliptical depressions below contact between dorsal centrum and neural arch	Absent	Absent	Absent	Present
Extension of the pleurocoels	Up to dorsal 1	Up to dorsal 4	Up to dorsal 2	?
Horizontal lamina along the base of neural spine	Absent	Absent	Absent	Present
Infradiapophysial lamina on dorsal 4	Single	Two converging laminae	Two converging laminae	
Hyposphene-hypantrum articulation	Throughout the dorsal series	Restricted to dorsals 1-5	?	Two distinct pits
Articular surface of proximal caudal centra	Amphiplatyan	Amphiplatyan	?	Moderately procoelous
Ventral surface of proximal caudal centra	Grooved	Flat	Grooved	
Neural spine of proximal caudales	Bifid cranially	Bifid cranially	Not bifid	
Mid- and distal chevrons	Not enlarged	Not enlarged	Not enlarged	Craniocaudally enlarged
Angle between proximal and distal ends of ulna	45°	90°	45°	
Manual ungual I	2/3 the length of the radius	1/2 the length of the radius	1/2 the length of the radius	
Manual ungual III	Half the size of ungual I	Half the size of ungual I	One third the length of ungual I	
Craniocaudal length of the pubic foot/proximodistal length of the pubis	0.49	> 0.60	0.61	
Proximodistal length of the pubis/craniocaudal width of the pubic shaft	27	14	< 18	
Greatest width of the paired pubes/proximodistal length of pubis	0.51	< 0.40	< 0.40	
Femoral head in cranial view	Angled dorsomedially	Angled dorsomedially	Angled dorsomedially	

Continuation of Table 1

Dorsal extension of lesser trochanter of femur	To the level of the base of the femoral head	To the level of the mid-height of the femoral head	To the level of the mid-height of the femoral head	
Distal condyle of femur	Mesial condyle extends further distally than lateral condyle	Both condyles extend to the same level distally	Both condyles extend to the same level distally	
Rostrolateral process developed into a ventral spine that overhangs the tibial shaft	Present	Absent	Absent	
Nutrient foramen caudal to distal end of fibular crest	Absent	Present	Present	
Cross-section of shaft of metatarsal III	Rectangular, plantar surface mediolaterally flat	Triangular, dorsal side wider than plantarside	Triangular, dorsal side wider than plantarside	Rectangular, plantar surface mediolaterally flat

Potential diagnostic character for Arkhane as a new *Allosaurus* species are in red color.

ACKNOWLEDGEMENTS

We should like to thank the current owner of Arkhane for the trust he has placed in us by entrusting us with the study of this fantastic new dinosaur. The members of the private company who discovered Arkhane and Eric Mickeler kindly communicated us all the necessary information to complete this study. Aldo Impens (Raphus SPRL) and Stéphane Berton (RBINS) did an incredible job in restoring some parts of the skeleton of Arkhane. Mathilde Cathelain, Pascale Golinvaux, and Thierry Hubin helped us respectively with the drawings and the photographs illustrating this report.

APPENDICES

Appendix 1
Selected osteological measurements of Arkhane

Table 2: Selected measurements of Arkhane

Anatomical part	Measurement (in cm)
First chevron	
Total length	25.2
Width proximal end	7.2
Craniocaudal width of proximal end	3.6
Scapula (left)	
Total length	75.5
Height proximal end	18.8
Height distal end	15.0
Humerus (left)	
Total length	34.5*
Maximal craniocaudal width of head	7.0
Ulna (right)	
Total length	27.0
Craniocaudal length of proximal end	9.5
Radius (right)	
Total length	22.5
Craniocaudal length of proximal end	5.8
Metacarpal I (left)	
Total length	8.8
Greatest transverse diameter, proximal end	5.1
Greatest transverse diameter, distal end	5.3
Least transverse diameter of shaft	4.0
Phalanx I-1 (left)	
Total length	13.4
Greatest transverse diameter, proximal end	5.5
Greatest transverse diameter, distal end	4.2
Least transverse diameter of shaft	3.5
Ungual I (left)	
Total length (dorsal lip to distal tip)	16.8
Maximal dorsoventral height	8.1

Continuation of Table 2

Phalanx II-1 (left)	
Total length	9.3
Greatest transverse diameter, proximal end	4.6
Greatest transverse diameter, distal end	3.2
Least transverse diameter of shaft	2.5
Phalanx II-2 (left)	
Total length	8.4
Greatest transverse diameter, proximal end	3.3
Greatest transverse diameter, distal end	3.1
Least transverse diameter of shaft	2.8
Metacarpal III (left)	
Total length	9.8
Greatest transverse diameter, proximal end	2.7
Greatest transverse diameter, distal end	3.4
Least transverse diameter of shaft	1.2
Phalanx III-1 (left)	
Total length	4.7
Greatest transverse diameter, proximal end	2.5
Greatest transverse diameter, distal end	1.6
Least transverse diameter of shaft	1.4
Phalanx III-2 (left)	
Total length	5.7
Greatest transverse diameter, proximal end	1.8
Greatest transverse diameter, distal end	1.4
Least transverse diameter of shaft	1.2
Ungual III (left)	
Total length (dorsal lip to distal tip)	7.7*
Maximal dorsoventral height	4.5*
Pubis (left)	
Total length	71.0
Distal foot length	35.0
Minimal dorsoventral width of the shaft	2.65
Ischium (right)	
Total length	71.1
Distal foot length	12.0
Minimal dorsoventral width of the shaft	3.7

Continuation of Table 2

Femur (left)	
Total length	87.0
Circumference at midshaft	31.5
Tibia (left)	
Total length	81.5
Circumference at midshaft	27.0
Proximal head: craniocaudal diameter	25.5
Fibula (left)	
Total length	74.0
Craniocaudal width of proximal head	16.0
Craniocaudal width of distal end	70.4
Metatarsal I (right)	
Total length	8.7*
Greatest transverse diameter, distal end	4.0
Least transverse diameter of shaft	3.4
Metatarsal II (right)	
Total length	34.6
Greatest transverse diameter, proximal end	8.2
Greatest transverse diameter, distal end	7.7
Least transverse diameter of shaft	4.6
Metatarsal III (right)	
Total length	39.0
Greatest transverse diameter, proximal end	6.8
Greatest transverse diameter, distal end	8.6
Least transverse diameter of shaft	4.8
Metatarsal IV (right)	
Total length	34.6
Greatest transverse diameter, proximal end	10.6
Greatest transverse diameter, distal end	7.5
Least transverse diameter of shaft	3.4

Measurements are in cm ; * refers to estimated value

Appendix 2
List of characters used for the phylogenetic analysis

SKULL

1. **Premaxilla**, inter-premaxillary suture in adults: open (0), fused (1).
2. **Premaxilla**, height/length ratio ventral to external naris: 0.5–2.0 (0), < 0.5 (1), > 2.0 (2).
3. **Premaxilla**, subnarial process and ventral border of naris: contacts nasals, excluding maxilla from narial margin (0), reduced and separate from nasals by maxillary contribution to narial margin (1).
4. **Premaxilla**, posterior extent of nasal process relative to posterior tip of subnarial process: even (0); posterior (1).
5. **Premaxilla**, form of premaxilla-nasal suture: V-shaped (0), W-shaped (1).
6. **Premaxilla**, proportions and position anterior to external nares: shorter than premaxilla ventral to nares, angle between anterior and alveolar margins $> 75°$ (0), longer than body ventral to nares, angle $< 70°$, external naris overlaps some of the premaxillary body (1); external naris entirely posterior to premaxillary body (2).
7. **Premaxilla**, diastema ('subnarial gap') adjacent to maxilla along dentigerous margin: absent (0), present (1).
8. **Premaxilla**, mediolateral constriction of posterior portion: absent (0), present (1).
9. **Premaxilla**, development of maxillary process: well–developed (0), reduced to a short triangle (1).
10. **Premaxilla**, morphology of subnarial foramen: distinct foramen (0), expanded channel (1).
11. **Premaxilla**, articulation with maxilla: planar (0), interlocking (1).
12. **Maxilla**, development of anterior ramus: anteroposteriorly short or absent (0), moderate (1), anteroposteriorly long(2).
13. **Maxilla**, orientation of anteriormost alveolus: vertical (0), angled anteriorly (1).
14. **Maxilla**, shape of ascending ramus: smooth curve or straight (0), abruptly changes orientation (1).
15. **Maxilla**, morphology of palatal process: long, ridged or fluted prong (0), long and plate-shaped (1).
16. **Maxilla**, position of palatal process: ventral, immediately dorsal to paradental plates (0), dorsal, immediately ventral to dorsal surface of maxillary anterior ramus (1).
17. **Maxilla**, anterior end of junction between medial wall and paradental plates: horizontal (0); inclined anteroventrally (1).
18. **Maxilla**, horizontal ridge (prominent 'lingual bar') between palatal process and antorbital fenestra: absent (0), present (1).

19. **Maxilla**, depth of paradental plates relative to anteroposterior width: low, < 1.8 (0); tall > 1.8 (1).

20. **Maxilla**, ventral extent of paradental plates relative to lateral wall: as far ventral (0); fall short (1).

21. **Maxilla**, arrangement of nutrient foramina on lateral surface: single row or no distinct pattern (0), two parallel rows (1).

22. **Maxilla**, anteroventral border of antorbital fossa: graded or stepped (0), demarcated by raised ridge (1).

23. **Maxilla**, anterior margin of antorbital fossa: rounded (0); squared (1).

24. **Maxilla**, ventral extent of antorbital fossa: moderate (0), absent (1), dorsoventrally deep (2).

25. **Maxilla**, position of anterior end of antorbital fossa relative to naris: posterior (0), ventral (1).

26. **Maxilla**, development of maxillary 'fenestra': absent (0), fossa (1), fenestra (2).

27. **Maxilla**, development of promaxillary fenestra: absent (0), present but shallow (1), present and extends into anterior ramus as a canal (2).

28. **Maxilla**, dimensions of promaxillary fenestra opening: small foramen (0), large fenestra (1).

29. **Maxilla**, development of pneumatic fossa (excavatio pneumatica) in ascending process: absent (0), present (1).

30. **Maxilla**, pneumaticity on medial side of posterior section of ascending ramus: absent (0), present (1).

31. **Maxilla**, posterior end of tooth row relative to orbit: beneath (0), anterior (1).

32. **Maxilla**, articulation with jugal: slot or groove (0), lateral shelf (1).

33. **Maxilla**, anteroposterior length of jugal contact relative to total jugal length: less than 50% (0), more than 50% (1).

34. **Maxilla and nasal**, external surface texture: smooth (0), sculptured (1).

35. **Nasal**, inter-nasal contact in adults: separate (0), partly or fully fused (1).

36. **Nasal**, posterior narial margin: absent or weak fossa (0), large fossa (1), laterally splayed hood (2).

37. **Nasal**, participation in antorbital fossa: absent or at edge (0), present (1).

38. **Nasal**, antorbital fossa in lateral view: visible (0); occluded by ventrolaterally overhanging lamina (1).

39. **Nasal**, pneumatic foramina: absent (0), present (1).

40. **Nasal**, development of dorsolateral surfaces: none, nasals low and dorsally convex (0), pronounced dorsolateral rims, sometimes with lateral crests (1), tall, parasagittal crests (2), inflated and forming a hollow midline crest (3).

41. **Nasal**, sculpturing: low rugosity (0), deeply rugose, bears large excresences (1) [inapplicable in taxa that lack craniofacial rugosity].

42. **Lacrimal**, anterior process: dorsoventrally deep (0), dorsoventrally narrow, includes antorbital fossa

and rim (1), dorsoventrally narrow, antorbital fossa only (2).

43. **Lacrimal**, morphology of lateral lamina of ventral process of lacrimal: anteriormost point situated around midheight of ventral process (0); anteriormost point situated dorsal to midheight of ventral process and a distinct rugose patch is present on the lateral surface (1).

44. **Lacrimal**, dorsal and ventral portions of antorbital fossa: separated by anterior projection of lateral lamina (0), continuous, lateral lamina does not project far anteriorly (1).

45. **Lacrimal**, lacrimal fenestra morphology: absent (0); present as small foramen (1); present as large oval opening with associated dorsal rugosity, swelling or 'horn' (2).

46. **Lacrimal**, openings in lacrimal recess: single (0), multiple (1).

47. **Lacrimal**, horn morphology: small rugosity (0); low, broad, rugose bar (1); triangular horn (2).

48. **Lacrimal**, suborbital process: absent (0), present (1).

49. **Lacrimal**, angle between anterior and ventral rami: $\sim 90°$(0), $< 75°$ (1).

50. **Lacrimal**, length of anterior process relative to ventral process: subequal (0), $\sim$75% (1).

51. **Jugal**, position of anterior end: posterior to internal antorbital fenestra, but reaching its posterior rim (0), excluded from internal antorbital fenestra (1), expressed at rim of internal antorbital fenestra, with distinct anterior process extending beneath it (2).

52. **Jugal**, pneumatisation: absent (0), internally hollowed and transversely inflated by foramen in posterior rim of antorbital fossa (1).

53. **Jugal**, antorbital fossa: absent (0), present (1).

54. **Jugal**, morphology of lacrimal articulation: abuts, no flange (0), overlapping, flange present (1).

55. **Jugal**, orientation of orbital margin: angled posterodorsally (0), vertical (1).

56. **Jugal**, dorsoventral size of posterior process: shallow (0), deep (1).

57. **Postorbital**, articulation with jugal: planar (0), grooved, ventral process with U-shaped cross-section (1).

58. **Postorbital**, suborbital flange: absent (0), present as small eminence (1), present as large flange (2).

59. **Postorbital**, ventral extent relative to ventral margin of orbit: substantially above (0), approximately same level (1).

60. **Postorbital**, participation in supratemporal fossa: fossa extends onto dorsal surfaces of anterior and posterior processes (0), anterior process only (1), posterior process only (2).

61. **Supraorbital shelf**, formed mostly by 'palpebral': absent (0), present (1).

62. **Postorbital**, anterior prominence: absent or small (0), large (1), contacts lacrimal (2).

63. **Postorbital**, articulation with squamosal: tongue-in-groove (0), helical (1).

64. **Laterosphenoid**, articulations: frontal and postorbital (0), postorbital only (1).

65. **Prefrontal**, condition in adults: separate, moderate (0), separate, reduced (1), partly or completely fused to postorbital (1).

66. **Prefrontal**, articulation with frontal: planar (0), peg-and-socket (1).

67. **Frontal**, exposure along orbital rim: broad (0), narrow or absent (1).

68. **Parietal**, articulation with supraoccipital: abuts (0), overlaps (1).

69. **Parietal**, development of median skull table: flat and broad (0), narrow with sagittal crest (1), very broad, widely separating upper temporal fenestrae (2).

70. **Parietal**, size and elevation of nuchal wedge and alae: moderate (0), tall and expanded (1).

71. **Supratemporal fossa**, anteromedial corner: open dorsally (0); partially roofed over by a small shelf of the frontalparietal (1).

72. **Squamosal**, constriction of lower temporal fenestra: absent (0), present (1).

73. **Squamosal**, anterodorsal lamina: emarginated by upper temporal fenestra (0); continuous (1).

74. **Squamosal**, flange covering quadrate head laterally: absent (0), present (1).

75. **Squamosal**, articulation with quadratojugal: at tip (0), absent (1), broad (2).

76. **Quadratojugal**, anteriormost point of ventral process relative to lower temporal fenestra: ventral (0), anterior (1).

77. **Quadrate**, pneumatisation: absent (0), present (1).

78. **Quadrate**, height of dorsal ramus relative to orbit height: less (0), greater (1).

79. **Quadrate**, axis in posterior view: vertical (0), oblique (1).

80. **Quadrate**, height of pterygoid flange relative to complete bone: 2/3 (0) subequal (1).

81. **Quadrate foramen**, present (0), absent (1).

82. **Quadrate**, axis in lateral view: vertical (0), anterior (1), posterior (2).

83. **Quadrate**, head shape in dorsal view: oval (0), subrectangular (1).

84. **Quadrate**, medial foramina adjacent to condyles: absent (0), present (1).

85. **Paroccipital process**, position of ventral rim of base relative to occipital condyle: at same level (0), below (1).

86. **Paroccipital process**, position of ventral edge of distal end relative to occipital condyle: at or above dorsal border of condyle, process approximately horizontal or dorsolaterally inclined (0), at or below mid-height of condyle, process ventrolaterally oriented (1).

87. **Supraoccipital**, anteroposterior depth of median ridge relative to occipital condyle length: less (0), greater (1).

88. **Supraoccipital**, width of knob relative to foramen magnum diameter: equal (0), 1.5x (1).

89. **Supraoccipital**, participation in foramen magnum: absent, exoccipitals contact dorsally (0), narrow, separating exoccipitals on dorsal edge of foramen (1), wide, supraoccipital extends ventrolaterally around foramen magnum (2).

90. **Basioccipital**, ventrolateral pair of pneumatic cavities invading neck of occipital condyle and joining medially: absent (0), present (1).

91. **Basioccipital**, sharp dorsoventrally oriented lamina situated immediately ventral to occipital condyle: absent (0), present (1).

92. **Basioccipital**, fossa ventral to occipital condyle in basioccipital apron: narrow and groove-like, one-half or less the width of the occipital condyle (0), broad depression approximately two-thirds the width of occipital condyle (1).

93. **Basioccipital**, notch along contact with exoccipital-opisthotic: absent (0), present (1).

94. **Basioccipital**, width of basal tubera relative to occipital condyle width: $\geq$ (0), $<$ (1).

95. **Basisphenoid**, location of basipterygoid processes relative to basal tubera: anterior or slightly anteroventral, basisphenoid recess opens ventrally (0), ventral, basisphenoid recess narrow and opens posteroventrally (1), anteroventrally, basisphenoid recess opens posteroventrally (2).

96. **Basisphenoid**, depth of basisphenoid recess: shallow (0), very deep (1).

97. **Basisphenoid**, shape of opening for basisphenoid recess: ovoid (0), teardrop-shaped (1).

98. **Basisphenoid**, depth of indentation between basal tubera and basipterygoid processes: deep notch (0), shallow embayment (1).

99. **Basisphenoid**, proportions of basipterygoid processes: elongate (0), broad (1).

100. **Braincase**, number of foramina (representing cranial nerves XII, XI and X) exiting ventrolateral to occipital condyle: two (0); three (1).

101. **Braincase**, ventral extension of subcondylar recess: pronounced (0); shallow/absent (1); narrow incisure (2).

102. **Braincase**, shape of ventral margin of paroccipital process and stapedial groove/foramen ovale: open curve (0); acute/closed curve (1).

103. **Braincase**, anteroposterior angle of occiput in lateral view: vertical (0), sloping anterodorsally–posteroventrally (1).

104. **Braincase**, morphology of trigeminal foramen: single (0), partly split (1), fully split (2).

105. **Braincase**, median ridge separating exits of left and right sixth cranial nerves: present (0), absent (1).

106. **Braincase**, number of tympanic recesses: two (0), three (1).

107. **Braincase**, internal carotid pneumatization: absent (0), fossa (1), opening (2).

108. **Braincase**, ossification of interorbital region: weak or absent (0), extensive, ossified sphenethmoid and interorbital septum (1).

109. **Palatine**, shape: triradiate (0), tetraradiate, well-developed jugal process (1).

110. **Palatine**, anteroposterior extent of maxillary flange: short (0), extended (1).

111. **Palatine**, morphology of jugal process: tapered process (0), expanded process (1).

112. **Palatine**, orientation of maxillary contact: lateral (0), ventral (1).

113. **Palatine**, pneumatic recess: absent (0), present (1).

114. **Pterygoid**, pocket on ectopterygoid flange: absent (0), present (1).

115. **Ectopterygoid**, dorsoventral depth: narrow (0), deep (1).

116. **Ectopterygoid**, ventral fossa: absent (0), present (1).

117. **Ectopterygoid**, lateral depth of ectopterygoid fossa: shallow (0), deep (1).

118. **Mandible**, size of external mandibular fenestra: small to moderate (0), large (1).

119. **Mandible**, position of anterior end of external mandibular fenestra relative to last dentary tooth: posterior (0), ventral (1).

120. **Dentary**, shape of anterior end in lateral view: blunt and unexpanded (0), dorsoventrally expanded, rounded, and slightly upturned (1), 'squared off' in lateral view via anteroventral process (2).

121. **Dentary**, size of mesialmost alveoli: subequal (0), third alveolus circular and enlarged (1).

122. **Dentary**, shape in dorsal view: straight (0), curves anteromedially (1).

123. **Dentary**, paradental groove: narrow along entire length (0), wide anteriorly defining a distinct gap between medial dentary wall and paradental plates (1).

124. **Dentary**, longitudinal groove housing dorsally situated row of neurovascular foramina on lateral surface: absent or weak (0), present and well-defined (1).

125. **Dentary**, number of Meckelian foramina: one (0), two (1).

126. **Dentary**, morphology of posterior end: notched by external mandibular fenestra (0), straight or slightly concave (1).

127. **Dentary**, morphology of surangular articulation just above external mandibular fenestra: small notch (0), large socket (1).

128. **Splenial**, contour of posterior edge: straight (0), curved (1), notched (2).

129. **Splenial**, size of splenial ('mylohyoid') foramen: small (0), large (1).

130. **Splenial**, foramen in ventral part: completely enclosed by bone (0), open anteroventrally (1).

131. **Surangular**, horizontal ridge on lateral surface below mandibular joint: weak or absent (0), strong (1).

132. **Surangular**, number of posterior surangular foramina: one (0), two (1).

133. **Mandibular glenoid**, morphology of medial edge: flat or rounded (0), projecting (1).

134. **Mandibular glenoid**, development of anterior wall: weak (0), tall (1).

135. **Retroarticular process**, length: long (0), blunt (1).

136. **Retroarticular process**, mediolateral width relative to posterior width of dentary: $\leq$ (0), $>$ (1).

137. **Retroarticular process**, orientation of attachment surface: posterodorsal (0), posterior (1).

138. **Paradental plates**, continuity and replacement groove: separated, groove present (0), forming a continuous medial lamina ('fused'), groove absent (1).

139. **Paradental plates**, visibility in medial view: widely exposed, subpentagonal and moderate–tall (0), obscured by medial wall of dentary, triangular apices only may be visible (1).

140. **Paradental plates**, surface texture: smooth (0), vertically striated or ridged (1).

141. **Teeth**, curvature: present, marked (0), reduced or absent (1).

142. **Teeth**, crown striations: absent (0), present (1).

143. **Teeth**, enamel wrinkles: absent (0), present, extending as bands across labial and lingual tooth surfaces (1), pronounced marginal enamel wrinkles (2).

144. **Teeth**, mid-crown cross-section: elliptical (0), circular (1).

145. **Teeth**, root shape: broad (0), tapered (1).

146. **Teeth**, maxillary and dentary, serrations: present (0), absent (1).

147. **Teeth, maxillary and dentary**, extent of anterior carina: to base of crown (0), at mid-height of crown or more dorsally (1).

148. **Premaxillary teeth**, arrangement of carinae: nearly symmetrical, on opposite sides (0), more asymmetrical, both on lingual side (1).

149. **Premaxillary teeth**, serrations: present (0), absent (1).

150. **Premaxillary teeth**, number: four (0), three (1), five (2), six/seven (3).

151. **Premaxillary teeth**, spacing: even (0), paired and spaced (1).

152. **Premaxillary teeth**, size of tooth 1 relative to others: subequal (0), smaller (1).

153. **Maxillary teeth**, number: $>$ 17 (0), 11–17 (1), $<$ 11.

154. **Maxillary teeth**, mid-tooth spacing: adjacent (0), with diastemata (1).

155. **Dentary teeth**, size and number relative to maxillary teeth: approximately equal (0), smaller and approximately 1.5 times as numerous (1).

AXIAL SKELETON

156. **Presacral vertebrae**, anterior face of anterior elements: flat (0), convex (1).

157. **Presacral vertebrae**, pleurocoel posterior to parapophysis (anterior pleurocoel) in anterior elements: absent (0), present (1).

158. **Presacral vertebrae**, posterior pleurocoel in anterior elements: absent (0), present (1).

159. **Presacral vertebrae**, vertebrae, extent of anterior pleurocoel: to D4 (0), to sacrum (1).

160. **Vertebrae**, internal structure of pneumatic centra: absent, 'pleurocoels' if present, form fossae, not foramina (0), camerate (1), camellate (2).

161. **Atlas**, length of epipophyses: moderate (0), elongate (1).

162. **Axis**, spinous process shape: dorsal end expanded transversely (0), tapers mediolaterally (1).

163. **Axis**, orientation of intercentrum ventral surface: horizontal or slightly anteroventral (0), tilted anterodorsally (1).

164. **Axis**, length of epipophyses: moderate (0), long (1), short (2).

165. **Axis**, morphology of spinopostzygapophyseal lamina: broad, well-developed (0), invaginated (1).

166. **Axis**, development of parapophyses: moderate/large (0), reduced/absent (1).

167. **Axis**, development of diapophyses: moderate (0), reduced or absent (1).

168. **Axis**, pleurocoels: absent (0), present (1).

169. **Cervical vertebrae**, morphology of anterior pleurocoel: single opening (0), two openings oriented anteroventralposterodorsal or very plastic morphology (1).

170. **Cervical vertebrae**, middle, shape of anterior pleurocoel: round (0), anteroposteriorly elongate (1).

171. **Cervical vertebrae**, anterior, ventral keel: present (0), absent or weak ridge (1).

172. **Cervical vertebrae**, anterior, demarcation of dorsal surface of neural arch from diapophyseal surface: gently sloping (0), ridge (prominent prezygapophyseal–epipophyseal lamina) (1).

173. **Cervical vertebrae**, position of parapophysis on centrum: anterior (0), middle (1).

174. **Cervical vertebrae**, articular surface of prezygapophyses: planar (0), flexed (1).

175. **Cervical vertebrae**, perimeter of anterior articular surface: not rimmed by a flattened peripheral band (0), flat, forming a distinct rim (1).

176. **Cervical vertebrae**, anterior, transverse distance between prezygapophyses relative to width of neural canal: $<$ (0), $>$, prezygapophyses situated lateral to neural canal (1).

177. **Cervical vertebrae**, anterior, morphology of epipophyses: low, blunt (0), long, thin (1), long, robust (2).

178. **Cervical vertebrae**, anteroposterior length of neural spines: nearly as long as centrum (0), $\leq 75\%$ centrum length (1).

179. **Cervical vertebrae**, longest post-axial elements: first five (0), last five (1).

180. **Cervical vertebrae**, middle, length/height ratio of centra: less than 3 (0), more than 3 (1).

181. **Dorsal vertebrae**, pneumaticity/webbing at base of neural spines: absent (0), present (1).

182. **Dorsal vertebrae**, accessory centrodiapophyseal lamina: absent (0), present (1).

183. **Dorsal vertebrae**, size of infraprezygapophyseal fossa: small (0), expanded (1).

184. **Dorsal vertebrae**, anterior, ventral keel: absent or developed as a weak ridge (0), pronounced, around 1/3 the height of centrum and inset from lateral surfaces (1).

185. **Dorsal vertebrae**, anterior, size of pneumatic foramen in centrum: small (0); enlarged (1).

186. **Dorsal vertebrae**, elevation of parapophyses: slightly elevated from centrum (0), project far laterally, more than half the diapophyseal length (1).

187. **Dorsal vertebrae**, orientation of hyposphene laminae: diverge ventrolaterally (0), parallel and sheet-like (1).

188. **Dorsal vertebrae**, position of parapophyses in posteriormost elements: on the same level as transverse process (0); distinctly below transverse process (1).

189. **Dorsal vertebrae**, distinct step-like ridge lateral to hyposphene, running posterodorsally from dorsal border of neural canal to posterior edge of postzygapophyses: absent (0); present (1); ridge present and is developed into a prominent lamina that bisects the infrapostzygapophyseal fossa in posterior dorsal vertebrae (2).

190. **Dorsal vertebrae**, middle and posterior, postzygapophyses with tab-like lateral extensions of articular facets: absent (0); present (1).

191. **Dorsal vertebrae**, morphology of neural spines: transversely compressed sheets (0), transversely broad anteriorly and posteriorly, central regions of lateral surface embayed by deep vertical troughs (1).

192. **Dorsal vertebrae**, posterior, inclination of neural spines: vertical or posterior (0), anterior (1).

193. **Dorsal vertebrae**, height of neural spines relative to centrum height: low, $\leq$ 1.3x (0), moderate, 1.4-1.8x (1); tall, $\geq$ 2.0x (2).

194. **Dorsal vertebrae**, posterior, centrum constriction: weak (0), strong (1).

195. **Dorsal vertebrae**, centrum length relative to height: more than 2 (0), less than 2 (1).

196. **Sacral vertebrae**, centrum pneumaticity: absent (0), pleurocoelous fossae (1); pneumatic foramina (2).

197. **Sacral vertebrae**, number: 2 (primordial sacrals only) (0), 5 (1 dorsosacral, 2 caudosacrals) (1), 6 (2 dorsosacrals, 2 caudosacrals) (2).

198. **Sacral vertebrae**, transverse dimensions of middle centra relative

to other sacrals: equivalent (0), constricted (1).

199. **Sacral vertebrae**, orientation of ventral margin of middle centra: approximately horizontal (0), strongly arched (1).

200. **Sacral vertebrae**, dorsal edge of neural spines: as thin as remainder of spine (0), transversely thickened (1).

201. **Sacral vertebrae**, pneumaticity of neural arches: weak or absent (0), paired fossa ventral to diapophyses (1).

202. **Caudal vertebrae**, anterior, morphology of ventral surface: flat (0), groove (1), ridge (2).

203. **Caudal vertebrae**, L-shaped neural spines: absent (0), present (1).

204. **Caudal vertebrae**, pleurocoels (large pneumatic foramina in centrum): absent (0), present (1).

205. **Caudal vertebrae**, vertebrae, anterior, centrodiapophyseal laminae on neural arch: weak or lacking (0), as prominent as in dorsal vertebrae, defining deep infradiapophyseal fossa that penetrates neural arch (pneumatic) (1).

206. **Caudal vertebrae**, anterior, proportions of neural arch base relative to centrum proportions: $<$ (0), $\geq$ (1).

207. **Caudal vertebrae**, middle, morphology of neural spines: rod-like and posteriorly inclined (0), subrectangular and sheet-like (1), rod-like and vertical (2).

208. **Cervical ribs**, articulation with cervical vertebrae in adults: separate (0), fused (1).

209. **Cervical ribs**, length of anterior process: short (0), long (1).

210. **Gastralia**, posteriormost gastral segments: separate (0), united into single, boomerang-shaped elements (1).

211. **Sacral ribs**, articulations in adults: separate (0), fused together (1).

212. **Sacral ribs**, position of posterior attachment to ilium: ventral (0), posterodorsal (1).

213. **Sacral ribs**, depth relative to ilium height: $<$ 85% (0), $\geq$ 90% (1).

214. **Chevrons**, morphology in middle caudal vertebrae: rodlike or only slightly expanded ventrally (0), L-shaped (1).

215. **Chevrons**, proximal articular surface: divided into anterior and posterior facets by distinct transverse ridge (0), no ridge, but low lateral mounds may be present, one on each side (1).

216. **Chevrons**, curvature: straight or gently curved (0), strongly curved (1).

217. **Chevrons**, anterior process: absent (0); present (1).

218. **Chevrons**, morphology of distal end in anterior and middle elements: expanded anteroposteriorly (0), unexpanded, tapers ventrally (1).

APPENDICULAR SKELETON

219. **Scapula**, angle between blade and acromion: gradual, oblique (0), abrupt, perpendicular (1).

220. **Scapula**, size of acromion process: moderate (0), marked (1).

221. **Scapula**, midshaft expansion of blade: absent (0), present (1).

222. **Scapula**, distal expansion of blade: marked (0), weak/absent (1).

223. **Scapula**, width ratio of blade: ≤ 7 (0), 7.5–9 (1), > 10 (2).

224. **Scapulocoracoid**, shape of anterior margin: indented or notched between acromial process and coracoid suture (0), smoothly curved and uninterrupted across scapula–coracoid contact (1).

225. **Scapulocoracoid**, glenoid lip: moderate (0), marked (1).

226. **Coracoid**, development of posteroventral process: low, rounded posteroventral eminence (0), pronounced, posteroventrally tapering process (1).

227. **Coracoid**, development of biceps tubercle (= acrocoracoid process): absent or poorly developed (0), conspicuous and well developed as tuber (1), developed as a posteroventrally oriented ridge (2).

228. **Coracoid**, prominent fossa on ventral surface posteroventral to glenoid (subglenoid fossa): absent (0); present (1).

229. **Humerus**, shape of head: elongate (0), globular (1).

230. **Humerus**, longitudinal torsion of shaft: absent (0), present (1).

231. **Humerus**, size of trochanters relative to midshaft diameter: $<$ (0), $>$ 150% (1) $>$ 250% (2).

232. **Humerus**, development of internal tuberosity: low/rounded (0), hypertrophied (1).

233. **Humerus**, length of deltopectoral crest relative to total bone length: $<$ 0.4 (0), 0.43–0.49 (1) $>$ 0.52 (2).

234. **Humerus**, height of deltopectoral crest: low (0), prominent (1).

235. **Humerus**, orientation of deltopectoral crest apex: anteriorly (0), anterolaterally (1).

236. **Humerus**, relative orientation of proximal distal condyles in anteroposterior view: parallel, humerus straight (0), distal canted (1).

237. **Humerus**, anterior surface of bone adjacent to ulnar condyle: smooth or gently depressed (0), bears well-defined fossa (1).

238. **Humerus**, shape of distal condyles: rounded (0), flattened (1).

239. **Radius and ulna**, development of radial external tuberosity and ulnar internal tuberosity: low, rounded (0), hypertrophied distal ends of radius and ulna broadened (1).

240. **Radius**, shaft: straight (0); curves laterally (1).

241. **Radius**, development of medial biceps tubercle: small or indistinct (0), hypertrophied (1).

242. **Ulna**, olecranon process: absent (0), present (1).

243. **Ulna**, morphology of olecranon process: transversely robust (0); transversely compressed and 'blade-like' (1).

244. **Ulna**, crest extending distally along posterior surface from olecranon process: absent (0), present (1).

245. **Ulna**, hypertrophied medial and lateral processes on proximal end: absent (0), present (1).

246. **Ulna**, length relative to minimum circumference: stout, < 2.3 (0); gracile > 2.6 (1).

247. **Carpus**, morphology and articulations of distal carpals: separate dc1 and dc2 over separate metacarpals, flattened proximodistally (0), fused dc1 and dc2, dc1 overlaps metacarpals I and II, flattened proximodistally (1), fused dc1 and dc2, dc1 overlaps metacarpals I and II, strongly arched proximodistally (2).

248. **Manus**, length relative to length of arm + forearm: $<$ (0), $\geq$ (1).

249. **Manus**, composition: digit IV and V present (0), digit IV present, digit V absent (1), MC IV present, IV phalanges and digit V absent (2), digits IV and V absent (3).

250. **Manual digits**, lengths: III longest (0), II longest (1).

251. **Metacarpals**, transverse width of proximal articular ends relative to minimum transverse shaft width: $<$ (0), $\geq$ 2x (1).

252. **Metacarpal I**, length to minimum width ratio: 1.4–1.9 (0), $\geq$ 2.4 (1).

253. **Metacarpal I**, length relative to length of metacarpal II: $>$ 50% (0), $<$ 50% (1).

254. **Metacarpal I**, extent of contact with metacarpal II relative to shaft length: $<$ 1/3 (0), 1/2 (1).

255. **Metacarpal I**, angle between facet for metacarpal II and proximal articular facet: perpendicular (0), obtuse (1).

256. **Metacarpal III**, position of base relative to those of other metacarpals: at same level (0), on palmar surface (1).

257. **Metacarpal III**, shape of proximal end: rectangular (0), triangular (1).

258. **Metacarpal III**, width relative to width of metacarpal II: $>$ 50% (0), $<$ 50% (1).

259. **Manual ungual I**, length:height ratio: $<$ 2.5x (0), $>$ 2.5x (1).

260. **Manual unguals**, proximal height:width ratio: transversely broad, $<$ 2.0 (0), transversely narrow, $>$ 2.4 (1).

261. **Pelvic elements**, articulations in adults: separate (0), fused (1).

262. **Ilium**, large external pneumatic foramina and internal spaces: absent (0), present (1).

263. **Ilium**, vertical ridge on lateral surface of blade dorsal to acetabulum: absent (0), low swollen ridge (1), low double ridge (2).

264. **Ilium**, posterior width of brevis fossa: subequal to anterior width, fossa margins subparallel (0), twice anterior width, fossa widens posteriorly (1).†

265. **Ilium**, height of lateral wall of brevis fossa relative to medial wall: taller along whole length (0), shorter anteriorly, exposing medial wall in lateral view (1).

266. **Ilium**, morphology between supraacetabular crest and brevis shelf on lateral surface: gap (0), continuous ridge (1).

267. **Ilium**, ventrolateral development of supraacetabular crest: large pendant 'hood' (0), reduced shelf (1).

268. **Ilium**, orientation of pubic peduncle: mostly ventral (0), mostly anterior or 'kinked' double facet with anterior and ventral components (1).

269. **Ilium**, shape of acetabular margin of pubic peduncle: transversely convex or flat (0); transversely concave (1).

270. **Ilium**, relative sizes of pubic and ischial articulations: subequal (0), pubic articulation $\geq$ 130% of iliac articulation (1).

271. **Ilium**, morphology of ischial peduncle: rounded (0), acuminate (1).

272. **Ilium**, pubic peduncle length to width ratio: $\leq$ 1 (0), 1.3–1.75 (1), $>$ 2 (2).

273. **Ilium**, ridge on medial surface adjacent to preacetabular notch: absent (0), present (1), strongly developed, forming a shelf (2).

274. **Ilium**, preacetabulum length relative to anterior edge of pubic peduncle: reaches anteriorly to same point as ('brachyiliac') (0), or well past ('dolichoiliac') (1).

275. **Ilium**, depth of preacetabular process: shallow (0), deep (1).

276. **Ilium**, anteroventral lobe of preacetabular process: absent (0), present (1).

277. **Ilium**, shape of dorsal margin: convex (0), straight (1).

278. **Ilium**, postacetabulum length relative to ischial peduncle length: $\leq$ (0), $>$ (1), 2x (2).

279. **Ilium**, depth of postacetabular process: shallow (0), deep (1).

280. **Ilium**, shape of posterior margin of postacetabular process: convex (0), concave (1), straight (2), with prominent posterodorsal process but lacking posteroventral process (3).

281. **Puboischiadic plate**, morphology and foramina/ notches: fully closed along midline, 3 fenestrae (0), open along midline, 1 fenestra (obturator foramen of pubis) and 1–2 notches (1), open along midline, 0 fenestrae, 1–2 notches (2).

282. **Pubis**, shaft orientation: straight (0), ventrally curved (1).

283. **Pubis**, articulation between apices in adults: unfused (0); fused (1).

284. **Pubis**, contact between distal portions: separate distally (0), contacting (1), contacting with slit-like opening proximal to distal expansion (interpubic fenestra) (2).

285. **Pubis**, angle between long axes of shaft and boot: 75–9° (0), $<$ 60° (1).

286. **Pubis**, morphology of symphysis: marginal (0), broad (1).

287. **Pubis**, morphology of obturator foramen: small and subcircular (0), large and oval (1).

288. **Pubis**, anterior expansion of distal end: absent (0), present (1).

289. **Pubis**, boot length relative to shaft length: $<$ (0), $>$ 30% (1), $>$ 60% (2).

290. **Pubis**, shape of boot in ventral view: broadly triangular (0), narrow, with subparallel margins (1).

291. **Pubis**, articulation with ilium: planoconcave (0), peg-and-socket (1).

292. **Ischium**, length relative to pubis length: 75–80% (0), ≤ 70% (1), > 80% (2).

293. **Ischium**, shaft orientation: straight (0), ventrally curved (1).

294. **Ischium**, articulation with ilium: planoconcave (0), peg-and-socket (1).

295. **Ischium**, morphology of antitrochanter: large and notched (0), reduced (1).

296. **Ischium**, notch ventral to obturator process: absent (0), present (1).

297. **Ischium**, morphology of symphysis: unexpanded (0), expanded as apron (1).

298. **Ischium**, cross-sectional shape of paired midshafts: oval (0), heart shaped, medial portions of shafts extend posteriorly as midline flange (1).

299. **Ischium**, morphology of distal end: rounded (0), expanded, triangular (1).

300. **Ischium**, articulation at distal end in adults: separate (0), fused (1).

301. **Femur**, head orientation: 45 anteromedial (0), 10–30° anteromedial (1), medial (2).

302. **Femur**, head angle: ventromedial (0), horizontal (medial) (1), dorsomedial (2).

303. **Femur**, groove on proximal surface of head oriented oblique to long axis of head ('articular groove'): absent (0), present (1).

304. **Femur**, oblique ligament groove on posterior surface of head: shallow, groove bounding lip does not extend past posterior surface of head (0), deep, bound medially by welldeveloped posterior lip (1).

305. **Femur**, placement of lesser trochanter relative to femoral head: does not reach ventral margin (0), rises past ventral margin (1), rises to proximal surface (2).

306. **Femur**, morphology of anterolateral muscle attachments at proximal end: continuous trochanteric shelf (0), distinct lesser trochanter and attachment bulge (1).

307. **Femur**, development of fourth trochanter: prominent semioval flange (0), very weak or absent (1).

308. **Femur**, distinctly projecting accessory trochanter (derived from lesser trochanter): weak, forms slightly thickened margin of lesser trochanter (0), present as triangular flange (1).

309. **Femur**, *M. femorotibialis externus* origin medially on anterodistal surface: faint, small rugose patch (0), pronounced rugose depression that extends to distal femur (1).

310. **Femur**, development of medial epicondyle: rounded (0), ridge (1).

311. **Femur**, distal extensor groove: absent (0), present (1).

312. **Femur**, morphology and orientation of tibiofibularis crest: broad (0), narrow, longitudinal (0), lobular, oblique (2).

313. **Femur**, infrapopliteal ridge connecting medial distal condyle and crista tibiofibularis: absent (0), present (1).

314. **Femur**, orientation of long axis of medial condyle in distal view: anteroposterior (0), posterolateral (1).

315. **Femur**, projection of lateral and medial distal condyles: approximately equal (0), lateral projects distinctly further than medial, distal surface of medial is gently flattened (1).

316. **Femur**, morphology of distal end: central depression connected to crista tibiofibularis by a narrow groove (0), anteroposteriorly oriented shallow trough separating medial and lateral convexities (1).

317. **Tibia** lateral malleolus: backs astragalus (0), overlaps calcaneum (1).

318. **Tibia** shape of edge of lateral malleolus: smoothly curved (0), tabular notch (1).

319. **Tibia** morphology of distal cnemial process: rounded (0), expanded proximodistally (1).

320. **Tibia** morphology of lateral (fibular) condyle: large (0), small and lobular (1).

321. **Tibia** anterolateral process of lateral condyle: absent or horizontal projection (0), prominent, curves ventrally (1).

322. **Tibia** anteromedial buttress for astragalus: absent (0), ventral (1), marked oblique step-like ridge (2), reduced oblique ridge (3), bluntly rounded vertical ridge on medial side (4).

323. **Tibia** morphology of fibular crest: narrow (0), bulbous (1).

324. **Tibia** development of fibular crest: extends to proximal end of tibia as high crest (0), extends to proximal end of tibia as low ridge (1), does not extend to proximal end of tibia (2).

325. **Fibula** depth of fibular fossa on medial aspect: groove (0), shallow fossa (1), deep fossa (2).

326. **Fibula** position of fibular fossa on medial aspect: posterior edge (0), central (1).

327. **Fibula** size of iliofibularis tubercle: faint scar (0), large (1), anterolaterally curving flange (2).

328. **Fibula** size of proximal end relative to width of proximal tibia: $< 75\%$ (0), $\geq 75\%$ (1).

329. **Astragalus** articulation between ascending process and fibula in adults: separate (0), fused (1).

330. **Astragalus** orientation of distal condyles: ventral (0), 30-45° anterior (1).

331. **Astragalus** ascending process morphology: absent (0), blocky (1), laminar (2).

332. **Astragalus** angle of dorsal margin of ascending process: low and oblique (0), high and oblique (1).

333. **Astragalus** ascending process height relative to depth of astragalar body: less (0), subequal (1), $>$ 1.6 times (2).

334. **Astragalus** prominent proximolateral extension: absent (0); present (1).

335. **Astragalus** round fossa at base of ascending process: absent (0), small (1), large (2).

336. **Astragalus** development of articular surface for distal end of fibula: large, dorsal (0), reduced, lateral (1).

337. **Astragalus** posterolateral crest: absent (0), present (1).

338. **Astragalus** posteromedial crest: absent (0), present (1).

339. **Astragalus** articulation with calcaneum in adults: separate (0), fused (1).

340. **Metatarsal I** length relative to length of metatarsal II: $\geq$ 50% (0), $<$ 50% (1).

341. **Metatarsal III** shape of proximal end: rectangular (0), shallow notch (1), deep notch (2).

342. **Metatarsal III** midshaft cross-sectional shape: rectangular (0), wedge-shaped, plantar surface pinched (1).

343. **Metatarsal III** relative proportions of shaft: short and thick, length:transverse width ratio $<$ 12.0 (0), long and gracile, ratio $>$ 12.5 (1).

344. **Metatarsal IV** proportions of distal end: broader than tall (0), taller than broad (1).

345. **Metatarsal V** morphology of distal end: articular (0), non-articular (1).

346. **Metatarsal V** length relative to length of metatarsal IV: $>$ 50% (0), $<$ 50% (1).

347. **Antarctometatarsus** absent (0), present (1).

348. **Pedal unguals** morphology of lateral and medial grooves: single (0), double (1).

349. **Pedal unguals** digits III and IV, cross-sectional shape: triangular (0), elliptical (1).

350. **Pedal unguals** digit II, mediolateral symmetry: symmetrical (0), asymmetrical (1).

351. **Pedal digit phalanges** length of I-1 + I-2 relative to III-1: greater (0), less than or equal (1).

Appendix 3
Phylogenetic coding of Arkhane, *Allosaurus fragilis*, and *Allosaurus 'jimmadseni'*

Arkhane

0 0 1 0 ? 0 0 0 0 ? 0 ? 0 0 ? ? ? ? ? ? 0 0 0 0 1 2 ? ? ? ? 1 1 0 0 ? ? 1 0 ? 1 0 0 0 ? 2
0 2 0 0 0 1 0 1 1 1 0 0 0 0 ? 0 1 ? ? ? ? 1 1 ? 0 ? 1 1 0 2 0 0 0 0 ? 0 2 ? 0 0 0 0 ? 1
0 0 0 1 1 0 1 ? ? ? ? ? ? ? ? ? ? ? 0 ? ? ? ? ? ? ? ? ? 0 0 0 ? 0 0 0 1 1 0 ? ? ?
1 1 1 1 1 1 1 1 0 0 0 0 1 0 ? 0 1 1 0 2 0 0 ? 0 1 1 1 0 0 ? 0 ? 0 ? ? ? ? 1 1 ? 0 ? 0
0 0 ? 0 1 ? ? 0 0 1 0 0 0 1 1 0 0 0 0 0 1 1 ? ? ? ? ? ? 1 1 0 0 0 0 0 ? ? ? ? ? 1 ? 1
1 0 1 1 0 1 2 0 0 ? ? ? 0 ? ? ? ? ? ? ? 1 0 0 0 0 1 0 0 0 1 ? 0 3 1 0 0 1 ? 1 1 1 ? 0
0 0 ? 2 0 1 2 0 1 ? 1 1 0 0 2 0 0 1 1 1 0 0 0 2
2 0 1 1 1 0 1 1 1 1 0 0 0 2 1 1 0 0 1 0 2 0 2 2 1 0 1 0 1 1 1 1 0 2 1 1 1 0 1 2 0 0 1 1 1 0 0 1 0 1

Allosaurus fragilis

0 0 1 0 1 [01] 0 0 0 0 0 1 0 0 0 1 0 1 0 0 0 0 0 0 0 0 2 1 0 1 1 1 1 0 0 0 1 1 0 1 1 0 0 0
0 2 1 2 [01] 0 0 1 0 1 1 1 0 0 0 0 0 0 0 1 0 1 1 1 1 1 0 0 0 1 1 0 2 0 0 0 0 0 0 2 0 0 1
1 0 1 1 0 0 0 1 1 0 1 0 0 1 0 0 1 0 2 0 1 2 0 1 1 1 1 1 1 1 1 1 1 0 0 0 0 0 0 0 1 1 0 2 0
1 1 1 1 1 1 1 1 1 0 0 0 0 1 0 0 0 1 1 0 2 0 0 1 0 0 1 1 0 0 1 ? 0 0 1 1 0 0 1 0 [01] 1
0 0 0 0 1 0 1 1 0 0 0 1 0 0 0 1 1 0 0 0 0 0 0 1 1 1 1 0 0 0 0 1 1 0 0 0 0 0 0 0 0 0 1 0 1 ?
1 1 0 1 1 0 1 2 0 0 1 2 0 0 1 1 1 0 1 0 1 1 0 0 0 0 1 0 0 0 1 1 0 3 1 0 0 1 1 1 1 1 1 1 0
0 0 0 1 1 1 0 1 0 0 1 0 2 1 1 1 1 0 1 1 0 2 0 1 2 1 1 ? 1 2 0 0 2 0 0 1 1 1 0 0 0 [12]
1 0 1 1 1 0 1 1 1 1 0 0 0 0 1 1 0 0 1 0 2 0 2 2 1 0 1 0 1 1 1 1 0 2 1 1 1 0 1 2 1 0 1 1 1 0 0 1 0 1

Allosaurus 'jimmadseni'

0 0 1 0 ? 0 0 0 0 0 0 0 1 0 0 ? ? ? ? ? ? 0 0 0 0 ? 2 ? ? 1 ? 1 1 0 0 ? 1 1 0 1 1 0 0
0 0 2 1 2 0 0 0 1 0 1 1 1 0 0 0 0 ? 0 1 0 ? 1 ? 1 1 ? 0 ? 1 1 0 2 0 0 0 0 ? 0 2 ? 0 1
1 0 ? 1 0 0 0 1 1 0 1 ? ? 1 ? ? ? ? ? ? ? ? ? 0 1 1 ? ? ? ? ? ? 1 0 0 0 ? 0 0 0 1 1
0 ? ? ? 1 1 1 1 1 1 1 1 0 0 0 0 1 0 ? 0 1 1 0 2 0 0 1 0 0 1 1 0 0 ? ? 0 0 ? ? 0 0 1 0
? ? 0 0 0 0 1 0 1 1 0 0 0 1 0 0 0 1 1 0 0 0 0 0 1 1 1 1 0 0 0 0 1 1 0 0 0 0 0 0 0 0 1 0
1 ? 1 1 0 1 1 0 1 2 0 0 1 2 0 0 1 1 1 0 1 0 1 1 0 0 0 0 1 0 0 0 1 ? 0 3 1 0 0 1 1 1 1 1
1 0 0 0 0 1 1 1 0 1 0 0 1 0 2 1 1 1 1 0 1 1 0 2 0 1 2 0 1 ? 1 2 0 0 2 0 0 1 1 1 0 0 0 2
1 0 1 1 1 0 1 1 1 1 0 0 0 0 1 1 0 0 1 0 2 0 2 2 1 0 1 0 1 1 1 1 0 2 1 1 1 0 1 2 1 0 1 1 1 0 0 1 0 1

REFERENCES

Baumel, J. J. (1993). *Handbook of avian anatomy: nomina anatomica avium*. Ed. by R. A. Paynter. 2nd ed. Vol. 23. Publications of the Nuttall Ornithological Club. The Nuttall Ornithological Club.

Bonaparte, J. F., F. E. Novas, and R. A. Coria (1990). *Carnotaurus sastrei Bonaparte, the horned, lighlty built carnosaur from the Middle Cretaceous of Patagonia*. Vol. 416. Contributions in Science. Los Angeles, California: Natural JHistory Museum of Los Angeles County.

Breithaupt, B. (1996). "Forty-seventh annual field conference guidebook". In: ed. by C. E. Brown, S. C. Kirkwood, and T. S. Miller. Wyoming Geological Association. Chap. The discovery of a nearly complete *Allosaurus* from the Jurassic Morrison Formation, eastern Bighom Basin, Wyoming, pp. 309–313.

Brinkman, P. D. (2010). *The second Jurassic dinosaur rush, museums and paleontology in America at the turn of the twentieth century*. Chicago: University of Chicago Press.

Britt, B. B. (1991). "The theropods of the Dry Mesa Quarry (Morrison Formation), Colorado: with emphasis on the osteology of *Torosaurus tanneri*". *Brigham Yound University, Geology Studies* 37, pp. 1–72.

Brusatte, S. L. and P. C. Sereno (2008). "Phylogeny of Allosauridae (Dinosauria: Theropoda): comparative analysis and resolution". *Journal of systematic palaeontology* 6, pp. 155–182.

Brusatte, S., R. B. J. Benson, and S. Hutt (2008). *The osteology of Neovenator salerii (Dinosauria: Theropoda) from the Wealden Group (Barremian) of the Isle of Wight*. Ed. by S. Brusatte. Monograph of the Palaeontographical Society. London: Palaeontographical Society.

Carrano, M. T., R. B. J. Benson, and S. D. Sampson (2012). "The phylogeny of Tetanurae (Dinosauria: Theropoda)". *Journal of Systematic Palaeontology* 10, pp. 211–300.

Charig, A. J. and A. C. Milner (1986). "*Baryonyx*, a remarkable new theropod dinosaur". *Nature* 324, pp. 359–361.

Chure, D. J. (1995). "Sixth symposium on Mesozoic terrestrial ecosystems and biota, short papers". In: *Sixth*. Ed. by L. Sun and Y. Q. Wang. Beijing: China Ocean Press. Chap. A reassessment of the gigantic theropod Saurophagus maximus from the Morrison Formation (Upper Jurassic) of Oklahoma, USA, pp. 103–106.

— (2000). "A new species of *Allosaurus* from the Morrison Formation of Dinosaur National Monument (UT-CO) and a revision of the theropod family allosauridae". Doctoral dissertation. Columbia: Columbia University.

Cope, E. D. (1878). "A new opisthocoelus dinosaur". *Amercian Naturalist* 12.6, pp. 406–408.

Coria, R. A. and P. J. Currie (2006). "A new carcharodontosaurud (Dinosauria, Theropoda) from the Upper Cretaceous of Argentina". *Geodiversitas* 28, pp. 71–118.

Coria, R. and L. Salgado (1995). "A new giant carnivorous dinosaur from the Cretaceous of Patagonia". *Nature* 377, pp. 224–226.

Currie, P. J. (2003). "Cranial morphology of tyrannosaurid dinosaurs from the Late Cretaceous of Alberta, Canada". *Acta Palaeontologica Polonica* 48, pp. 191–226.

Currie, P. J. and K. Carpenter (2000). "A new specimen of *Acrocanthosaurus atokensis* (Theropoda, Dinosauria) from the Lower Cretaceous Antlers Formation (Lower, Aptian) of Oklahoma, USA". *Geodiversitas* 22, pp. 207–246.

Currie, P. J. and X. J. Zhao (1993). "a new carnosaur (Dinosauria, Theropoda) from the Jurassic of Xinjiang, People's Republic of China". *Canadian Journal of Earth Science* 30, pp. 2037–2081.

Dalman, S. G. (2014). "Osteology of a large allosauroid theropod from the Upper Jurassic (Tithonian) Morrison Formation of Colorado, USA". *Volumina Jurassica* 12.2, pp. 159–180.

DePalma, R. A., D. A. Burnham, L. D. Martin, P. L. Larson, and R. T. Bakker (2015). "The first giant raptor (Theropoda: Dromaeosauridae) from the Hell Creek Formation". *Paleontological Contributions* 14, pp. 1–16.

Dong, Z., S. Zhou, and Y. Zhang (1983). "Dinosaurs from the Jurassic of Sichuan". *Palaeontologica Sinica, New Series C* 162, pp. 1–136.

Foth, C., S. Evers, B. Pabst, O. Mateus, A. Flisch, M. Patthey, and O. W. M. Rauhut (2015). "New insights into the lifestyle of *Allosaurus* (Dinosauria: Theropoda) based on another specimen with multiple pathologies". *PeerJ Preprints* 3, e824v1.

Galton, P. M., K. Carpenter, and S. G. Dalman (2015). "The holotype pes of the Morrison dinosaur *Camptonotus amplus* Marsh, 1879 (Upper Jurassic, wester USA) - is it *Camptosaurus*, Sauropoda or Allosaurus?" *Neues Jahrbuch für Geologie und Paläontologie Abhandlungen* 275.3, pp. 317–335.

Galton, P. M. and J. A. Jensen (1979). "A new large theropod dinosaur from the Upper Jurassic of Colorado". *Brigham Young University Geology Studies* 26, pp. 1–12.

Gao, Y. (1992). "*Yangchuanosaurus hepingensis* – a new species of carnosaur from Zigong, Sichuan". *Vertebrata PalAsiatica* 30.4, pp. 313–324.

Gauthier, J. A. (1986). "Saurischian monophyly and the origin of birds". In: *The origin of birds and evolution of flight*. Ed. by K. Padian. San Francisco: California Academy of Sciences, pp. 1–55.

Gilmore, C. W. (1920). *Osteology of the carnivorous Dinosauria in the United States National museum: with special reference to the genera Antrodemus (Allosaurus) and Ceratosaurus*. Washington: Government printing office, p. 224.

Goloboff, P. A., J. S. Farris, and K. C. Nixon (2008). "TNT, a free program for phylogenetic analysis". *Cladistics* 24.5, pp. 774–786.

Hammer, W. R. and W. J. Hickerson (1994). "A crested theropod dinosaur from Antarctica". *Science* 264, pp. 828–830.

Hanna, R. R. (2002). "Multiple injury and infection in a sub-adult theropod dinosaurs (*Allosaurus fragilis*) with comparisons to allosaur pathology in the Cleveland-Lloyd Dinosaur Quarry Collection". *Journal of Vertebrate Paleontology* 22.1, pp. 76–90.

Harris, J. D. (1998). "A reanalysis of *Acrocanthosaurus atokensis*, its phylogenetic status, and paleobiogeographic implications, based on a new specimen from Texas". *New Mexico Museum of Natural History and Science, Bulletin* 13, pp. 1–75.

Holland, W. J. (1906). "The osteology of *Diplodocus* Marsh". *Memoirs of the Carnegie Museum* 2, pp. 225–264.

Holtz, T. R. (2004). "The Dinosaurias". In: ed. by D. B. Weishampel, P. Dodson, and H. Osmólska. 2nd. California: University of California Press. Chap. Tyrannosauroidea, pp. 111–136.

Imlay, R. W. (1980). "Jurassic paleobiogeography of the conterminous United States in its continental setting". *U.S. Survey Professional Paper* 1062, pp. 1–134.

Johnson, E. A. (1992). "Depositional history of Jurassic rocks in the area of the powder river basin, Northeastern Wyoming and Southeastern Montana U.S." *Geological Survey Bulletin* 1917, pp. 1–38.

Leidy, J. (1873). "Contribution to the extinct vertebrate fauna of the western territories". *Report of the U.S. Geological Survey of the Territories* I, pp. 14–358.

Loewen, M. A., S. D. Sampson, M. T. Carrano, and D. J. Chure (2003). "Morphology, taxonomy, and stratigraphy of *Allosaurus* from the Upper Jurassic Morrison Formation". *Journal of Vertebrate Paleontology* 23.3, 72A.

Madsen, J. H. (1976a). "A second new theropod dinosaur from the Late Jurassic of east central Utah". *Utah Geology* 3, pp. 51–60.

— (1976b). *Allosaurus fragilis: a revised osteology*. Bulletin (Utah Geological and Mineral Survey). Utah: Utah Geological and Mineral Survey, Utah Department of Natural Resources.

Madsen, J. H. and S. P. Welles (2000). *Ceratosaurus (Dinosauria, Theropoda): a revised osteology*. Miscellaneous Publication 00-2. Utah: Utah Geological Survey.

Malafaia, E., P. Dantas, F. Ortega, and F. Escaso (2007). "Cantera Paleontológica". In: ed. by O. Cambra-Moo, C. Martimez-Pérez, B. Chameri, F. Escaso, S. De Estebar Trivigno, and J. Marugán-Lobón. Cuenca, Portugal: Diputación Provincial de Cuenca. Chap. Nuevos restos de *Allosaurus fragilis* (Theropoda: Carnosauria) del yacimiento de Andrés (Jurásico Superior; Centro-Oeste de Portugal), pp. 255–272.

Marsh, O. C. (1877). "Notice of new dinosaurian reptiles from the Jurassic formation". *American Journal of Science and Arts* 14.84, pp. 514–516.

— (1878). "Notice of new dinosaurian reptiles". *American Journal of Science and Arts* 15.87, pp. 241–244.

— (1879). “Principal characters of American Jurassic dinosaurs. Part II”. *American Journal of Science. Series 3* 17.97, pp. 86–92.

Mateus, O., A. Walen, and M. T. Antunes (2006). “Paleontology and geology of the Upper Jurassic Morrison Formation”. In: ed. by J. R. Foster and S. G. Lucas. Vol. 36. Albuquerque, New Mexico: New Mexico Museum of Natural History and Science Bulletin. Chap. The large theropod fauna of the Lourinha Formation (Portugal) and its similarity to that of the Morrison Formation, with a description of a new species of *Allosaurus*, pp. 123–129.

Molnar, R. E. (1991). “The cranial morphology of *Tyrannosaurus rex*”. *Palaeontographica Abteilung A* 217, pp. 137–176.

Osmólska, H. (1996). “An unusual theropod dinosaur from the Late Cretaceous Nemegt Formation of Mongolia”. *Acta Palaeontologica Polonica* 41, pp. 1–38.

Paul, G. S. and K. Carpenter (2010). “*Allosaurus* Marsh, 1877 (Dinosauria, Theropoda): proposed conservation of usage by designation of a neotype for its type species *Allosaurus fragilis* Marsh,1877”. *Bulletin of Zoological Nomenclature* 67.1, pp. 53–56.

Pérez-Moreno, B. P., D. J. Chure, and C. Pires (1999). “On the presence of *Allosaurus fragilis* (Theropoda: Carnosauria) in the Upper Jurassic of Portugal: First evidence of an intercontinental dinosaur species”. *Journal of the Geological Society* 156, pp. 449–452.

Rauhut, O. W. M. (2003). “The interrelationships and evolution of basal theropod dinosaurs”. *Special Papers in Palaeontology* 69, pp. 1–213.

Sereno, P. C., D. B. Dutheil, M. Iarochene, H. C. E. Larsson, G. H. Lyon, P. Magwene, C. A. Sidor, D. J. Varricchio, and J. A. Wilson (1996). “Predatory dinosaurs from the Sahara and Late Cretaceous faunal differentiation”. *Science* 272, pp. 986–991.

Sereno, P. C., J. A. Wilson, H. C. E. Larsson, D. B. Dutheil, and H.-D. Sues (1994). “Early Cretaceous dinosaurs from the Sahara”. *Science* 266, pp. 267–270.

Smith, D. K. (1998). “A morphometric analysis of *Allosaurus*”. *Journal of Vertebrate Paleontology* 18.1, pp. 126–142.

Stovall, J. W. and W. J. Langston (1950). “*Acrocanthosaurus atokensis*, a new genus and species of Lower Cretaceous Theropod from Oklahoma”. *The American Midland Naturalist* 43, pp. 696–728.

Stromer, E. (1931). “Ergebnisse der forschungsreisen prof. E. Stromers in den Wüsten Ägyptens. II. Wirbeltier-Reste der Baharîjestufe (unterstes Cenoman). 10. Ein skelett-rest von *Carcharodontosaurus* nov. gen.” *Abhandlungen der Bayerischen Akademie der Wissenschaften Mathematisch-naturwissenschaftliche Abteilung, Neue Folge* 9, pp. 1–23.

Winslow, N. S. and P. L. Heller (1987). “Evaluation of unconformities in Upper Jurassic and Lower Cretaceous nonmarine deposits, Bighorn Basin, Wyoming and Montana, U.S.A.” *Sedimentary Geology* 53, pp. 181–202.

Zhao, X.-J. and P. J. Currie (1993). “A large crested theropod from the Jurassic of Xinjiang, People’s Republic of China”. *Canadian Journal of Earth Sciences* 30, pp. 2027–2036.